University of Alberta

Prediction of Load-Sharing Mechanisms and Patterns of Human Cervical Spine Injuries Due to High-Velocity Impact Using Finite Element Method.

by

Tanvir Mustafy

A thesis submitted to the Faculty of Graduate Studies and Research in partial fulfillment of the requirements for the degree of

Master of Science

in

Structural Engineering

Department of Civil & Environmental Engineering

Fall 2013
Edmonton, Alberta

Dedication

Dedicated to my father Mr. Mukter Hussain, my mom Mrs. Tamiza Akter and my sister Dr. Tania Jebin.

Abstract

The purpose of the current study was to investigate the loading rate dependency, load-sharing and injury mechanisms of the C2-C3 cervical spine unit. A ligamentous bio-realistic finite element model was constructed considering comprehensive geometrical representation at tissue level components and material laws that include strain rate effect, bone fracture and ligament failure. The model has been validated for both quasi-static and dynamic loading scenarios. The study demonstrated four important findings: 1) Cervical segment response is rate dependent as it showed distinctive responses under different rates of loading; 2) Ligaments are the primary load-bearing structure for in plane and out of plane loading; 3) Depending on the loading rate and direction, capsular ligaments, articular facets represent vulnerable sites and they possess risk of failure under impact complex loading. 4) This model provides detailed biofidelic kinematic and local tissue response up to failure, leading to injury prediction in major and/minor injury conditions.

Acknowledgement

It pleasures me immensely to recount the people, the figures of flesh and blood, who have helped me through my endeavor, sometimes by just "being a friend or a dedicated ear that listened", sometimes by helping me technically or philosophically to overcome the hurdles in my research. First and foremost, I would like to thank my supervisor, Professor Dr. Marwan El-Rich, who has supported me throughout my thesis with his patience and knowledge. I attribute the level of my master's degree to his encouragement and effort and without him this thesis, would not have been completed or written. Throughout my thesis-writing period, he provided encouragement, sound advice, good teaching, good company, and lots of good ideas. This research work would not have been possible without his patronage. One simply could not wish for a better or friendlier supervisor.

I would like to thank my co-supervisor, Professor Dr. Kodjo Moglo for the continuous support of my research, for his patience, motivation, enthusiasm, and immense knowledge. His guidance helped me in all the time of research and writing of this thesis. I appreciate all his contributions of time, ideas, and funding to make my last two years' experience productive and stimulating.

In my daily work I have been blessed with a friendly and cheerful group of fellow students and kind professors. I am indebted to those friendly students and professors for providing a stimulating and fun environment in which to learn and grow. I would like to express my utmost gratitude to Dr. Samer Adeeb and Dr. Kajsa Duke for their unflagging support and wise advice. Their wisdom, knowledge and commitment to the highest standards inspired and motivated me.

I am also grateful to Amin Komeili, Behzad Vafaeian, Muntaseer Kainat, Mohamad Najari, Celal Cakiroglu, Fatemeh Moghaddam, Sadegh Naserkhaki, Faisal Agah and Hongru Zhao for their kindness, friendship and support,

I wish to thank Kamrul Islam and Jonathon Schofield for helping me get through the difficult times, and for all the emotional support, comraderie, entertainment, and caring they provided.

Lastly, and most importantly, I wish to thank my parents, Mukter Hussain and Tamiza Akter. Their love provided me inspiration and was my driving force. I owe them everything and wish I could show them just how much I love and appreciate them. They bore me, raised me, supported me, taught me, and loved me. To them I dedicate this thesis. Also I would like to thank my dearest sister, Dr. Tania Jebin who has inspired me through the tantrum of brainstorming in those caffeine empowered nights of simulation run and through all the falls and rises I've gone through in Canada reminding me what the science fiction writer Jim Butcher once said "When everything goes to hell, the people who stand by you without flinching - they are your family".

Table of Contents

Chapter 1: Introduction

1.1 Background and Motivation

The cervical spine is subject to injuries caused by different types of accidents and/or extreme movements. The most common causes of injuries are related to sport and motor vehicle accidents. Contact sports such as American football, ice hockey, rugby, and wrestling carry a high risk for neck injuries. Another group exposed to a high risk of neck injury is Air Force and helicopter pilots. The extreme loads applied to the neck during activities such as high g-maneuvers, crashes, or emergency ejections while wearing helmets with substantial mass, are known to cause acute injuries to the cervical spine. Neck injury stands as an important issue in crash safety, where 14% of all car crash injuries occur in this region [1].

The anatomy of the cervical spine makes it very vulnerable against different load. Cervical spine injuries are mostly occurred due to the spinal injuries rather than the lower spinal regions [2]. According to Yoganandan et al [2], the craniocervical junction (Occiput–C2) is the primary location of cervical injury. This junction is vulnerable due to the flexibility of the upper portion of the spine. Because of the stiffness change between the upper cervical spine and the stiffer thoracic spine, the inferior portion of the cervical spine segment has a higher value of incidence.

There are two major classes of neck injuries, vertebral fractures and soft tissue injuries (International Classification of Diagnosis version 10). These injuries usually refer to the global loading mode, which represents the motion of the head relative to the torso. But this reference is not always accurate as there is a difference between the local loading mode between two consecutive vertebrae and the global motion. As for an example, the distraction loading on the top of head can results in distraction, flexion and extension loading in different motion segments. Global motions are shown in (Fig.1), while the local loading modes are shown in (Fig.2).

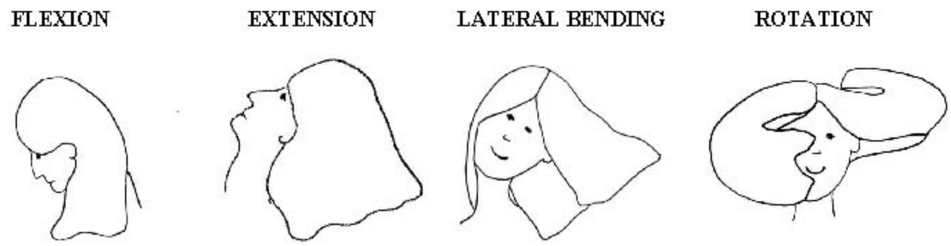

Figure 1: Global motions of the head compared to the torso [3].

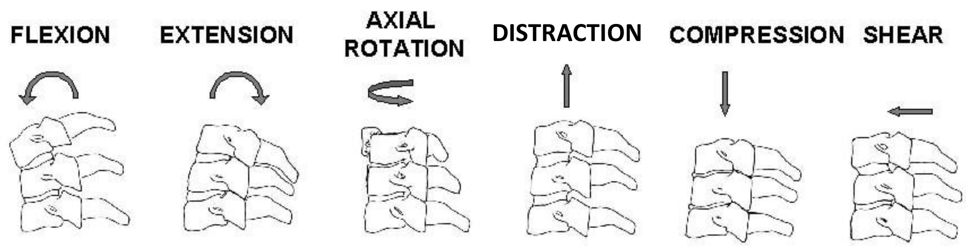

Figure 2: Local motions of lower cervical spine segments, due to different loading modes [3].

There are different kinds of vertebral fractures. A brief overview of the vertebral fractures are given below.

1. Atlas Fractures

A multipart fracture of the first cervical vertebra is often called Jefferson's fracture, although the Jefferson's fracture properly refers to a four-part fracture [3]. This injury may be fatal since the nerve roots leaving the spinal canal at this level are in control of the autonomous system.

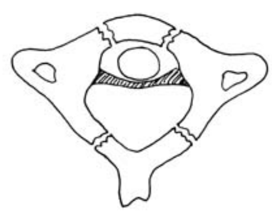

Figure 3: Multipart fracture / Jefferson's fracture [3]

2. Axis Fractures

Axis fractures have a high death rate, where many die at the scene of accident and will therefore be neglected in statistical studies based on hospital reviews [3]. There are three major types of axis fractures: dens fracture, hangman's fracture, and vertebral body fractures [3].

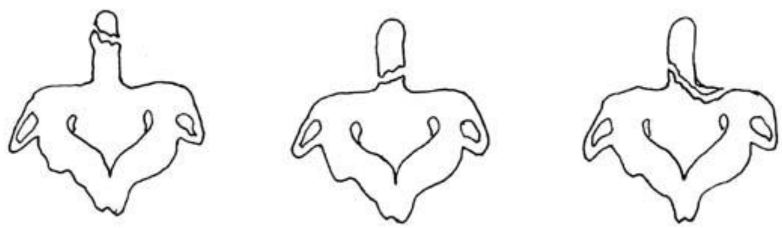

Figure 4: Odontoid fracture / Dens fracture [3]

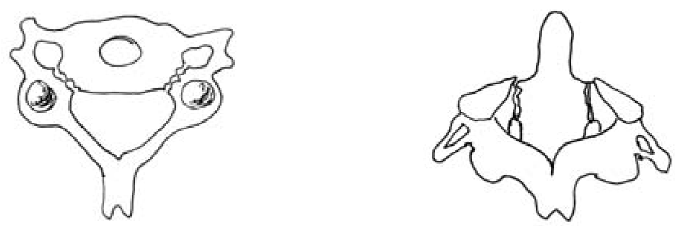

Figure 5: Hangman's fracture, superior and posterior view of C2 with fractured pedicles [3]

3. Lower Cervical Spine Fractures

- Burst Fracture

In burst fractures the vertebral body disintegrates into several smaller fragments (Fig.6a). This injury is frequently combined with fractures to the endplates and injury of the intervertebral disk [3].

- Teardrop Fracture

The teardrop fracture is characterized by a triangular shaped bone segment that fractures from the inferior part of the vertebral body (on the anterior side) (Fig.6b). The injury is considered highly unstable in extension because the ALL is ruptured. The injury is stable in flexion since all the posterior ligaments are intact [3].

- Wedge Fracture

The wedge fracture is a failure of the anterior vertebral body (Fig.6c). This injury is thought to be the result of a flexion bending moment and a compression forces on the vertebral motion segment [3].

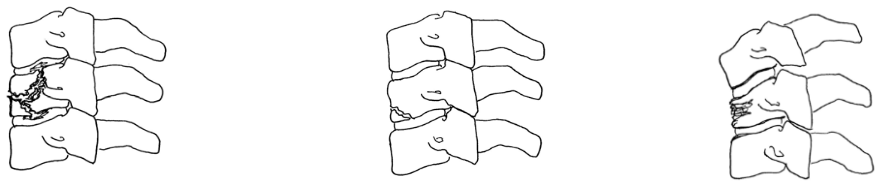

(a) (b) (c)

Figure 6: a) Burst fracture. b) Teardrop fracture. c) Wedge fracture [3].

4. Posterior Element Fracture

   Fracture of the posterior elements of the cervical spine occur throughout the upper and lower cervical spine. This fracture can be isolated, but multiple fractures are frequent (Fig.7). These fractures include fractures of the laminae, the pedicles, the spinous processes, and the pars interarticularis. The bony structures that protect the spinal cord are injured [3].

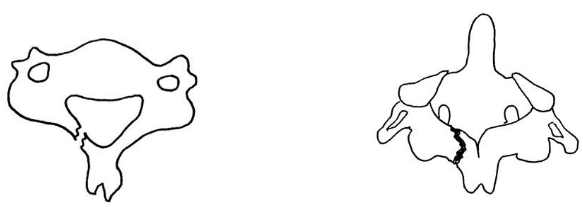

(a) (b)

Figure 7: Fracture of spinous process, (a) Superior view, (b) Posterior view [3]

Soft tissue injury are categorized into several types. They are,

- Facet Dislocation

In facet dislocations the superior vertebra is displaced anteriorly compared to the inferior vertebra, thus locking the facet joints. A dislocation can be either unilateral or bilateral, that is injury to only one or both of the facet joints. The bilateral facet dislocation causes a significant reduction of neural canal diameter, and is therefore often associated with spinal cord injuries [3].

- Occipitoatlantal Dislocation

Dislocation at this level is the result of local tension in combination with other loading modes [3].

- Atlantoaxial Subluxation

Atlantoaxial subluxation refers to injuries where one or both facet surfaces on C1 are displaced anterior or posterior to the facet surfaces on C2. Depending on the severity of displacement the alar, transverse, and capsular ligaments can be ruptured [3].

- Rupture of Ligaments

Ligament ruptures result from severe tensile strains in the ligaments. At first some of the collagen fibers break and if the tensile loading continues to increase the elastin fibers will start to fail, until complete failure of the ligament occurs. Tensile strains in anterior ligaments result from global extension motions, while posterior ligaments fail in global flexion [3].

- Subfailure of Ligaments

Lately, spinal researchers are hypothesizing that subfailure of the ligaments can be responsible for diffuse symptoms occurring in patients after low energy trauma. When the ligaments are stretched some of the collagen fibers may fail without any noticeable effect on spinal stiffness, this is defined as subfailure [3].

- Rupture of the Disc

Intervertebral disc trauma is frequently combined with vertebral body. Compression in combination with flexion or extension may cause this type of injury [3].

To mitigate the frequency of these life threatening and costly neck injuries, the auto industry is trying to improve the safety mechanism. And to achieve this they are operating a good amount of advanced testing and analysis. In vehicular design aspect, finite element models of the cervical spine can be used to simulate the load-sharing response and predict injury in different crash scenarios. Understanding the cervical spine response to these different rate-dependent loading that represents the crash condition, can contribute in the design & validation of these computation models. A mentionable number of research efforts have focused on determining the head and neck (HN) complex kinematics and kinetics under different types of loading [4]. The methods adopted for carrying out these studies are mostly experimental (dummy or post mortem human surrogate) [5].

Many factors and parameters could influence the investigation results such as specimen age, number of units tested, specimen orientation, loading protocol and biological variation of the tissues. Clinical studies have shown the influence of muscle tension due to awareness of the coming impact on resulting neck injury symptoms. Hence, these methods have a limitation of predicting the localized stress and strain fields within each structure of the cervical spine due to the fact of high cost and ethical issues. Mathematically developed models such as the Finite Element (FE) method can be used also to investigate the structural response of HN complex to external loading, it permits to find the internal response such as stress and strain resulted to external loading in the individual tissue level which can be used to predict injuries based on tissue level criteria. For a finite element model to be accurate in injury prediction, the consideration of realistic (bio-fidelic) geometry and material properties during modelling is very important [6]. And the segment should be detailed enough yet due to the time and effort required for subject-specific spinal model development, one segment is often used.

Testing and Validating FE models by comparing results to experimental data obtained in-vivo or from in vitro human cadaver experiments are necessary. Subject-specific validation studies data rely mainly on the data extracted from the same specimen which was considered to build the models. Therefore, different parametric variability in material properties of specimen found during experimental test could be a useful tool for calibrating a model in order to enhance its ability to mimic subject-specific experimental behavior. Also, the model should take into account accurate geometry and material properties, representative loading conditions, and proper verification and validation (V & V) using experimental studies. FE models have to include time-dependent constitutive material laws when used to investigate the spinal response under dynamic and rapid loading scenarios such us high speed car crashes [7] compared against high strain rate experimental data if accurate prediction of occupant response is needed as the neck injuries occur mainly during the high speed car crashes [7].

Investigations have been done on measuring experimentally the quasi-static response of the cervical spine in flexion and extension [8], [9], [10], [11]. Data from these investigations was used to establish FE models [12]. But even so, the models which have been validated against quasi-static experimental data cannot be used to predict the response under high rate loading conditions [13]. There is a paucity of data on the dynamic response of cervical spine segments [14]. Ligament studies from the recent literatures reported that cervical spine ligament show increased stiffness at higher strain rates [15], [2], [16]. Intervertebral discs in the lumbar spine also confirms about the loading rate dependency [17], [18], [19]. This rate dependent response might resulted from the viscoelastic nature of the ligaments and disc. In flexion, the posterior longitudinal ligament (PLL), the interspinous ligament (IL) and the ligamentum flavum (LF) act significantly to resist motion through tension. The disc also takes part in resisting the load by anterior side compression and posterior side tension [20]. In extension case, the anterior longitudinal ligament (ALL) is under tension along with the capsular ligament (CL), thus these ligaments take part significantly in extension along with the disc. Hence the stiffness response of the spinal segment is dependent on load sharing between ligaments, bone, disc and zygapophyseal joints for sagittal movements, which strongly implies that the complete spinal response should also be rate dependent.

Alongside of investigating the load-rate effect on the cervical spine it is also very important to prepare an accurate model at the tissue level to predict injury under various impact loading conditions. For investigation of load distribution mechanism under different impact loading scenarios several FE spinal models were used; [21], [22], [23], [24], [25], [26].These models have not considered the nonlinear viscoelastic properties for spinal material. Study by Kumaresan et al. [27] has developed a detailed model of C4-C6 segment considering non linearity in the materials. In that model, disc was modeled with annulus fibers and ground substance along with linear elastic solid elements for the nucleus pulposus, which is believed to be the first model to include anisotropic behavior of the disc. Ligaments were modelled as non-linear springs. A study by Wheeldon et al. [11] constructed C2, C7 and T1 to the C4-C6 model by Kumaresan et al. [28], thus having a model of the complete C2-T1 segment. An investigation by Clausen et al. [21] used non-linear material properties for the ligaments in an FE model of the C5-C6 complex. In order to investigate the fracture fixation methods in the cervical spine, several studies were done by some other investigators [27], [29], [30], [31], [32], [33].

Unlike individual loading applications, there is a paucity of biomechanical data on the human cervical spine under combined complex loading. A work of combined tension-extension has been done by [33], [33]. Tensile loading has been reported to cause occipitoatlantal dislocation, Hangman’s fracture (fracture of both pedicles or pars interarticularis), anterior longitudinal ligamentous rupture, disk rupture, horizontal fracture of the vertebral body, teardrop fracture, bilateral facet dislocation, and unilateral facet dislocation [33]. This study investigated the neck injury criterion by imposing combined axial tension and bending to postmortem human subject ligamentous cervical spines. Another study [34] has been conducted on combined bending and axial loading scenario. It investigated the lateral, anterior and posterior passive bending responses of the cervical spine [34]. Still there remains lack of data about the injury propagation and response of the soft tissue in case of the combined loading.

In this current study a bio-realistic FE model of the ligamentous cervical spine segment of C2-C3 has been developed and validated against numerous dynamic loading scenarios for the evaluation of global kinematics and tissue-level response. This model was used to investigate two significant aspect of the cervical spine segment: 1) Loading rate effect on cervical spinal load-sharing under impact, and 2) Injury mechanism of the spinal unit due to the combined complex loading scenarios.

1.2 Outline of the Thesis

This thesis contains four chapters. Chapter 2 and 3 will be submitted to two biomechanics specialized journals which were enclosed as **Paper I** and **Paper II**. Finally, summary and conclusions were discussed in Chapter 4.

1.3 References

[1] A. B. T. B. I. G. P. Robertson, "Spinal Injury Patterns Resulting from Car and Motorcycle Accidents.," *Spine, 27,* vol. 24, pp. 2825-2830., 2002.

[2] P. F. B. J. R. J. S. A. ,. L. S. Yoganandan N., "Dynamic response of human cervical spine ligaments.," *Spine*, vol. 14, p. 1102–10, 1989.

[3] K. Brolin, "Cervical Spine Injuries - Numerical Analyses and Statistical Survey," Sweden, 2002.

[4] A. e. a. Patwardhan, *Spine Vol 25(12);,* pp. 1548-54., 2000.

[5] Z. a. P. T. Dvir, "Cervical muscles strength testing: Methods and clinical implications," *J. of Manipulative and Physiological Therapeutics Spine ; 25(12),* vol. 15, pp. 1548-54., 2008.

[6] M. A. P. J. W. E. B. C. a. A. C. E. El-Rich, "Finite Element Investigation of the Loading Rate Effect on the Spinal Load- Sharing Changes under Impact Conditions," *J. Biomech., ,* vol. 42, no. 9, p. 1252–1262., 2009.

[7] J. C. D. P. M. Fice, "Cervical Spine Model To Predict Capsular Ligament Response In Rear Impact.," *Annals of Biomedical Engineering,,* vol. 39 (8), pp. 2152-2162, 2011.

[8] R. B. Nightingale, "Flexion and extension structural properties and strengths for male cervical spine segments," *Journal of Biomechanics (3),* vol. 40, p. 535–542., 2007.

[9] R. W. B. K. K. M. B. NIightingale, "Comparative bending strengths and structural properties of the upper and lower cervical spine.," *Journal of Biomechanics,,* p. 725–732., 2002.

[10] M. C. J. V. A. O. T. C. J. N. K. S. E. Panjabi, "Mechanical properties of the human cervical spine as shown by three-dimensional load-displacement curves.," *Spine, 26(24);,* pp. 2692-700., 2001.

[11] P. F. K. S. Y. N. Wheeldon JA, "Experimental flexion/extension data corridors for validation of finite element models of the young, normal cervical spine.," *J Biomech. (2),* vol. 39, pp. 375-80. , 2006.

[12] M. Panzer, *Numerical modelling of the human cervical spine in frontal impact,* Waterloo: University of Waterloo., 2006.

[13] A. C. G. A. E.-R. M. A. P. Wagnac E, "Calibration of hyperelastic material properties of the human lumbar intervertebral disc under fast dynamic compressive loads.," *J Biomech Eng ,* vol. 133, 2011.

[14] L. P. F. Y. N. L. Y. Voo, "Static and dynamic bending responses of the human cervical spine.," *Journal of Biomechanical Engineering, 120(6);,* pp. 693-6., 1998.

[15] L. J. L. V. Shim V.P.W., "A Technique for Dynamic Tensile Testing of Human Cervical Spine Ligaments," *Exper Mechanics,,* vol. 46, p. 77–89, 2006.

[16] M. J. C. N. C. D. Mattucci SF, "Strain rate dependent properties of younger human cervical spine ligaments," *Journal of Mechanical Behaviour & Biomedical Materials,* vol. 10, pp. 216-26, 2012.

[17] A. M. C. D. S. M. Kemper, "The Influence of Strain Rate on the Compressive Stiffness Properties of Human Lumbar Intervertebral Discs.," *Biomed. Sci. Instrum*, vol. 43, p. 176–181, 2007.

[18] S. K. A. M. D. B. P. M. F. Duma, "Biomechanical Response of the Lumbar Spine in Dynamic Compression," *Biomed. Sci. Instrum,*, vol. 42, p. 476–481, 2006.

[19] O. M. D. T. M. L. F. Izambert, "Dynamic stiffness and damping of human intervertebral disc using axial oscillatory displacement under a free mass system," *European spine journal*, vol. 12(6), pp. 562-6, 2003.

[20] S. M. Nikolai Bogduk, "Biomechanics of the cervical spine. I: Normal kinematics," *Clinical Biomechanics* , pp. 633-648, 2000.

[21] J. Clausen, "Unicinate process and Luschka joints influence the biomechanics of the cervical spine:quantification using a finite element model of the C5–C6 segment.," *JournalofOrthopaedic Research,* vol. 15, p. 342–347., 1997.

[22] N. L. F. a. S. W. Maurel, "A three-dimensional parameterized finite element model of the lower cervical spine. Study of the influence of the posterior articular facets," *Journal of Biomechanics,* vol. 30, pp. 921-931, 1997.

[23] K. S. V. L. P. F. Yoganandan N, "Finite element model of the human lower cervical spine: parametric analysis of the C4-C6 unit," *Jo. Biomechanical Engineering,* vol. 119, no. 1, pp. 87-92, 1997.

[24] H. Ng, "Statistical factorial analysis on the material property sensitivity of the mechanical response of the C4–C6 under compression,anterior and posterior shear.," *JournalofBiomechanics,* Vols. 37,, p. 771–777., 2004..

[25] N. H. Teo EC, "Evaluation of the role of ligaments, facets and disc nucleus in lower cervical spine compression and sagittal moments using finite element method," *Med. Eng. & Physics,* vol. 23, pp. 155-164, 2001b.

[26] A. D. B. D. H. R. L. D. D. R. Wilcox R, "An invetsigation of the burst fracture mechanism using a combined experimental and finite element approach," Calgary, 2002.

[27] S. Kumaresan, "Finite element modeling of cervical laminectomy with graded facetectomy.," *Journal of Spinal Disorders* , Vols. 10(1),, p. 40–46., 1997.

[28] S. Kumaresan, "Finite element modeling of the cervical spine:role of intervertebral disc under axial and eccentric loads," *Medical Engineering and Physics* , vol. 21, p. 689–700., 1999.

[29] K. S. Y. N. P. F. C. J. Voo LM, "Finite element analysis of cervical facetectomy," *SPINE,* vol. 22, no. 9, pp. 964-969, 1997.

[30] R. Natarajan, "Anterior cervical fusion: a finite element model study on motion segment stability including the effect of osteoporosis," *Spine,* vol. 25 (8), p. 955–961, 2000.

[31] K. H. J. C. K. J. S. M. N. R. A. H. A. G. Lim TH, "Effect of Endplate Conditions and Bone Mineral Density on the Compressive Strength of the Graft-Endplate Interface in Anterior Cervical Spine Fusion," *SPINE,* vol. 26, no. 8, pp. 951-956, 2001.

[32] G. V. T. V. C. C. Puttlitz CM, "A Finite Element Investigation of Upper Cervical Instrumentation," *SPINE,* vol. 26, no. 22, pp. 2449-2455, 2001.

[33] M. D. B. D. S. W. Pitzen TR, "Initial stability of cervical spine fixation: predictive value of a finite element model," *J. Neurosurg (Spine 1),* vol. 97, pp. 128-134, 2002.

[34] R. W. N. F. L. C. C. E. F. S. M. Alan T. Dibb, "Tension and Combined Tension-Extension Structural Response and Tolerance Properties of the Human Male

Ligamentous Cervical Spine," *Journal of Biomechanical Engineering* , vol. 131, AUGUST 2009.

[35] B. J. D. J. G. P. B. S. M. G. James H. McElhaney, "Combined Bending and Axial Loading Responses of the Human Cervical Spine".

Chapter 2

Investigation of Loading Rate Effects under Impact Conditions on the Ligamentous Cervical Spinal Load-Partitioning Using Finite Element Model of Functional Spinal Unit C2-C3.

A Journal Paper will be submitted to the Journal of Biomechanics:

This paper is enclosed in this chapter next as **Paper I**

Paper I

Investigation of Loading Rate Effects under Impact Conditions on the Ligamentous Cervical Spinal Load-Partitioning Using Finite Element Model of Functional Spinal Unit C2-C3.

Tanvir Mustafy[a], Marwan El-Rich[a], Wissal Messfar[b] and Kodjo Moglo[b]

[a]*Department of Civil and Environmental Engineering, University of Alberta, Canada;*
[b]*Department of Mechanical & Aerospace Engineering, Royal Military College of Canada*

Corresponding Author:

Marwan El-Rich
Department of Civil and Environmental Engineering
Markin/CNRL Natural Resources Engineering Facility
9105 116th St
Edmonton, Alberta, Canada
T6G 2W2

Phone: 1(780) 492-6678
Email: elrich@ualberta.ca

Abstract

The cervical spine functions as a complex mechanism that responds to sudden loading in a unique manner, due to intricate structural features and kinematics. Impact load at high-velocity rate releases important energy over a short time period and can induce spinal fractures. In the current study, the spinal load-sharing under pure compression and sagittal flexion and extension at two different loading rates was compared using a bio-realistic Finite Element (FE) model of the ligamentous cervical spine segment C2-C3. This model was developed using a comprehensive and realistic geometrical representation of spinal components and material laws that include strain rate dependency, bone fracture, and ligament failure. The model's results in terms of range of motion, articular facets contact pressure, and ligaments forces and failure properties were compared to experimental published findings. The structural response was markedly different under the highest velocity. The stress in the annulus and intradiscal pressure (IDP) in the nucleus increased with the rotation rate. The fastest rotation of C2 has increased significantly the IDP (1.42 MPa_flexion) and the stress in the outer annulus (0.38 MPa_extension and 1.9 MPa_flexion). Also the fastest extension caused facet contact stresses reaching up to 7.72 MPa. The highest ligament stress was obtained for capsular ligament (CL) under fastest flexion and it reached the rupture value. For sagittal rotations, the ligaments were the primary load-bearing structure in the segment. Load sharing among disc, facet joints, cortical and cancellous bone and vertebral endplates have showed dissimilar trends with different rates of loadings. These findings suggest that the loading rates have a significant effect on the load-sharing and failure mechanisms of the cervical spine under different loading conditions.

Keywords: cervical motion segment; high speed impact; experimental validation; load sharing

Introduction

Cervical spine injury represents 14% of total car crash injuries and the second cervical vertebra (C2) was the most commonly injured level [1]. Legislations in conjunction with the automotive industry are continuously working to develop new technologies to improve vehicle safety and protective equipment that prevents serious and costly neck injury through advanced testing and analyses. Despite advances in automotive safety, cervical spine injuries sustained in motor vehicle collisions continue to occur too often [2] [3]. Investigating the response of the cervical spine at different loading rate scenario that represents a car crash situation can provide important findings that would help in the design process and validation of lab based simulations. The finite element method has been used to investigate individual cervical segments, portions of the cervical spine, and full cervical spines with musculature [4], [5]. Neck injuries take place during high speed car crashes, so comparing results with experimental data can increase accuracy in the FE model [6] [7]. Major number of studies regarding the cervical spine have been confined to quasi-static simulations to investigate the load-sharing behavior of local tissue [8] [9] [10]. Only a fewer studies have tried to evaluate the occupant injury risk during automotive collisions [11] [12] [4], but most of these studies were limited in impact velocity and sub-catastrophic failure. Cervical spine ligaments have shown increased stiffness with the higher strain rates in some recent studies [13] [14] [7]. Intervertebral discs studies in the lumbar spine have also confirmed the load rate dependency [15] [16] [17]. In flexion, the interspinous ligament, the posterior longitudinal ligament, and the ligamentum flavum resist motion through tension mechanism. The disc also contributes in opposing the motion through anterior compression and posterior tension [18]. The specialized structure of the intervertebral disc enables itself for showing these highly demanding functions. As the spine is loaded in compression or bending, tensile loads are transmitted to the angled, lamellar collagen fiber structure of the annulus fibrosus. In extension, the anterior longitudinal ligament is the only ligament that remain in tension, thus it is the only ligament to contribute in extension along with the disc. In addition, anterior side capsular ligament contributes in taking some of the loading through tension [18]. At higher levels of flexion, the ligaments carried most of the load and in extension, the facets were the main source of joint stiffness [19]. The stiffness of a segment in flexion or extension is dependent on the load sharing between the disc and ligaments, therefore it implies that the segment response should also be rate dependent. The viscoelastic nature of the ligaments and disc suggests that dynamic effects might play an important role in the response of the cervical spine to high rate loading. These materials are relatively difficult to characterize since tissues are typically anisotropic with non-linear, viscoelastic behavior [5] [20], and must be represented using a continuum approach. Furthermore, most of the existing cervical spine models used 1D ligaments [19] and modeled ligaments as straight line [21] [22] and cable [23] [24] [25] elements. As a result, these studies are not capable of showing the stress position and/concentration in ligaments which may affect the spinal load sharing mechanism and lead to inaccurate predictions of injury in the case of impact loading scenario.

In order to address these issues, a refined three-dimensional finite-element model (FEM) of the C2-C3 segment has been developed to evaluate the compression and rotation rate effects during rapid axial and sagittal movements and this model has been validated in component level for both quasi-static and dynamic loading scenarios. The current study focuses on the loading rate effects and load-sharing responses at the component level using the complete C2-C3 functional cervical unit, which is comprised of comprehensive geometrical representation of tissue level components and material laws, that include strain rate effect, bone fracture, and ligament failure.

Materials and methods

- ### Geometric modeling and meshing

A 3-D nonlinear complex finite element (FE) model of C2-C3 spinal unit was developed and constructed based on a 39 year old adult male from CT scans and MRI images. The images were provided by the Human Visible Project organization and were taken at 1 mm intervals in the axial plane. Using Mimics Software, we reconstructed the geometry of the bony structures (cervical vertebrae (C2-C3)) using CT scan images and the intervertebral disc using MRI images. The mesh geometries obtained by the reconstruction software was converted to a CAD model using the scan-to-3D functionality in SolidWorks software without altering the real reconstructed geometry of the parts. This allows for an accurate partition of complex parts and mesh improvements. Here, the complete functional unit of C2-C3 has been considered. The vertebral bodies and posterior elements were modeled by taking into account the separation of the cortical shell (including bony endplate and facet joints) and cancellous bone using 3-nodes shell and 4-nodes solid elements, respectively. All shell elements had 1.0 mm thickness and characteristic length close to 0.5mm. The intervertebral disc was created between the intervening endplates. It was subdivided into nucleus pulposus and annulus fibrosus with a proportion (56 % annulus and 44 % nucleus) according to the histological findings [26].

The annulus was filled with 5 layers of 8-nodes solid elements and was reinforced in the radial direction by 5 collagenous fiber layers using unidirectional nonlinear springs resisting tensile load only and organized in concentric lamellae with crosswise pattern close to ±35 [27]. The surrounding ligaments, the anterior (ALL) and posterior (PLL) longitudinal ligaments, intertransverse (ITL), flavum (FL), capsular (JC) ,intertransverse (ITL), supraspinous (SSL) and interspinous (ISL) ligaments were modelled as 2D elements (Fig. 1).

The geometrical properties of soft tissues were taken from the literature [4]. All ligaments were modeled with 4-nodes shell elements. In total, the mesh of the C2–C3 model contained 105,000 nodes and 447,000 elements, with characteristic length ranges from 0.5 to 1.0 mm. The final mesh sizes of the components (vertebral bodies, intervertebral disc (IVD), and ligaments) were selected through sensitivity analysis, which ensured that the selected mesh resolutions were not significantly less accurate than finer mesh resolutions. This approach made an efficient way of balancing between accuracy and computing time/ cost. Also the prony series used for the ligaments modelling were implemented in different ranges (maximum shear modulus value 800 to 1500) to measure the effect of the variation in stress distribution among the ligaments. The pattern of the stress distribution remained same for different ranges of values but the maximum stress varied from 10% to 15%. And the parametric value of C_{10} and C_{01} from the hyper-elastic modelling of disc were taken from a calibrated range of values [32]. Which ensures the acceptable change of values inside that range will result in very slight change in the ouput of stress.

- <u>Material constitutive laws</u>

Bony components were assumed as isotropic materials and followed a symmetric and strain rate-dependent elasto-plastic material law (Johnson–Cook) (Table 1a) allowing computing von Mises hardening with ductile damage until potential rupture (Fig. 1).

Before reaching the plasticity limit, as long as the equivalent stress remains below the yield limit, the material behaves as linear elastic. When it reaches the onset of plastic deformation the equivalent stress at constant temperature was described with the relation:

$$\sigma = (a + b\varepsilon_p^n) * \left\{1 + \ln\left(\frac{\dot{\varepsilon}}{\dot{\varepsilon}_0}\right)\right\},$$

where σ equivalent stress, a yield stress, b hardening modulus, n hardening exponent, ε_p plastic strain (true strain), $\dot{\varepsilon}$ current strain rate, and $\dot{\varepsilon}_0$ reference strain rate. Once the ultimate deformation level ($\varepsilon_{\max}$) is reached, failure is modeled without any damage effect using a kill element model [28] [29]. In case of shell elements, the ruptured element gets deleted. In case of solid elements, the ruptured element has its deviatoric stress tensor permanently set to zero, but there is no deletion of the element. Strain-rate dependency of the bone structure was investigated through a sensitivity analysis.

The nucleus is modelled as fluid cavity structure [30]. The properties of the annulus fibrosus were governed by hyper-elastic material law based on a first-order Mooney–Rivlin formulation, while the fibers were modeled using nonlinear elastic material [31] (Table 1b). The formulation for the strain energy function of the Mooney–Rivlin model has been described below,

$$W = C_{10}(I_1 - 3) + C_{01}(I_2 - 3) + \frac{(J-1)^2}{d},$$

Where, C_{10}, C_{01} are material constants; I_1, I_2 first and second invariants of the deviatoric components of the left Cauchy- Green strain tensor; J local volume ratio; d = 2/K;

$$K = 6(C_{10} + C_{01}) / 3(1 - 2\upsilon),$$

The calibration method used by [32] has been implemented in this model as this material law does not incorporate strain rate dependency into its formulation.

Progressive failure mechanism was introduced in the ligament elements to produce a more biofidelic failure response. The ligaments were governed by visco-elastic (Time dependent Prony Series) material laws [33] (Table 1c). The relaxation modulus for this material has the form,

$$G(t) = G_\infty + \sum_{i=1}^{N} G_i e^{-t/t_i},$$

Where G_∞ is the steady-state stiffness, and G_i, t_i, $i = 1...N$ are the time constants and stiffnesses of the Maxwell elements. These parameters are used directly as the properties of the material. The sum of exponentials is known as the `Prony Series.'

Tied contact between the disc and vertebral bony endplates was used to represent disc avulsion. Frictionless contact interfaces were assumed between the diverse parts of the model to avoid any possible penetration. This interface was also used between the facet surfaces to calculate the contact forces. Development of the complete C2–C3 cervical full functional segment (Fig. 2) was based on the best available material properties at the tissue level (Table 1a, 1b and 1c). All simulations were performed using the explicit dynamic finite-element solver Abaqus (Version 6.12).

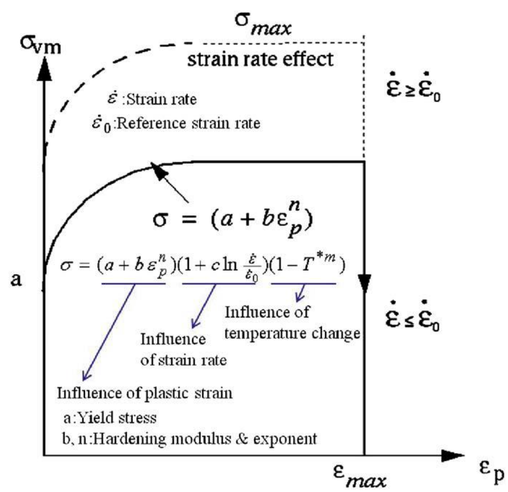

Figure 1: Johnson–Cook elasto-plastic material law used to model the structural behavior of the bone structure [29]

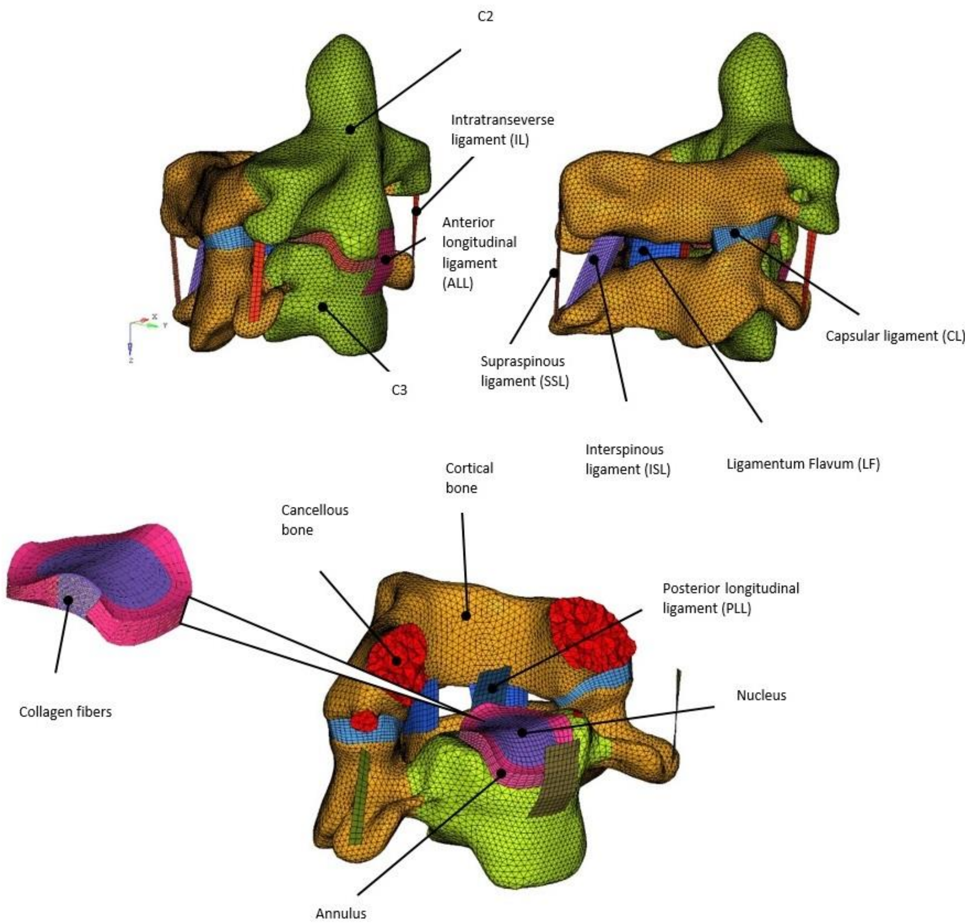

Figure 2: Functional spinal unit C2-C3 of the Cervical Spine Model

Table 1a: Material properties of vertebral components

Material Properties	*Vertebral Components*					
	Cortical	Reference	Endplate	Reference	Cancellous	Reference
Density (10^{-6} kg/mm^3)	1.83	[34]	1.06	[19]	0.17	[9]
Young modulus, E(MPa)	16800	[35]	5600	[19]	100	[9]
Poisson ratio, υ	0.3	[35]	0.3	[9]	0.29	[9]
Yield stress, a (MPa)	110	[35]	6	[35]	1.92	[9]
Hardening modulus b (MPa)	100	[36]	100	[36]	20	[36]
Hardening exponent, n	0.1	[36]	1	[36]	1	[36]
Failure plastic strain,(10^{-3}) ε_p	9.68	[36]	20	[37]	14.5	[37]
Maximum stress (MPa)	155	[38]	7.5	[38]	2.23	[39]
Strain rate coefficient, c	1	-	1	-	1	-

Table 1b: Material properties of disc components

Material Properties	*Disc Components*				
	Nucleus pulposus	Annulus matrix	References	Collagenous fibres	References
Density (kg/mm^3)	1.00E-06	1.20E-06	[34]	Nonlinear elastic curve	[31]
Poisson ratio, υ	0.495	0.45	[27]		
C_{10}	0.12	0.18	[27]		
C_{01}	0.03	0.045	[27]		

Table 1c: Material properties of spinal components

	Spinal ligaments								
	Constitutive models	Young modulus, E(MPa)	Poisson ratio, υ	Density (10^{-6} kg/mm^3)	Update coef., E1 (MPa/ms)	Update coef., E2 (MPa)	Failure strain, ε1	Failure strain, ε2	References
Ligaments	2D Viscoelastic material with time dependent Prony series								
ALL	Viscoelastic	11400	0.4	1	469.4	45.6	0.68	0.90	[40]
PLL		9120	0.4	1	1432.1	39.4	0.38	0.50	[30], [32]
ISL		3400	0.39	1	98.3	8.3	1.10	1.30	[30], [32]
IL		17100	0.49	1	98.3	8.3	1.10	1.30	[5], [32]
CL		7700	0.39	1	3.6	6	1.75	1.85	[30], [32]
LF		2400	0.39	1	199.7	6.5	1.01	1.25	[5], [32]
SSL		8550	0.4	1	476.5	8.3	0.94	1.08	[5], [32]

- <u>Model validation under quasi-static loading conditions</u>

a) Range of motion:

The model was evaluated in flexion, extension by comparing the simulated response with the measured range-of-motion for the C2-C3 vertebrae [41] at 2 Nm (Fig.3).The simulated range-of-motion was defined as the angle where the reactive moment of the model reached 2 Nm. The model results showed good agreement with all the studies for extension at levels up to 2 Nm and was moderately more compliant compared to the flexion results data. Also finite element results have been compared with the different investigation results for both extension and flexion up to 2 Nm. In addition, the FEA result shows good agreement with compared data (Fig.8).

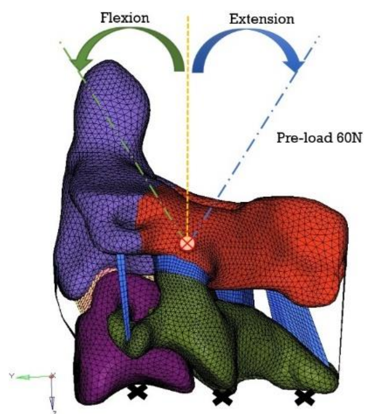

Figure 3: Loading set up for range of motion test

b) Contact Pressure:

The contact pressure in the facet joint during sagittal bending (Fig.4) has been compared with the cadaveric specimen test data [42].

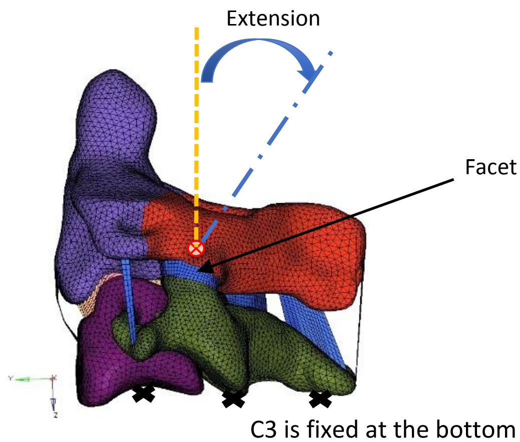

Figure 4: Loading set up for contact pressure test

The results have been evaluated for extension case only. The result found from FEA showed good agreement with the experimental corridor.

c) Ligaments:

Ligaments have been validated against the strain rate dependent experimental data [7]. The ligaments were tested at quasi-static (0.5 s−1), medium (20 s−1) and high (150–250 s−1) strain rates (Fig.5). Deformation vs force data have been plotted. The model results showed fair agreement with all of the ligaments results.

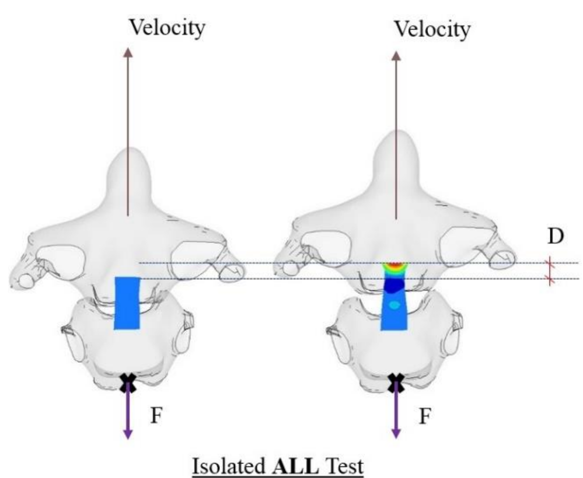

Figure 5: Loading set up ligament test (ALL)

- <u>Model validation under dynamic loading conditions</u>

a) Ligament Rupture/failure:

Ligaments have been validated against the failure strain and failure stress criterion [7]. Results were found to be in good agreement with the experimental data. Failure elongation values were also investigated for the ligaments and the values fitted inside the deviation range of the reported data.

b) Bone Rupture:

The elasto-plastic material property of the bone has been taken from the literature with reference to the validated data [36].

- <u>Loading rate investigation</u>

For compression test, two different rates of 1.2 m/s and 0.02 m/s axial loading were applied on the C2 vertebrae to get 0.3 mm amount of displacement in both rates (Fig.6). For stability condition, C3 was fixed at the bottom.

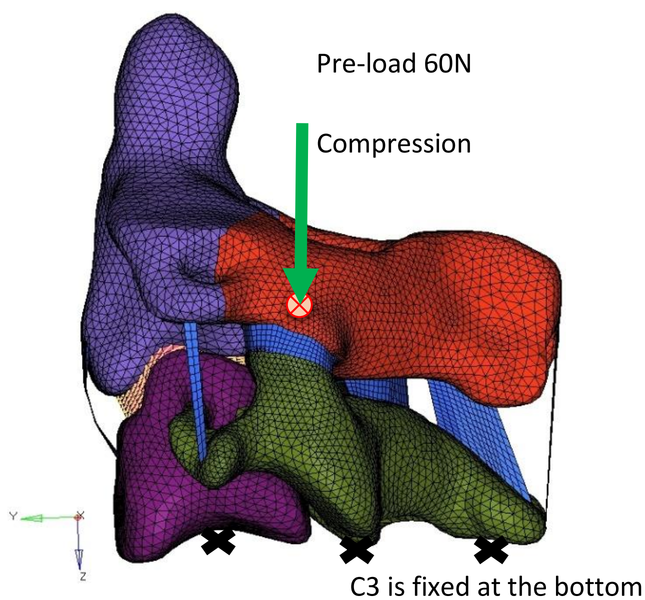

Figure 6: Loading set up for compression test

For sagittal rotation test, two different rates of 8°/ms , 0.4°/ms have been applied in both flexion and extension conditions to get 2.5 degree of rotation while the C3 was fixed at the bottom (Fig.7). For all the tests, Von Mises stress in vertebral endplates, intradiscal pressure (IDP) changes (stress in the nucleus pulposus) in the nucleus were calculated. The ligaments stresses were evaluated in their fibers directions and the contact forces were assessed in the facet joints. Also, strain energy variation in all components was investigated to assess the spinal load-sharing distribution. All the loading rates were selected based on the values resulted from impact analysis studies by [43].

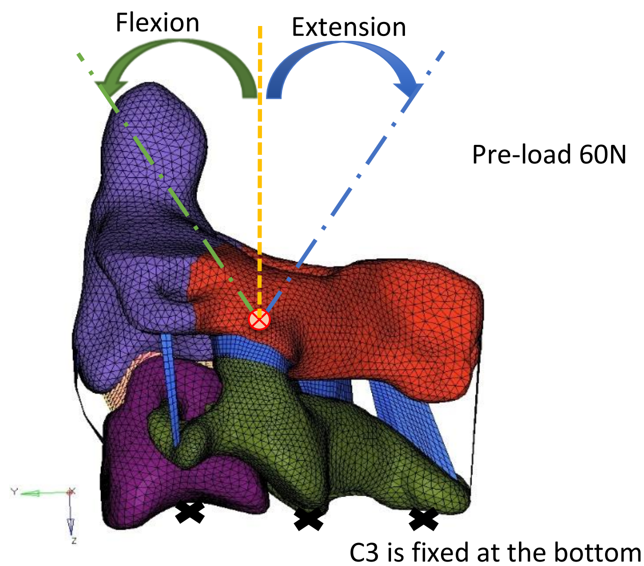

Figure 7: Loading set up for sagittal rotation test

Boundary and Loading conditions

The sagittal plane, transverse plane, and the coronal plane were defined by the axes “Y” and “Z”, axes “Y” and “X”, and axes “X” and “Z” respectively.

The movement of superior vertebra was allowed in sagittal plane only during flexion-extension rotations. The inferior vertebra was fully constrained at the bottom for all cases. C2-C3 segment model was compared against a number of in vitro studies of the human cervical spine segment which includes the loading at slower rates (predominantly disc response) and loading at faster rates in accordance to include the ligaments and facet joints. These studies were picked for validation purpose based on the type of experiment, the usefulness of the experimental data for validation, the historical use of the experimental data, and the general agreement of the experimental data with other studies in the literature. For each simulation cases a 60N of preload was applied to the superior vertebra to simulate the head weight [44]. As loading response was not distinctively different to the placement of center of rotation location for a unit segment in the superior-inferior side, so the loading has been applied on the centroid of C2 vertebra which is consistent with the loading methods adapted in [44]. Most of the experimental studies were load-controlled [46] [42] [47], so controlled load was applied in the comparison analyses in accordance with the experimental studies.

Model validation results

a) Range of motion:

The calculated moment-rotation curve of the C2 vertebrae for both flexion and extension are shown in (Fig.8). The curves are fitted within the experimental corridor (Fig.8), however the model appeared to be stiffer than the corresponding experimental one in flexion (Fig.8) and the decrease in stiffness seen by the experimental curves was not obtained by the model.

FEA results have been compared for both cases up to 2 Nm with the available experimental and numerical study results to assess the flexibility of the model. And in both cases of flexion (Fig. 9a) and extension (Fig.9b), the model shows a fair amount of range of motion compared with other studies.

b) Contact Pressure:

The contact pressure in the facet joint was in agreement with the previous experimental data [42] (Fig.10).

c) Ligaments:

Ligament strains that were inside the experimental range was defined by [7]. Ligaments tensile forces were also found to be in good agreement with experimental data. ALL, PLL, ISL, CL and LF ligaments are tested according to the test condition described in the referred paper. Here all the results for the ligaments are shown (Fig. 11) for all three quasi-static (0.5 s^{-1}), medium (20 s^{-1}) and high (150–250 s^{-1}) strain rates.

d) Ligament Rupture/failure:

Ligaments have been tested for all three quasi-static (0.5 s−1), medium (20 s−1) and high (150–250 s−1) strain rates. Moreover, the results are in good agreement with the experimental results [7]. Here the comparison of the results between FEM results and experimental data are presented in table 2.

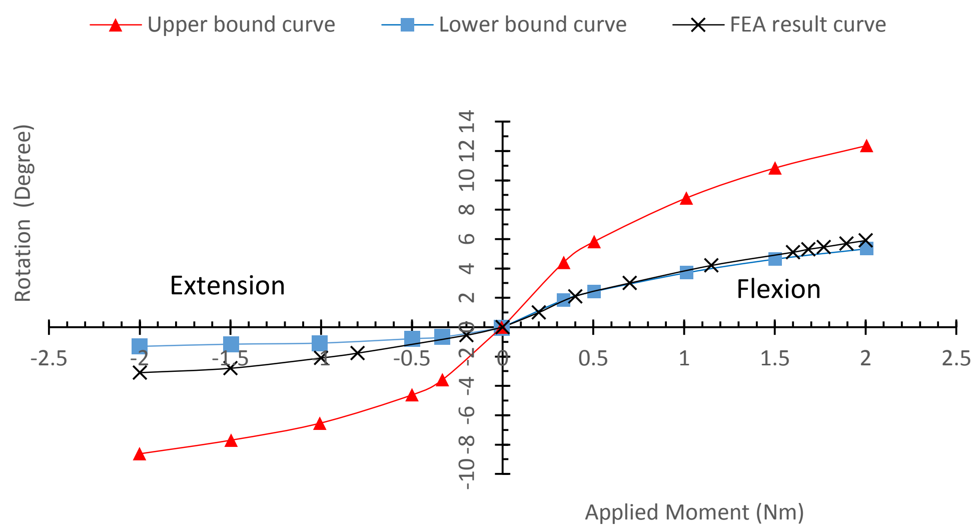

Figure 8: C2–C3 model response to flexion and extension loading compared with experimental data.

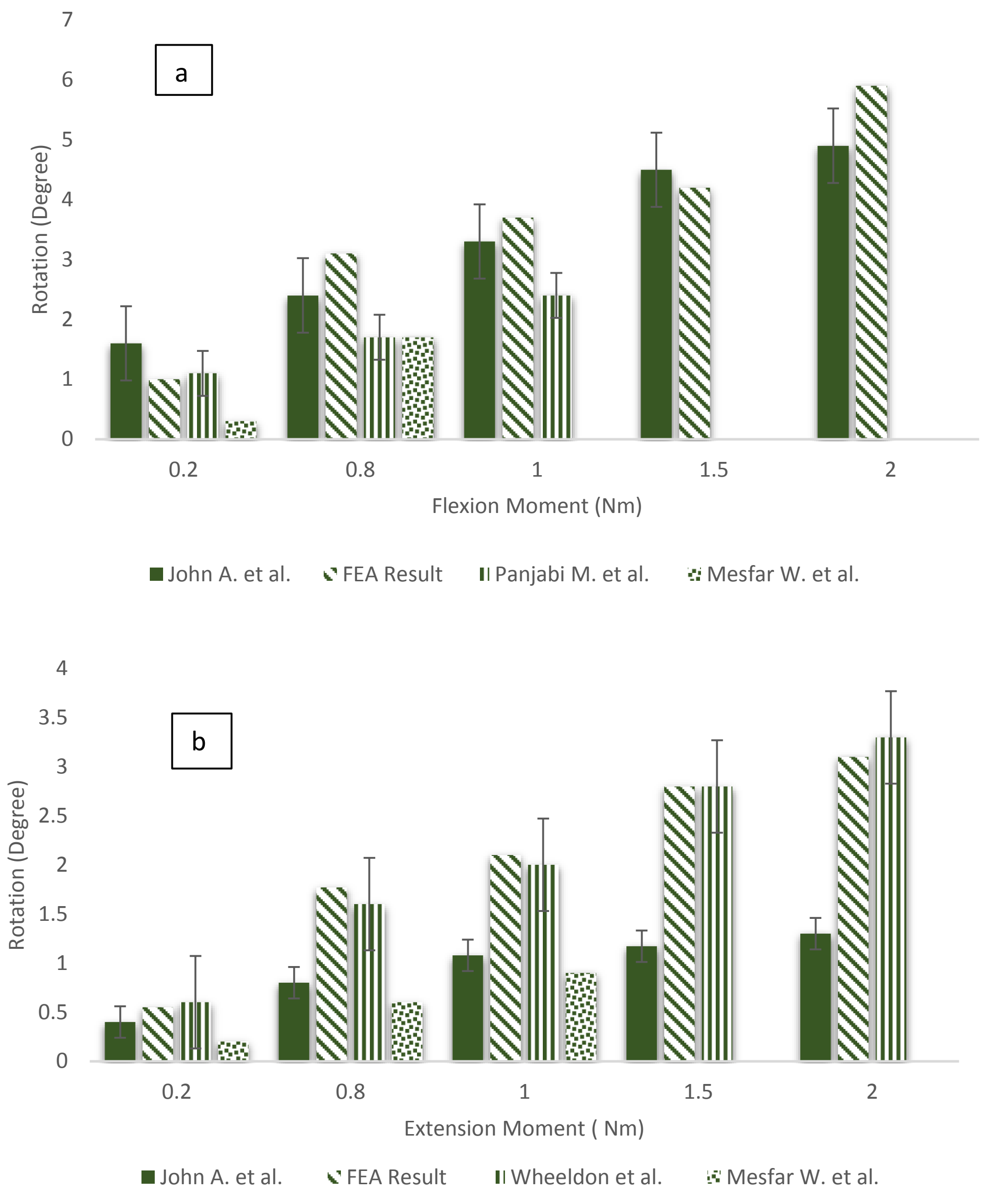

Figure 9: C2–C3 model FEA response to (a) flexion and (b) extension loading compared with other relevant studies

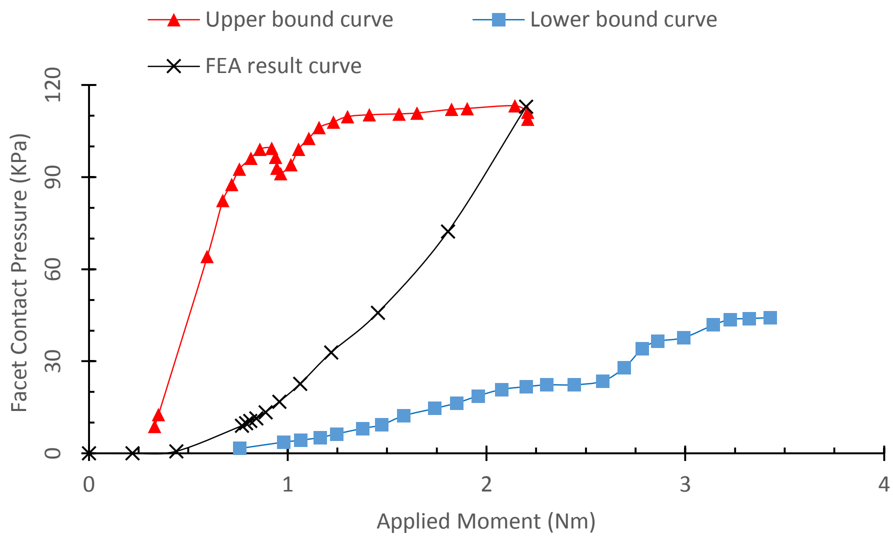

Figure 10: Right facet contact pressure in extension loading compared with experimental data.

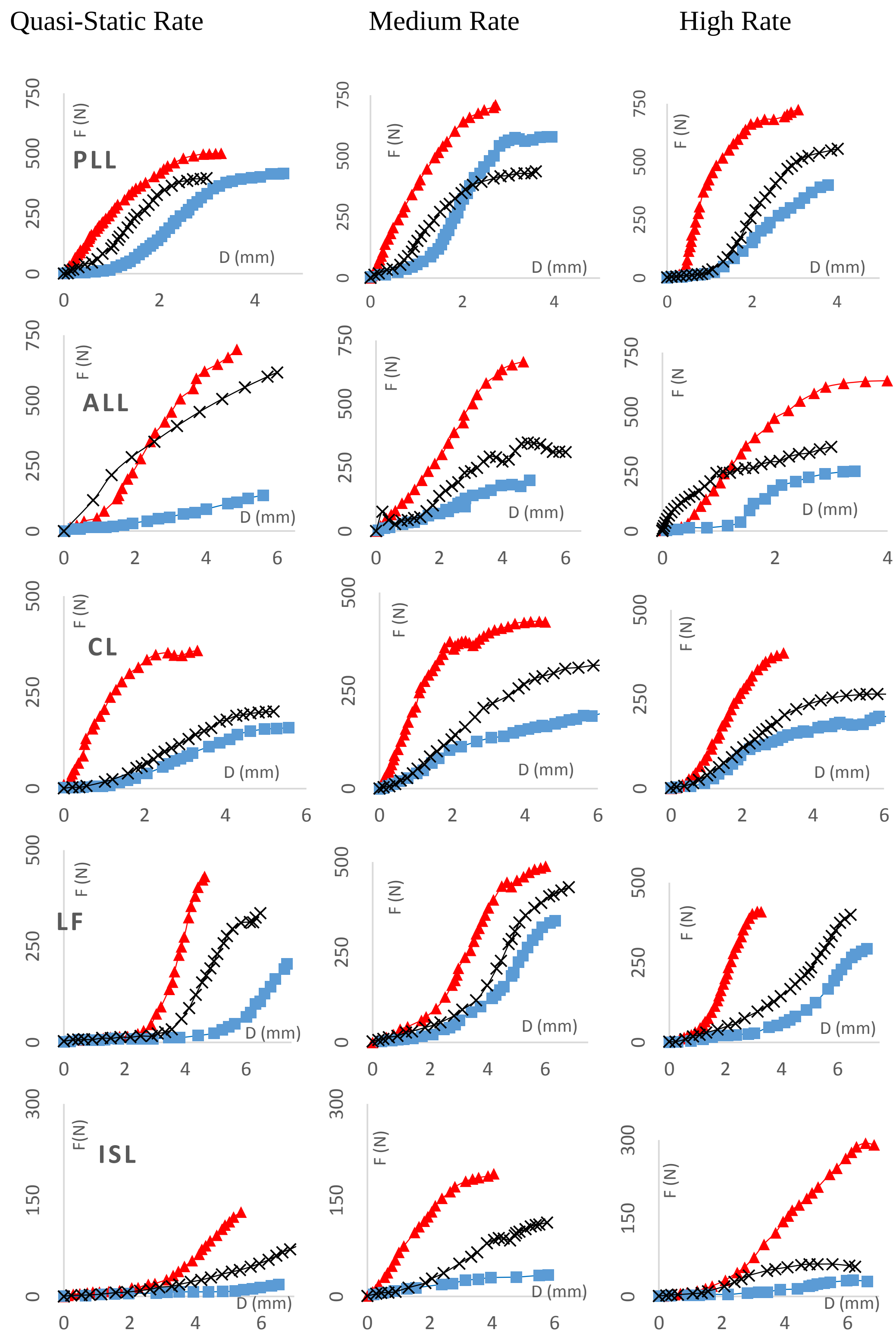

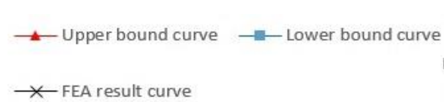

Figure 11: Ligament curves for each strain rate, shown from left: quasi-static (0.5 s−1), medium (20 s−1), and high rate (150–250 s−1).

Table 2: Ligaments test data

Ligament	*Rate*	*Failure elongation (mm)*		*Failure stress (MPa)*		*Failure strain*	
		FEM result	Experimental result	FEM result	Experimental result	FEM result	Experimental result
ALL	Quasi-static	3.30	3.97 (±1.05)	24.7	31.9 (±13.2)	1.10	1.15 (±0.49)
	Medium	3.22	3.89 (±1.49)	28.1	35.8 (±14.9)	0.87	0.93 (±0.41)
	High	3.11	3.79 (±0.98)	33.65	45.6 (±11.9)	0.78	0.90 (±0.31)
PLL	Quasi-static	2.01	2.68 (±1.06)	25.2	29.3 (±12.1)	0.68	0.76 (±0.31)
	Medium	2.13	2.87 (±0.89)	33.1	43.8 (±19.3)	0.61	0.73 (±0.21)
	High	2.06	2.78 (±0.70)	28.3	39.4 (±15.2)	0.55	0.65 (±0.20)
CL	Quasi-static	3.56	4.37 (±1.42)	2.87	3.5 (±1.2)	0.83	0.97 (±0.32)
	Medium	3.77	4.18 (±1.89)	4.43	6.0 (±2.2)	0.94	1.12 (±0.51)
	High	3.87	4.33 (±1.78)	4.65	6.1 (±1.7)	1.03	1.11 (±0.46)
LF	Quasi-static	4.54	5.61 (±1.38)	4.33	5.6 (±2.4)	0.52	0.62 (±0.12)
	Medium	4.33	4.92 (±1.53)	6.53	8.0 (±3.1)	0.47	0.58 (±0.13)
	High	4.67	4.18 (±1.50)	5.32	6.5 (±2.4)	0.58	0.52 (±0.16)
ISL	Quasi-static	5.22	6.72 (±1.91)	4.12	4.5 (±2.9)	0.61	0.65 (±0.17)
	Medium	4.15	4.70 (±1.50)	6.33	7.5 (±6.5)	0.33	0.40 (±0.12)
	High	3.89	4.64 (±1.25)	7.88	8.3 (±6.2)	0.31	0.45 (±0.12)

Loading rate investigation results

- Intervertebral disc

Disc (nucleus) exhibits more stress (0.75 MPa) than the annulus itself (0.25 MPa) at the same amount of displacement (0.3 mm) for the compression case. Also the pattern remains similar for extension and flexion but for flexion at faster rate (8 degree/ms), annulus carried more loading (1.9 MPa) than the nucleus (1.4 MPa). For compression case faster rate carries more stresses in nucleus (0.75 MPa) and annulus (0.25 MPa) comparing to the slower rate for nucleus (0.45 MPa) and annulus (0.23 MPa). Also in both flexion and extension the higher stress is noticed at the higher rates for both nucleus and annulus (Fig.12).

- Articular Facets

For contact pressure in the facets, they do not have the symmetric behaviour. So, left and right facet showed different value at the same amount of displacement for compression case and at the same amount of rotation for flexion-extension case. For compression and extension cases right facet has higher stresses than the left one. In flexion case left facet takes the higher loading (Fig.13). For the same amount of displacement (0.3 mm), faster rate produced more stress (10.3 MPa) than the slower rate (8.3 MPa) in the right facet. And for the same amount of rotation (2.5 degree), faster rate produced more stress (7.08 MPa) than the slower rate (5.89 MPa) in the right facet in case of extension whereas faster rate produced more stress (5.03 MPa) than the slower rate (1.47 MPa) in the left facet in case of flexion (Fig.13).

- Vertebral end plates

For vertebral end plate stress, in compression case, 7.44 MPa stress is obtained in the faster rate compared to the 3.51 MPa (Fig.14). In flexion the faster rate produce more stress (7.61 MPa) than the slower rate (3.74 MPa) whereas in extension the faster rate produce more stress (7.52 MPa) than the slower rate (4.55 MPa) (Fig.14).

- Ligaments

In flexion all ligaments were recruited except ALL while only ALL and CL ligaments were recruited under extension (Fig.15a). The greatest values were obtained for the CL ligaments (9.1 MPa in faster rotation comparing to 5.7 MPa in slower rotation) (Fig.15b). Also stress distribution in the ligaments for the faster rotation case has been shown in (Fig.15). It shows clearly the importance of modelling the ligaments as 2D elements to find out the stress concentration location from the ligaments.

- Spinal load-sharing

The normalized strain energy for all spinal components was plotted against displacement and rotation for compression and bending respectively (Fig. 16 and 17).

Under compression with faster rate, strain energy of cancellous bone represented 58% of the total strain energy compared to the cortical bone (33%) and disc (17.93%). An alternation in load sharing between vertebral endplate and disc occurred around 0.098 mm of displacement (Fig.16). Under compression with slower rate, strain energy of cortical bone represented 47.58% of the total strain energy compared to the disc (29%) and cancellous bone (26%) (Fig.16). There is almost no strain energy in the articular facets for both cases (Fig.16).

Under flexion with faster rate, ligaments carried a significant portion (63%) of the total strain energy compared to the disc (11.6%), cancellous bone (13.83%) and cortical bone

(8.55%) (Fig.16). An alternation in load sharing between cancellous bone and disc occurred around 1.71 degree of rotation (Fig.16). Under extension with faster rate, strain energy of ligaments represented a significant portion (50.15%) of the total strain energy compared to the disc (9.26%), cancellous bone (20%) and cortical bone (19.76%) (Fig.16). Also an alternation in load sharing between cancellous bone, cortical bone and disc occurred around 1.85 degree of rotation (Fig.16). There is almost no strain energy in the articular facets for both cases (Fig.16).

Under flexion with slower rate, ligaments carried a significant portion (54%) of the total strain energy compared to the disc (34.6%), cancellous bone (3.16%) and cortical bone (7.79%) (Fig. 16). An alternation in load sharing between ligaments and disc occurred around 0.38 degree of rotation (Fig.16). Under extension with slower rate, strain energy of ligaments represented a significant portion (58.26%) of the total strain energy compared to the disc (18%), cancellous bone (6.64%) and cortical bone (10.63%) (Fig.11). There is almost no strain energy in the articular facets for both cases (Fig.16).

From the collagen fibres strain energy curves (Fig.17), it can be seen that the trend of the load carrying pattern of the collagen fibres agree with the load carrying pattern of disc. In addition, it can be noticed that the three different layers contribute differently in load sharing mechanism, which is an important finding of this work.

Compression

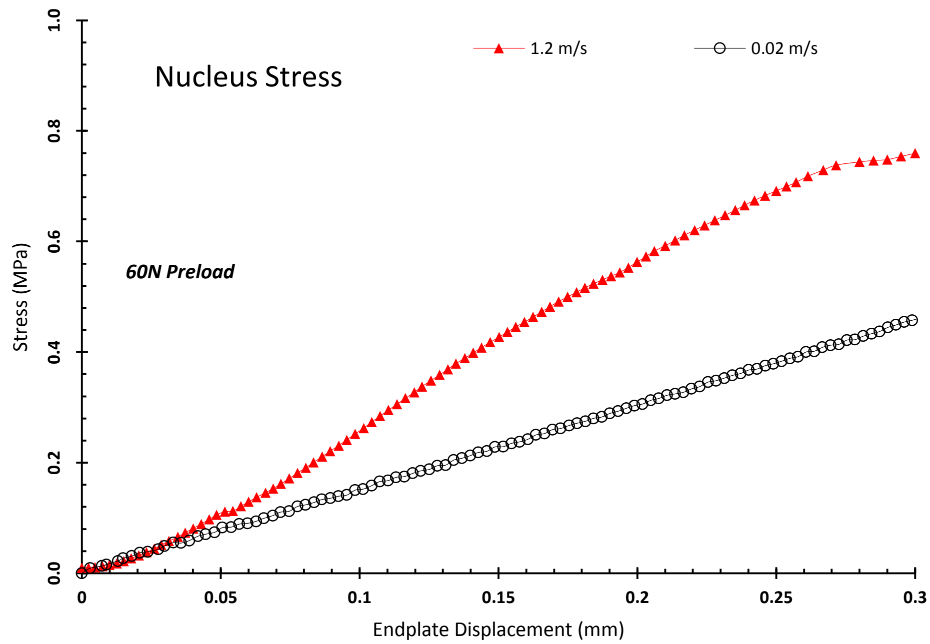

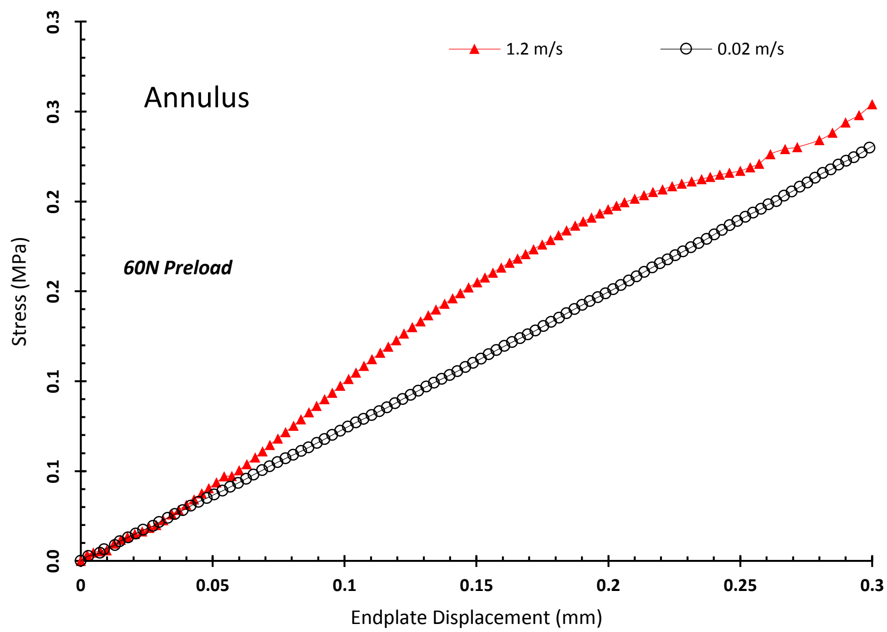

<u>Flexion and Extension</u>

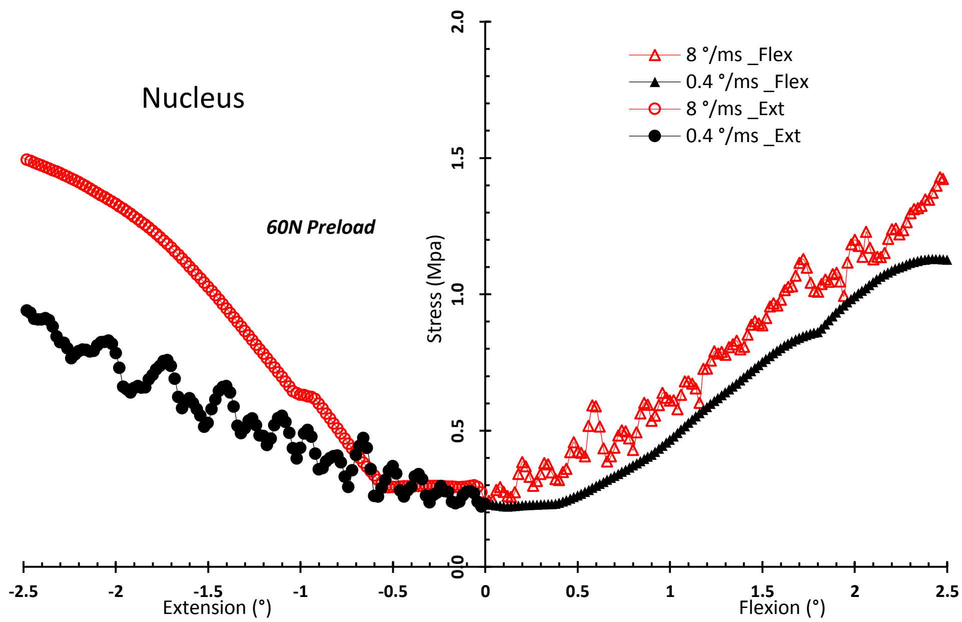

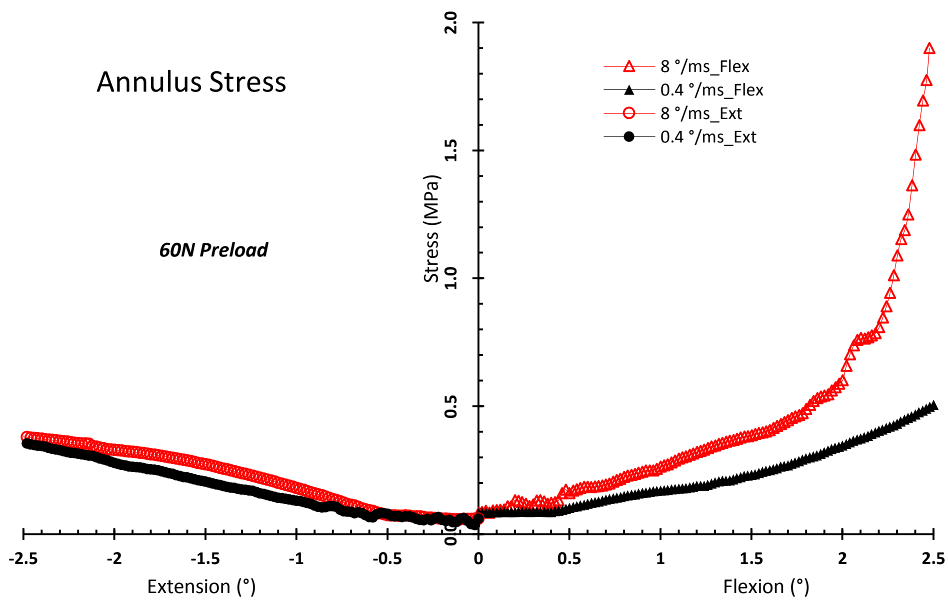

Figure 12: Disc stress and Annulus stress plotted against displacement and rotation for compression, flexion and extension rotation cases

Compression

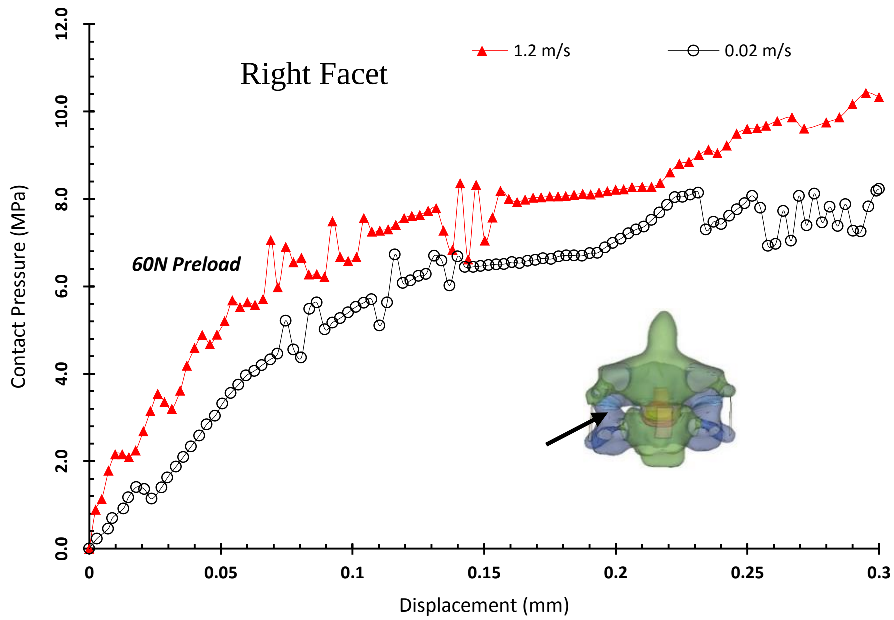

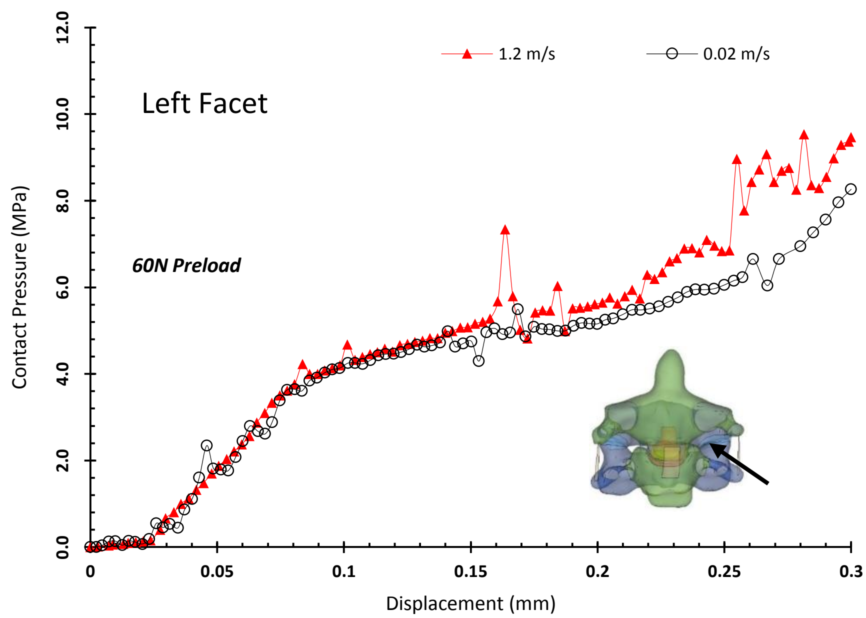

<u>Flexion and Extension</u>

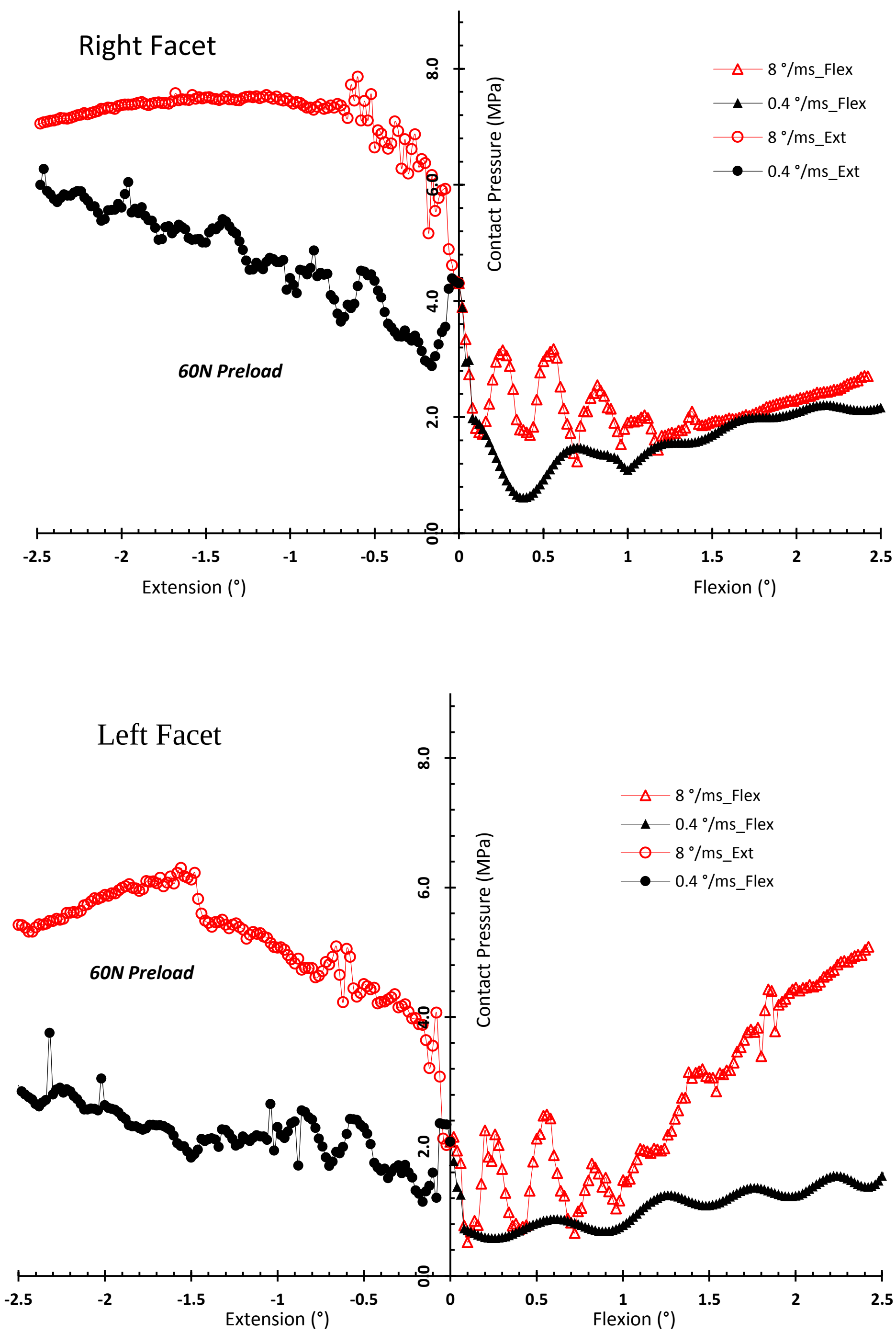

Figure 13: Contact pressure in facet joint for flexion and extension

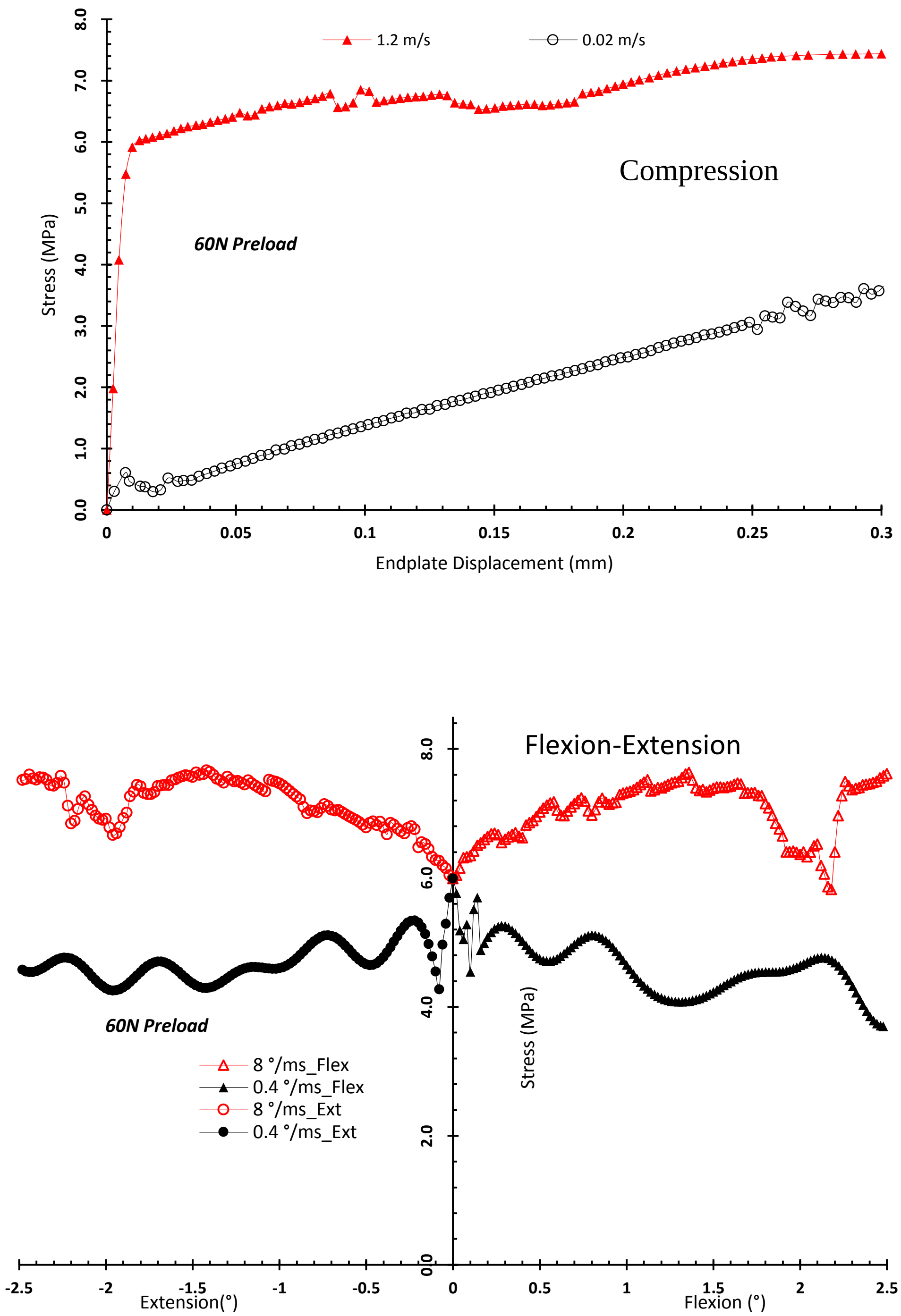

Figure 14: Stress in vertebral endplate for different loadings

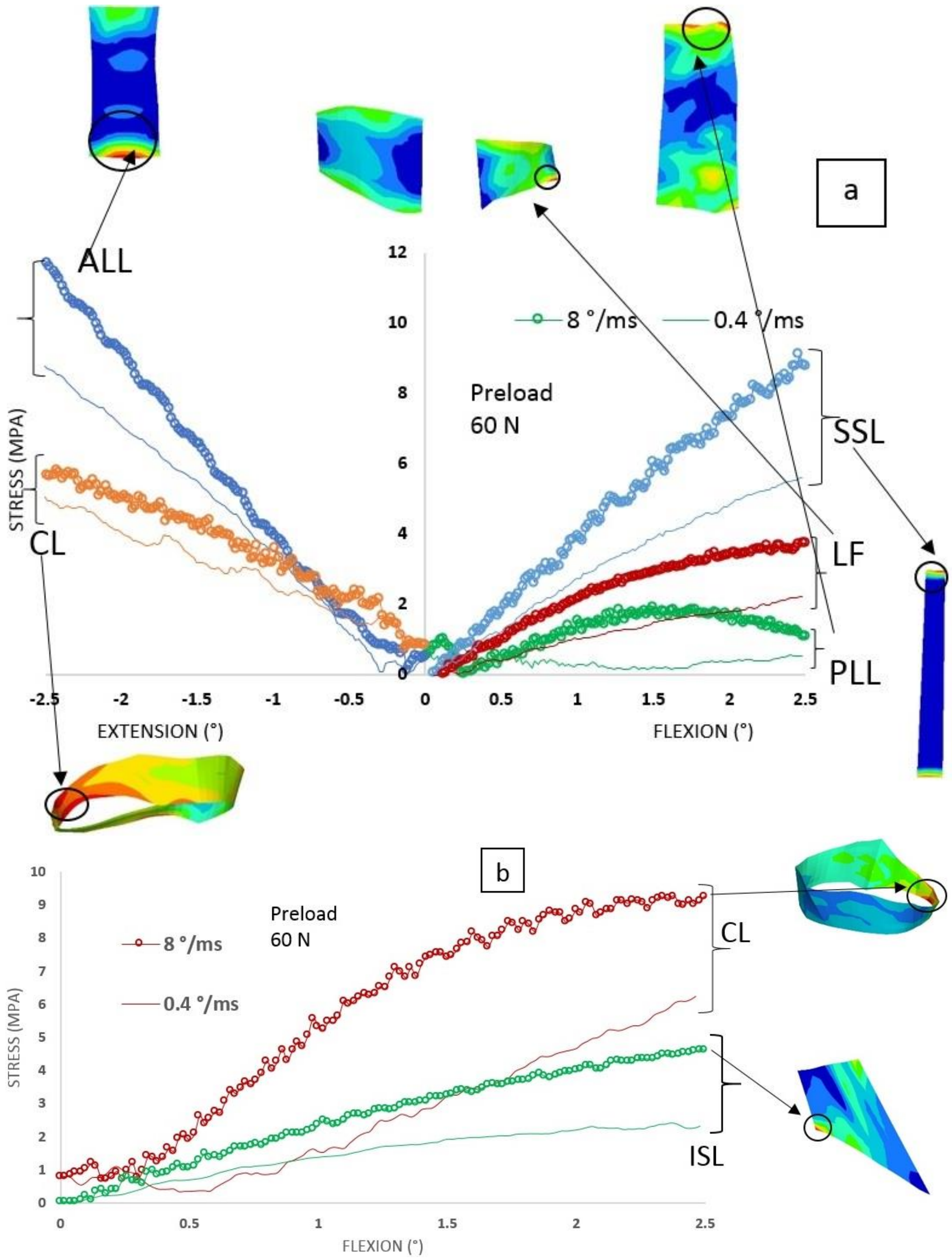

Figure 15: Ligament stresses evaluated in their fibre directions directions under flexion (right) and extension (left) at the different rates and Ligament Stress (S11) distribution under the fastest extension and flexion.

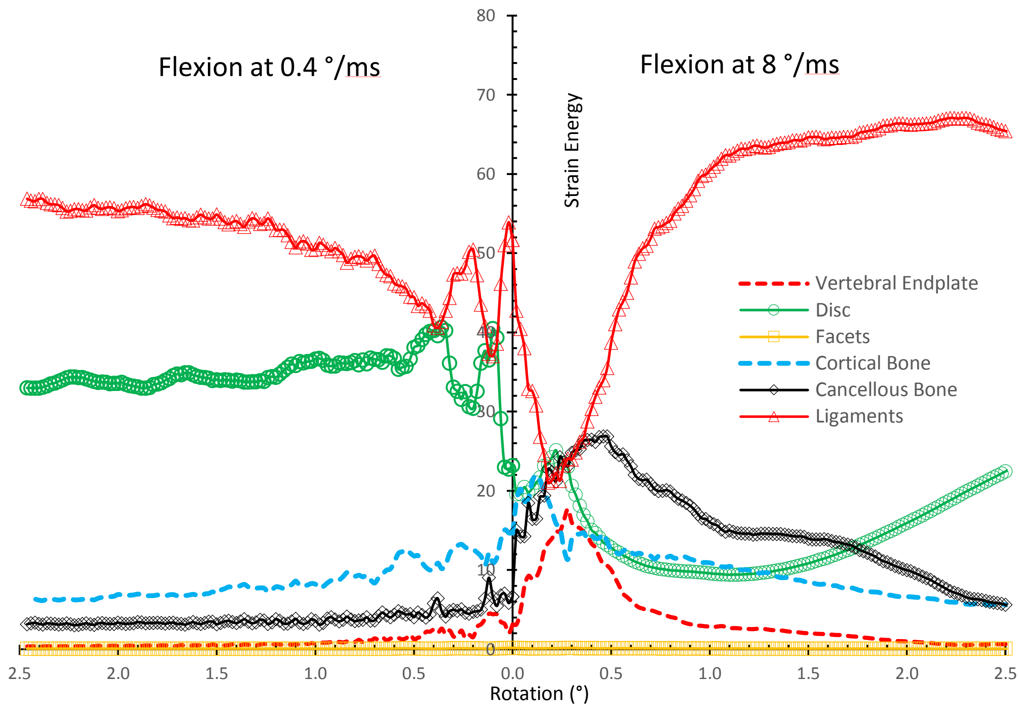
Flexion at 0.4 °/ms
Flexion at 8 °/ms
Strain Energy
Vertebral Endplate
Disc
Facets
Cortical Bone
Cancellous Bone
Ligaments
Rotation (°)
80
70
60
50
40
30
20
10
0
2.5
2.0
1.5
1.0
0.5
0.0
0.5
1.0
1.5
2.0
2.5

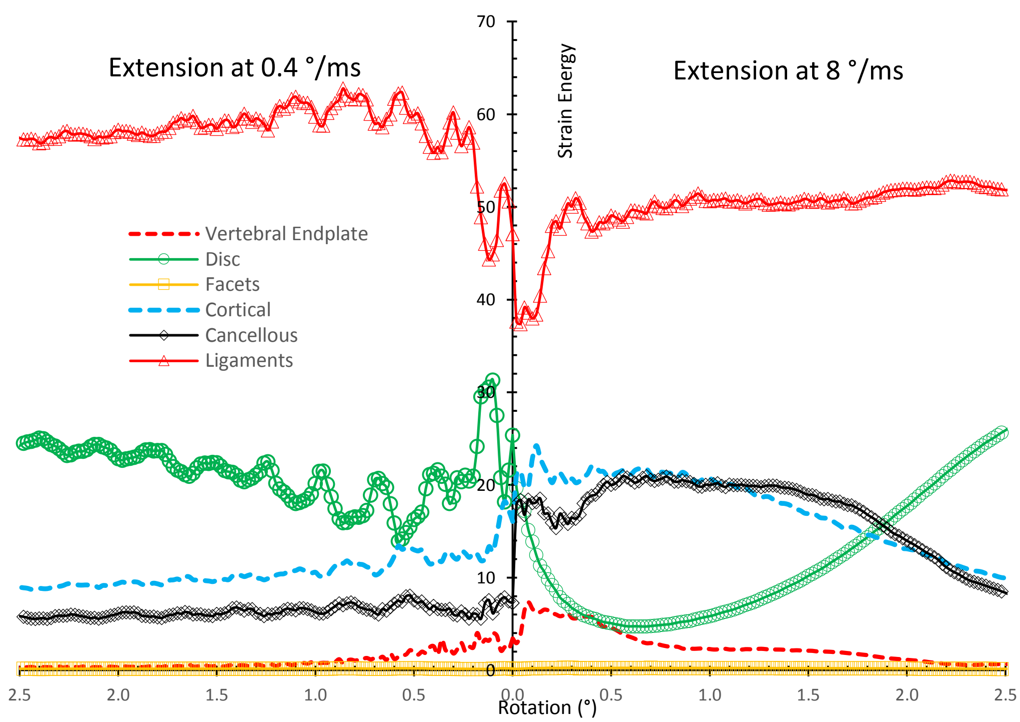
Extension at 0.4 °/ms
Extension at 8 °/ms
Strain Energy
Vertebral Endplate
Disc
Facets
Cortical
Cancellous
Ligaments
Rotation (°)
70
60
50
40
30
20
10
0
2.5
2.0
1.5
1.0
0.5
0.0
0.5
1.0
1.5
2.0
2.5

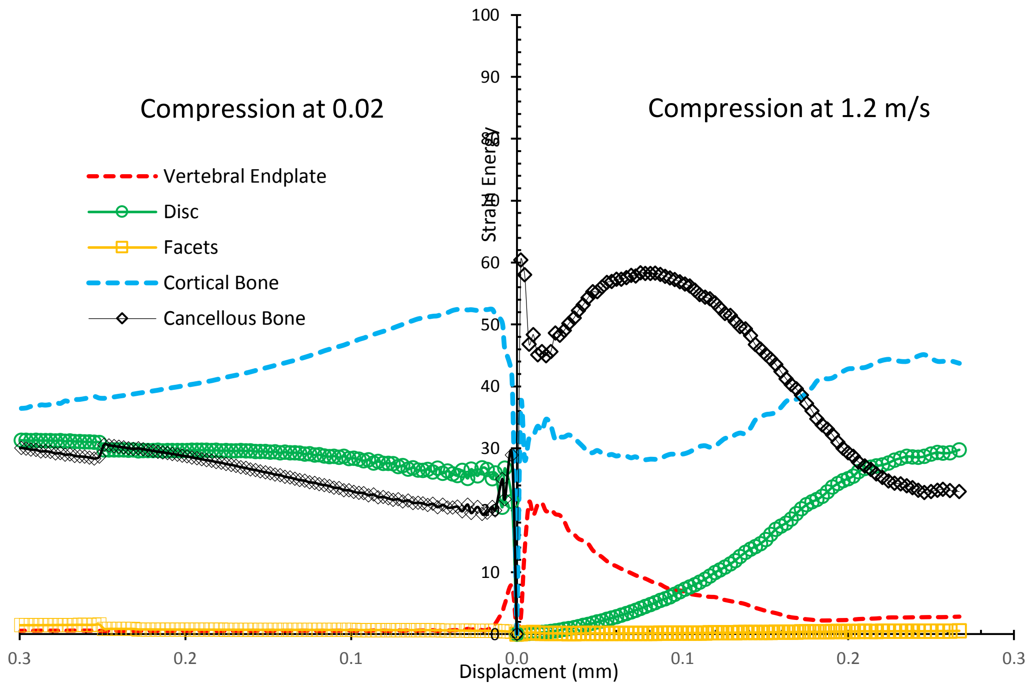

Figure 16: Strain Energy curve for all modes of loading.

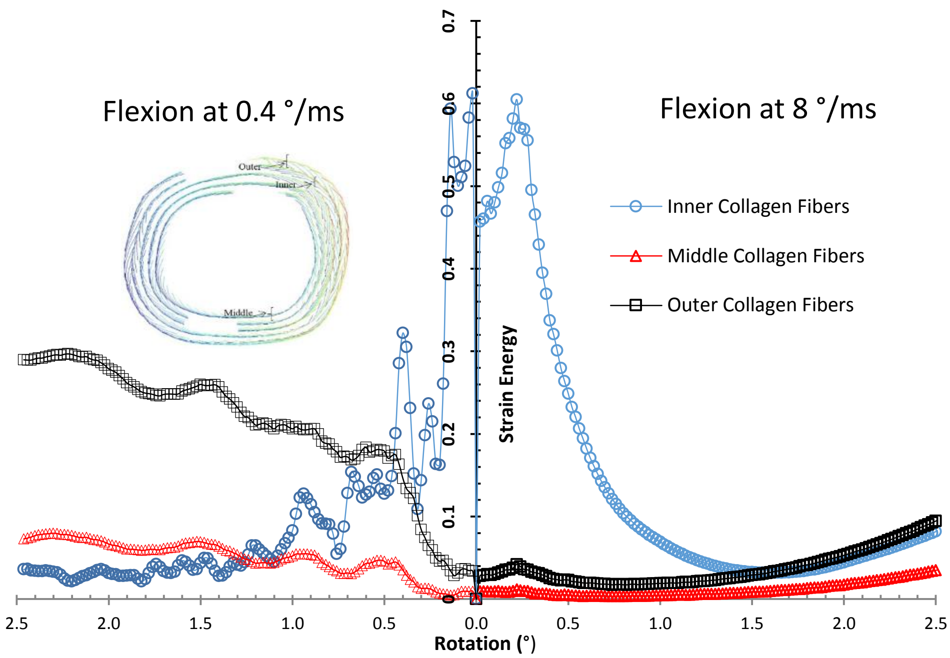

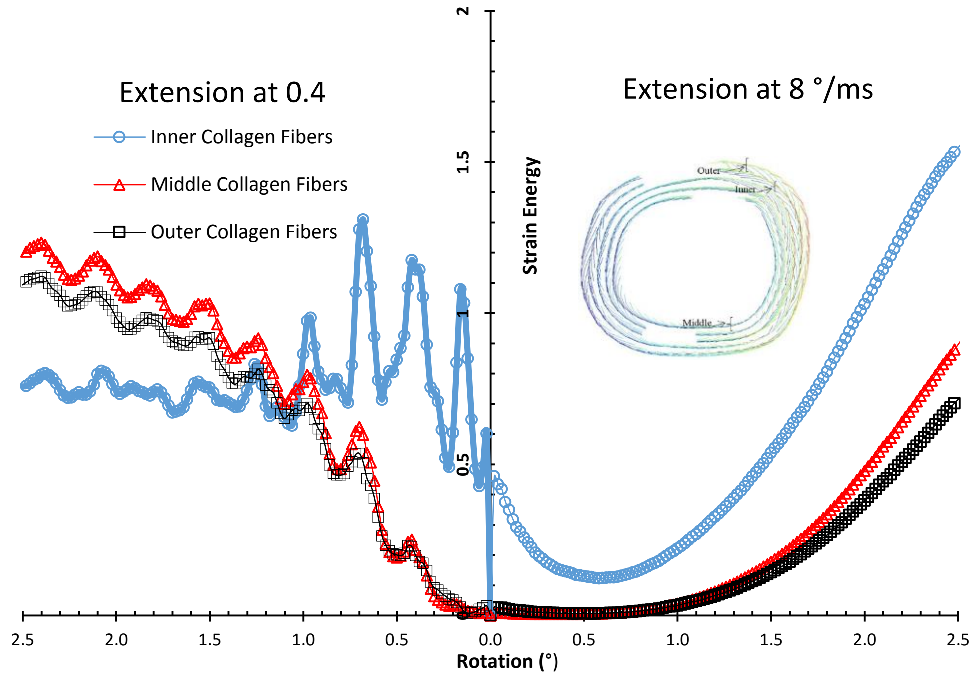

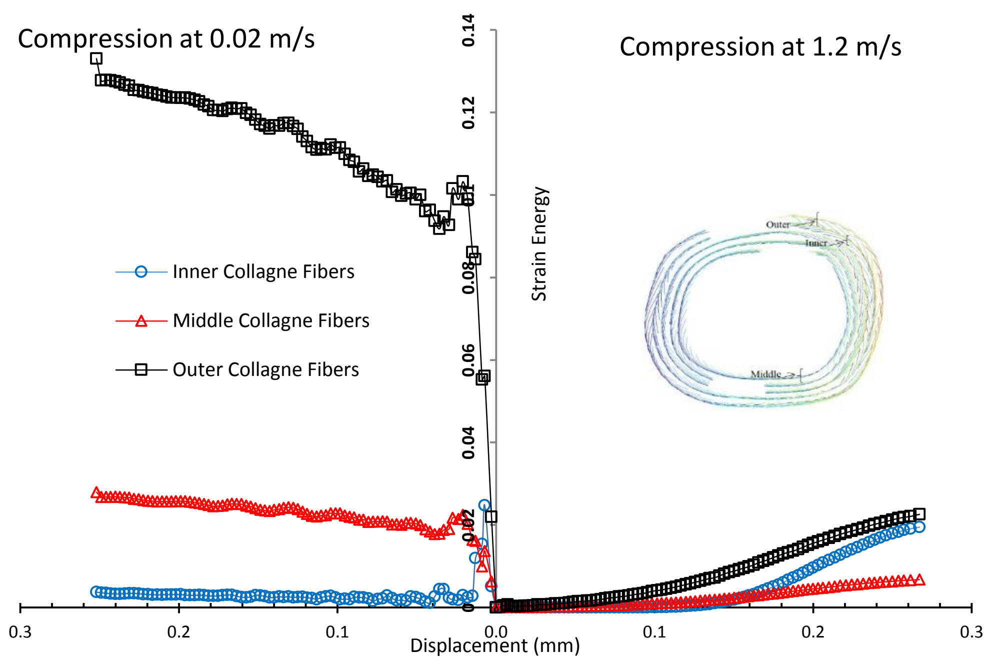

Figure 17: Strain Energy curve for the collagen fibres for all modes of loading

Discussions and Conclusions

A detailed FE model of the spinal complex structure was built, focusing on accurate geometric and material representation at the local tissue level to investigate the loading rate effects on the spinal load-sharing in dynamic loading conditions. It should be noted here that the model was not calibrated against any test conditions or data. Moreover, this C2-C3 cervical spine model has almost tripled the number of elements comparing to the existing models. Also in this model, the 2D ligaments with viscoelastic properties have been implemented which is a major contribution of this current model. The tissue material properties that have been used here were taken from a wide range of experimental studies, and were implemented using nonlinear constitutive models to create a complete cervical spine segment model, which was capable of showing rate effects in different dynamic loading conditions. Whereas many existing models have used overestimated material properties to compensate the 2D ligaments and to achieve agreeable response.

In this analysis the disc failure is not analyzed. But the maximum value of stress in the nucleus was compared with the available experimental literature data. For the compression test, the pressure in the nucleus was 0.75 MPa, which is reasonably below the 3.35 MPa peak value of the disc pressure [48] measured from the experimental compression test. For flexion case in the slower rate, the nucleus pressure was 1.12 MPa which is below the rupture value 1.18 MPa [49]. But for the faster rate the maximum value is 1.39 MPa which indicated that there is a disc rupture taken place in the model. Also for the slower extension rate the value (0.91 MPa) did not cross the peak value but for the faster rate, the maximum value was 1.47 MPa, which again indicated a disc rupture in the model [49].

The C2–C3 model has been validated against a number of in vitro studies of the cervical spine unit including different rates of loading. The structural response of the model fell within the experimental corridors for the applied load conditions including flexion and extension. In general, the predicted response of the model was within the single standard deviation response corridors for both low and high load levels. The model showed good compliance for extension loading, but there is some disparity in the flexion results. It was suggested that the differences between the datasets could be attributed due to the differences in specimen age, fixation, and resulting boundary conditions [50]. Since flexion motion relies heavily on the disc loading, variation in the disc geometry or material property may be a more significant factor in explaining the differences between the flexion results with less difference in the extension results. The compliance of the model was within the statistical corridors of the experimental results; however, the standard deviations of the experimental data were relatively large. This is attributed to high compliance in this direction for the loads considered, and the pooling of data from various regions of the cervical spine. Studies by [51] were also considered but had similarly large variations. Some of this variation may be explained by the sensitivity of the response to the load location, as predicted in this study.

Ligament failure was supported by this model. The stress was not uniformly distributed over the ligaments and was concentrated in specific region of each ligament. This confirmed the benefit of the 2D geometrical representation in ligament modeling. The implementation of viscous material properties allowed studying the ligaments under various loading rates conditions. However, the results depend on the viscous properties given in the model. Since very limited information was available on the structural behavior of cervical spinal ligaments in dynamic loading conditions, the used viscous parameters were based on the values used in [33]. At the same time, in the present model, it was assumed that any slight variation in the viscosity parameters would not significantly modify the results trends. Further improvements of the ligaments model (integration of the toe-in region, implementation of threshold data for damage and failure process in dynamic loading conditions, extended validation of the strain-rate effects according to the range of tested velocity, etc.) could be performed once experimental data will be available.

The fluid-like behavior of the nucleus was simulated according to Kumaresan et al.[33]. The fluid-flow in the disc and porous bone was not simulated since the current model studied only the immediate effect of fast movements on the load-sharing changes over the spinal structures.

The stress values and distribution in the different ligaments depended on their stiffness and orientation with respect to the center of rotation [52]. Stress was mostly concentrated in the attachment regions of ligaments to the bone that may lead to ligaments tear. For flexion loading the most posterior ligaments, SSL and ISL give the greater stress value and for extension case the most superior ligament, ALL gives the greater stress which is reasonable from the geometric point of view. This study investigated sagittal symmetric movements and did not consider neuromuscular responses, which may underestimate the effect on the load-sharing changes over the spinal components.

For all the modes of loading conditions, internal energy of the components of the cervical unit has been analyzed (Fig.16). For all modes of sagittal loading considered, for both rates, ligaments were the primary load-bearing structure in the segment. At higher levels of each loading, the ligaments carried most of the load. This is an important finding given that most hyperflexion soft tissue injuries occur in the disc and posterior ligaments [53]. In flexion case, for the slower rate the disc is the second most load carrier in the segment; whereas for the faster rate, at the beginning of loading the vertebral endplate takes more loading than the disc and with higher degree of loading the behavior alters. For the extension case, the cortical and cancellous bone proved to be the second most load bearer among other components. For slower rate the load sharing of these two components remain same along loading but for the faster rate the load sharing pattern alters with time. For the compression case, the loading pattern stays the same as extension case. These results are the most significant findings of this study. These results provide insight into cervical spine behavior as the distribution of load within the cervical spine has not yet been measured experimentally. In Goel et al. [23], reported similar conclusions with a C5–C6 FE model that included compressive preload; however, they did not report the load in the ligaments during flexion. In general, the segment model described in this study provides good prediction of response over a wide range of loads and different modes of loading. It should be noted that this model was developed for dynamic loading at non-injurious levels.

Future work will address more complex types of loading such as combined rotations and translations that could potentially lead to more severe injuries resulting from early contact between bone components and to an amplified strain level on ligaments.

Acknowledgements

This study was supported by Department of National Defense, Directorate of Technical Airworthiness and Engineering Support (DTAES 6) and Surgeon General's Health Research Program (SGHRP). Also some of the valuable data about the processing of the model has been received from the Royal Military College of Canada. Natural Sciences and Engineering Research Council of Canada (NSERC) (engage) grants supported partially this study as well.

References

[1] A. B. T. B. I. G. P. Roberston, "Spinal Injury Patterns Resulting from Car and Motorcycle Accidents.," *Spine, 27,* vol. 24, pp. 2825-2830., 2002.

[2] D. M. D. M. P. R. Jackson AB, "A demographic profile of traumatic spinal cord injuries: change and sustainability over 30 years," *Arch Phys Med Rehabil,* vol. 85, pp. 1740-1748, 2004.

[3] S. A. B. R. S. P. S. M. Prasad VS, "Characteristics of injuries to the cervical spine and spinal cord in a polyttrauma patient poluation: experience from a regional trauma unit.," *Spinal Cord,* vol. 37, pp. 560-568, 1999.

[4] M. Panzer, *Numerical modelling of the human cervical spine in frontal impact,* Waterloo: University of Waterloo., 2006.

[5] N. Yoganandan, "Finite element applications in cervical spine modeling," *Spine (15),* vol. 21, p. 1824–1834, 1996.

[6] J. C. D. P. M. FICE, "Cervical Spine Model To Predict Capsular Ligament Response In Rear Impact.," *Annals of Biomedical Engineering, ,* vol. 39 (8), pp. 2152-2162, 2011.

[7] M. J. C. N. C. D. Mattucci SF, "Strain rate dependent properties of younger human cervical spine ligaments," *Journal of Mechanical Behaviour & Biomedical Materials,* vol. 10, pp. 216-26, 2012.

[8] S. Kumaresan, "Finite element modeling of cervical laminectomy with graded facetectomy.," *Journal of Spinal Disorders ,* Vols. 10(1),, p. 40–46., 1997.

[9] H. Ng, "Nonlinear finite-element analysis of the lower cervical spine (C4–C6) under axial loading," *Journal of Spinal Disorders ,* vol. 14(3), p. 201–210., 2001.

[10] H. Ng, "Statistical factorial analysis on the material property sensitivity of the mechanical response of the C4–C6 under compression,anterior and posterior shear.," *JournalofBiomechanics,* Vols. 37,, p. 771–777., 2004..

[11] P. Halldin, "Investigation of conditions that affect neck compression-flexion injuries using numerical techniques," 2000.

[12] F. Meyer, "Human neck finite element model development and validation against original experimental data," 2004.

[13] L. J. L. V. Shim V.P.W., "A Technique for Dynamic Tensile Testing of Human Cervical Spine Ligaments," *Exper Mechanics,,* vol. 46, p. 77–89, 2006.

[14] P. F. B. J. R. J. S. A. ,. L. S. Yoganandan N., "Dynamic response of human cervical spine ligaments.," *Spine,* vol. 14, p. 1102–10, 1989.

[15] A. M. C. D. S. M. Kemper, "The Influence of Strain Rate on the Compressive Stiffness Properties of Human Lumbar Intervertebral Discs.," *Biomed. Sci. Instrum,* vol. 43, p. 176–181, 2007.

[16] S. K. A. M. D. B. P. M. F. DUMA, "Biomechanical Response of the Lumbar Spine in Dynamic Compression," *Biomed. Sci. Instrum, ,* vol. 42, p. 476–481, 2006.

[17] O. M. D. T. M. L. F. Izambert, "Dynamic stiffness and damping of human intervertebral disc using axial oscillatory displacement under a free mass system," *European spine journal,* vol. 12(6), pp. 562-6, 2003.

[18] N. C. D. C. Jeff Barker, "High rate behaviour of the cervical spine segments," 2012.

[19] D. Matthew B.Panzer, "C4–C5 segment finite element model development,validation,and load-sharing investigation," *Journal of Biomechanics,* vol. 42, p. 480–490, 2009.

[20] Y. Fung, "Mechanical Properties of Living Tissue,seconded.," *Biomechanics,Springer,NewYork*, 1993.

[21] M. K. J. De Jager, "Mathematical head-neck models for acceleration impacts," PhD. Thesis, Technical University of Eindhoven., 1996.

[22] M. J. van der Horst, "Human head neck response in frontal, lateral and rear end impact loading: modelling and validation.," PhD. Thesis, Technical University of Eindhoven., 2002.

[23] V. Goel, "Prediction of load sharing among spinal components of a C5–C6 motion segment using the finite element approach," *Spine (6),* vol. 23, p. 684–691, 1998.

[24] S. Y. N. a. P. F. A. Kumaresan, "Finite element modeling approaches of human cervical spine facet joint capsule.," *Journal of Biomechanics* , vol. 31, pp. 371-376., 1998.

[25] N. L. F. a. S. W. Maurel, "A three-dimensional parameterized finite element model of the lower cervical spine. Study of the influence of the posterior articular facets," *Journal of Biomechanics,* vol. 30, pp. 921-931, 1997.

[26] J. Pooni, "Comparison of the structure of human intervertebral discs in the cervical,thoracic and lumbar regions of the spine.," *Surgical and Radiologic Anatomy,* vol. 8, p. 175–182., 1986..

[27] H. K. A. H. F. S. U. C. L. W. H. Schmidt, "Intradiscal pressure, shear strain, and fiber strain in the intervertebral disc under combined loading," *Spine* , vol. 32, p. 748–755., 2007.

[28] A. P. W. E. A. C. Garo A, "Calibration of the mechanical properties in a finite element model of a lumbar vertebra under dynamic compression up to failure," *Med Biol Eng Comput* , vol. 49, p. 1371–1379, 2011.

[29] M. A. P. J. W. E. B. C. a. A. C. E. El-Rich, "Finite Element Investigation of the Loading Rate Effect on the Spinal Load- Sharing Changes under Impact Conditions," *J. Biomech.,* , vol. 42, no. 9, p. 1252–1262., 2009.

[30] K. Yang, "Compressibility measurement of human intervertebral nucleus pulposus," *Journal of Biomechanics* , vol. 21, p. 865, 1988.

[31] A. A. A. S. S. Shirazi-Adl, "Mechanical response of a lumbar motion segment in axial torque alone and combined with compression," *Spine,* vol. 11, p. 914–927, 1986.

[32] A. C. G. A. E.-R. M. A. P. Wagnac E, "Calibration of hyperelastic material properties of the human lumbar intervertebral disc under fast dynamic compressive loads.," *J Biomech Eng* , vol. 133, 2011.

[33] S. Kumaresan, "Finite element modeling of the cervical spine:role of intervertebral disc under axial and eccentric loads," *Medical Engineering and Physics* , vol. 21, p. 689–700., 1999.

[34] C. K. Y. L. C. H. Y. J. J. G. V. Lee, "Impact response of the intervertebral disc in a finite-element model," *Spine* , vol. 25, p. 2431–2439, 2000.

[35] D. Reilly, "The elastic modulus for bone," *Journal of Biomechanics,* vol. 7, p. 271–275., 1974..

[36] P.-J. A. E. W. C. B. C.-E. A. Marwan El-Rich, "Finite element investigation of the loading rate effect on the spinal load-sharing changes under impact conditions," *Journal of Biomechanics* , vol. 42 , p. 1252–1262, 2009.

[37] D. S. C. Jennifer A. DeWit, "Cervical spine segment finite element model for traumatic injury prediction," *Journal of Mechanical Behaviour of Biomedical Materials,* vol. 10, pp. 138-150, 2012.

[38] D. K. T. Kopperdahl, "Yield strain behavior of trabecular bone," *Journal of Biomechanics* , vol. 31, p. 601–608, 1998.

[39] R. T. A. C. R. Ochia, "Effect of loading rate on endplate and vertebral body strength in human lumbar vertebrae.," *Journal of Biomechanics,* vol. 36, p. 1875–1881, 2003.

[40] Y. N. P. F. Kumaresan S, "Finite element analysis of the cervical spine: a material property sensitivity study," *Clinical Biomechanics,* vol. 14, no. 1, pp. 41-53, 1999.

[41] P. F. K. S. Y. N. Wheeldon JA, "Experimental flexion/extension data corridors for validation of finite element models of the young, normal cervical spine.," *J Biomech. (2),* vol. 39, pp. 375-80. , 2006.

[42] B. J. W. C. G. B. W. W. W. B. Jaumard NV, "Contact pressure in the facet joint during sagittal bending of the cadaveric cervical spine.," *J Biomech Eng. ,* vol. 133, no. 7, 2011.

[43] S. Hedenstierna, "3D Finite Element Modeling of Cervical Musculature and its Effect on Neck Injury Prevention," 2008.

[44] A. e. a. Patwardhan, *J. of Spine ,* vol. 25, no. 12, pp. 1548-54, 2000.

[45] M. S. P. V. F. S.-. w. W. Panjabi, "Three-dimensional load–displacement curves due to forces on the cervical spine," *Journal of Orthopaedic Research* , vol. 4, p. 152–161., 1986.

[46] S. A. J. P. F. M. D. R. J. C. J. L. S. Yoganandan N, "Injury Biomechanics of the Human Cervical Column," *Spine (Phila Pa 1976),* vol. 15, no. 10, pp. 1031-9., 1990 Oct.

[47] P. F. S. A. J. R. J. L. S. Yoganandan N, "Strength and kinematic response of dynamic cervical spine injuries.," *Spine (Phila Pa 1976),* vol. 16, no. 10, pp. 511-7., 1991 Oct.

[48] G. D. L.-P. N. P.A. Cripton, "A minimally disruptive technique for measuring intervertebral disc pressure in vitro: application to the cervical spine," *Journal of Biomechanics* , vol. 34, p. 545–549, 2001.

[49] M. ,. W. H. ,. M. ,. N. H. ,. M. ,. H. U. ,. M. ,. G. I. J. ,. M. P. C. M. ,. M. ,. P. J. T. ,. M. ,. a. B. W. C. ,. M. Ryan M. Kretzer, "Adjacent-Level Range of Motion and Intradiscal Pressure After Posterior Cervical Decompression and Fixation," *SPINE* , vol. 37, no. 13, p. pp E778–E785, 2012.

[50] R. B. Nightingale, "Flexion and extension structural properties and strengths for male cervical spine segments," *Journal of Biomechanics (3),* vol. 40, p. 535–542., 2007.

[51] M. K. Mesfar W., "The Influence of head weight on the biomechanical response of the cervical spine under applied moments," 2011.

[52] M. G. V. T. K. Panjabi, "Physiologic strains in the lumbar spinal ligaments. An in vitro biomechanical study.," *Spine* , vol. 7, p. 192–203., 1982.

[53] R. Crowell, "Cervical injuries under flexion and compression loading," *Journal of Spinal Disorders (2)*, vol. 6, p. 175–181., 1993.

Chapter 3:
Investigation of the Injury Mechanisms of the Ligamentous Cervical Spine Unit under Combined Complex Loading

A Journal Paper will be submitted to the Clinical Biomechanics:

This paper is enclosed in this chapter next as **Paper II**

Paper II

Investigation of the Injury Mechanisms of the Ligamentous Cervical Spine Unit under Combined Complex Loading

Tanvir Mustafy[a], Kodjo Moglo[b] and Marwan El-Rich[a]

[a]*Department of Civil and Environmental Engineering, University of Alberta, Canada;*
[b]*Department of Mechanical & Aerospace Engineering, Royal Military College of Canada*

Corresponding Author:

Marwan El-Rich
Department of Civil and Environmental Engineering
Markin/CNRL Natural Resources Engineering Facility
9105 116th St
Edmonton, Alberta, Canada
T6G 2W2

Phone: 1(780) 492-6678
Email: elrich@ualberta.ca

Abstract

Neck injuries are very acute types of injuries and they can cause devastating if not life threatening consequences. Cervical spine injury is a common cause of mortality and morbidity in young adults. Predicting cervical spine response in major/minor injury resulting from vehicular accidents is essential to improve our understanding of the injury mechanism and occupant protection. In the current study, a bio-realistic finite element model (FEM) of the ligamentous cervical spine segment C2-C3 has been used for the evaluation of global kinematics and tissue-level response. The objective of this study was to use the segment for predicting tissue-level failure under six combined complex loading conditions: flexion-distraction/compression, extension-distraction/compression, lateral bending-distraction and axial rotation-distraction which could take place in vehicle impact conditions. The predicted failure locations were in agreement with the reported cervical spine injuries for different modes of loading. C2 vertebral endplate ruptured almost in every loading case, and ligaments failure stresses were reached in the Intertransverse ligaments (IL) and Capsular ligaments (CL). Facets were ruptured and cancellous bone near facet joints reached failure stress limit in case of extension, axial rotation and lateral bending scenarios. This study showed that under almost all loading conditions, ligaments were the primary load-bearing structure in the segment except for flexion-compression case where cancellous bone carried a major portion (70%) of the total loading. From the injury assessment results it reveals that the lateral bending-distraction case can be considered as the most critical loading scenario where major number of components failed during the load application.

Keywords: combined-complex loading; cervical spine; injury; bone fracture; ligament tear; finite-element analysis

Introduction

Cervical spine injury resulting from high impact loading is a well-known problem. The cervical spine remains to be the major location for serious motor vehicular accidental injuries. An estimation of 40 % to 65 % of all spine-related injuries are caused by motor vehicle accidents, where cervical spine being the major injury site [1]. Hence again, a frequent rate of occurrence of minor injuries to the cervical spine in rear impact vehicular accidents (commonly known as whiplash) can eventually leave a victim with long-term pain and disability [1]. Finite element (FE) models are often used to assess the injury potential of occupants during motor vehicle collisions. FE models of cervical motion segments were developed for investigating load distribution among cervical segments and biomechanical secondary effects to impact; [2], [3], [4], [5], [6], [7]. The former mentioned cervical models used linear elastic materials. A detailed model of C4-C6 segment developed by Kumaresan et al. [8] has been considered the first model which accounted for the anisotropic behavior of the disc. Non-linear spring elements were used for modelling the ligaments. Validation was assessed in quasi-static flexion, compression and torsion. In a parametric study of the material properties of the lower cervical spine [9] separately varied the different properties of the cervical tissues. [10] used non-linear material properties for the ligaments in an FE model of the C5-C6 complex. Also to investigate the fracture fixation methods in cervical segment several studies were done in past, [11], [12], [13], [14], [15], [16]. Unlike individual loading applications, there is a paucity of biomechanical data on the human cervical spine under combined complex loading. A work of combined tension-extension has been done by [17]. Tensile loading has been reported to cause occipitoatlantal dislocation, Hangman's fracture, anterior longitudinal ligamentous rupture, disc rupture, horizontal fracture of the vertebral body, teardrop fracture, bilateral facet dislocation, and unilateral facet dislocation [17]. This study investigated the neck injury criterion by imposing combined axial tension and bending to postmortem human subject ligamentous cervical spines. Another study [18] has been conducted on combined bending and axial loading scenario. It investigated the lateral, anterior and posterior passive bending responses of the cervical spine [18]. Still there remains lack of data about the injury propagation and response of the soft tissue in case of the combined loading. In order to improve our understanding of cervical spine injuries under impact complex loads, a ligamentous segment of the cervical spine has been used to investigate the injury mechanism, load sharing and failure propagation in six different major injury conditions [19]. To accomplish the objectives of this research, a segmental unit C2-C3 of ligamentous cervical spine has been used which has already been developed and validated against numerous dynamic loading scenarios. This model is developed considering a detailed geometrical representation of tissue level components and material laws that include the progressive failure of ligaments, onset of bone fracture and element deletion procedure based on critical plastic strain failure for bone and failure strain and stress for ligaments.

Materials and methods

- Geometric modeling and meshing

Using the CT scan and MRI images of a 39 year old male, a finite element (FE) model of C2-C3 spinal unit has been developed. The bony structures (cervical vertebrae (C2-C3)) were contructed using the CT scan images and with the aid of Mimics software. The intervertebral disc geometry was contructed using the MRI images for better accuracy. The meshing of different segments were completed using the Hypermesh software. Ligaments were constructed based on the insertion points in the bone and were meshed using Hypermesh software. The ligaments were modelled as 2D elements. The bony structures were modelled using the 3-nodes shell elements and the cancellous bone was modelled using the 4-nodes solid elements. The intervertebral disc has been created based on the MRI images and it was subdivided into annulus fibrosus and nucleus pulposus with a proportion (56 % annulus and 44 % nucleus) according to the histological findings [21]. The annulus was modelled with 8 nodes solid elements and was reinforced with the non-linear collagen fibers. The collagen fibers are modelled with the nonlinear elastic property from the literature [22].

- Material constitutive laws

The bony structures comprising the cortical, cancellous bone and vertebral endplates were modelled following the symmetric and strain rate-dependent elasto-plastic material law (Johnson–Cook) (Table 1a). The equivalent stress at constant temperature during the onset of plastic deformation was defined by the following equation:

$$\sigma = (a + b\varepsilon_p^n) * \left\{1 + \ln\left(\frac{\dot{\varepsilon}}{\dot{\varepsilon}_0}\right)\right\}, \text{[24]}$$

The nucleus is modelled as fluid cavity structure [25]. A common reference node is shared by the other hydrostatic fluid elements which are used to model the nucleus. Nucleus pulposus was modelled as an incompressible body. And hydrostatic fluid elements are used to fill the cavity which cover the nucleus boundary and also share common nodes between cavity and standard elements of annulus fibrosus.

Hyper-elastic material law has been used to model the annulus fibrosus. This law was based on a first-order Mooney–Rivlin formulation. The formulation used by this law for strain energy function is given below,

$$W = C_{10}(I_1 - 3) + C_{01}(I_2 - 3) + \frac{(J-1)^2}{d}, \text{[24]}$$

$$K = 6(C_{10} + C_{01}) / 3(1 - 2\upsilon), \text{[24]}$$

Maximum failure strain and failure stress were used to model the ligaments. This method ensures the progressive failure scenario in ligaments. The ligaments are modelled based on the visco-elastic (Time dependent Prony Series) material laws. [9] (Table 1c). The formulation for the relaxation modulus of this material is given below,

$$G(t) = G_\infty + \sum_{i=1}^{N} G_i e^{-t/t_i},$$

There is a non-uniformity in the mesh pattern between the disc and the vertebral endplate. To mitigate this difference a tied contact has been used between the two components. The model experienced large deformations and to avoid any penetrations, frictionless contact interfaces were assumed between diverse parts. For the measurement of contact force in the facets, surface to surface contact interfaces were implemented. All simulations were performed using the explicit dynamic finite-element solver Abaqus (Version 6.12). The material properties used for the C2-C3 complete cervical segment were taken from the available material properties at the tissue level from different literatures (Table 1).

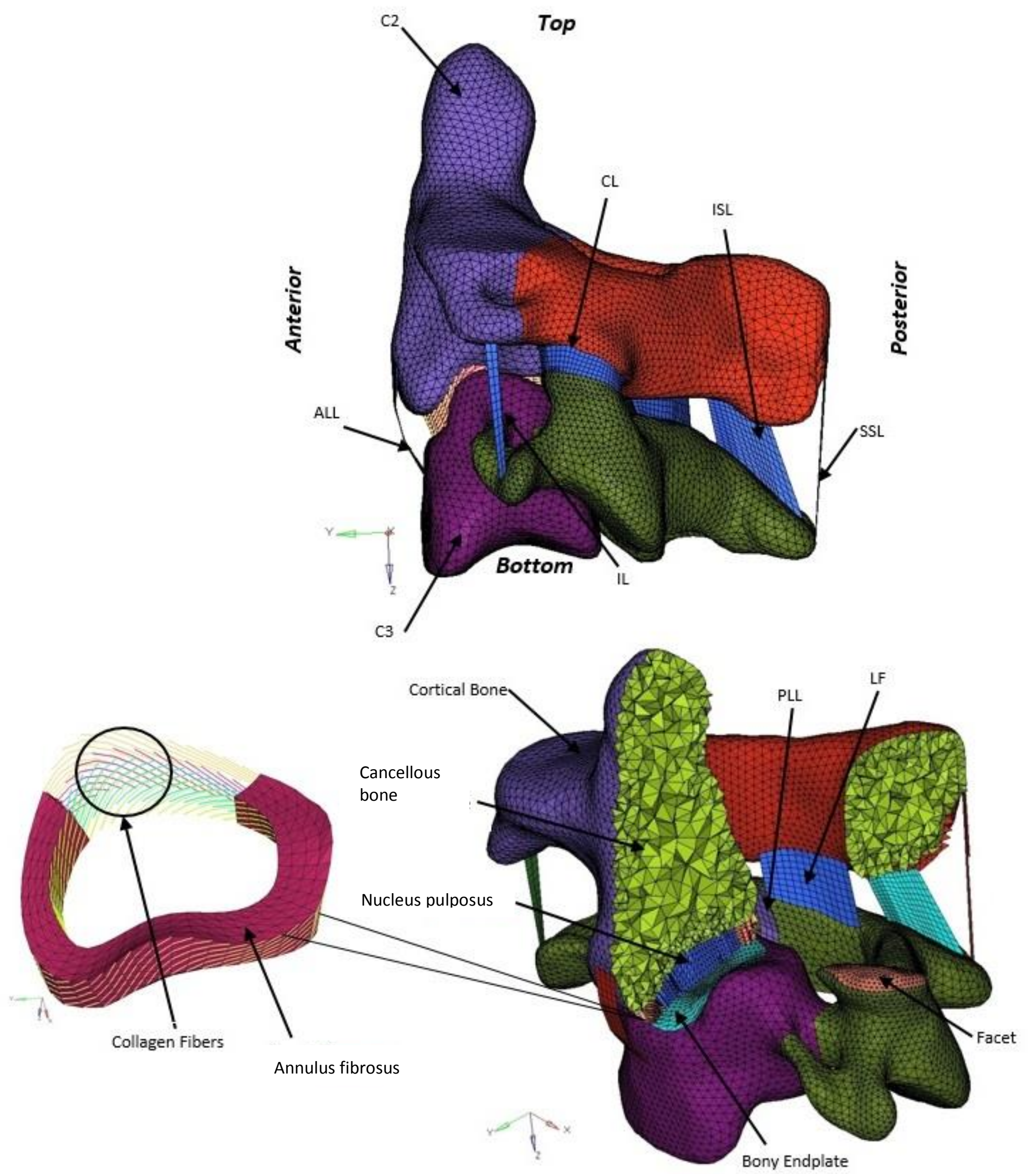

Figure 1: Functional spinal unit C2-C3 of the Cervical Spine Model

Table 1a: Material properties of vertebral components

Material Properties	*Vertebral Components*					
	Cortical	Reference	Endplate	Reference	Cancellous	Reference
Density (10^{-6} kg/mm^3)	1.83	[34]	1.06	[19]	0.17	[9]
Young modulus, E(MPa)	16800	[35]	5600	[19]	100	[9]
Poisson ratio, υ	0.3	[35]	0.3	[9]	0.29	[9]
Yield stress, a (MPa)	110	[35]	6	[35]	1.92	[9]
Hardening modulus b (MPa)	100	[36]	100	[36]	20	[36]
Hardening exponent, n	0.1	[36]	1	[36]	1	[36]
Failure plastic strain,(10^{-3}) ε_p	9.68	[36]	20	[37]	14.5	[37]
Maximum stress (MPa)	155	[38]	7.5	[38]	2.23	[39]
Strain rate coefficient, c	1	-	1	-	1	-

Table 1b: Material properties of disc components

Material Properties	*Disc Components*				
	Nucleus pulposus	Annulus matrix	References	Collagenous fibres	References
Density (kg/mm^3)	1.00E-06	1.20E-06	[34]	Nonlinear elastic curve	[31]
Poisson ratio, υ	0.495	0.45	[27]		
C_{10}	0.12	0.18	[27]		
C_{01}	0.03	0.045	[27]		

Table 1c: Material properties of spinal components

Spinal ligaments

	Constitutive models	Young modulus, E(MPa)	Poisson ratio, υ	Density (10^{-6} kg/mm^3)	Update coef., E1 (MPa/ms)	Update coef., E2 (MPa)	Failure strain, ε1	Failure strain, ε2	References
Ligaments	2D Viscoelastic material with time dependent Prony series								
ALL	Viscoelastic	11400	0.4	1	469.4	45.6	0.68	0.90	[40]
PLL		9120	0.4	1	1432.1	39.4	0.38	0.50	[30], [32]
ISL		3400	0.39	1	98.3	8.3	1.10	1.30	[30], [32]
IL		17100	0.49	1	98.3	8.3	1.10	1.30	[5], [32]
CL		7700	0.39	1	3.6	6	1.75	1.85	[30], [32]
LF		2400	0.39	1	199.7	6.5	1.01	1.25	[5], [32]
SSL		8550	0.4	1	476.5	8.3	0.94	1.08	[5], [32]

- Loading scenarios

1. Sagittal rotation with axial forces (distraction and/ compression)

For sagittal rotation test, a rotation of 8° at 8°/ms was applied about the medio-lateral axis in both flexion and extension scenarios while the C3 vertebra was fixed at the bottom (Fig.2).

2. Axial rotation with axial force (distraction)

For axial rotation test, a rotation of 8° at 8°/ms was applied about the superior-inferior axis to the left side of the C2 vertebra (Fig.2).

3. Lateral bending with axial force (distraction)

For lateral bending test, a rotation of 8° at 8°/ms was applied about the anterior-posterior axis towards the left side of the C2 vertebra (Fig.2).

For the implementation of the simultaneous combined loading condition, for sagittal rotation cases all rotations are combined with either compression or distraction of 100N. And for axial rotation and lateral bending cases, the respective loading is accompanied with a 100N distraction. A 60N of preload was applied to the superior vertebra to simulate the head weight [37].

For all the tests, Von Mises stress in vertebral endplates, intradiscal pressure (IDP) changes (stress in the nucleus pulposus) in the nucleus were calculated. The ligaments stresses were evaluated in their fibers directions and the contact forces were assessed in the facet joints. In addition, strain energy variations in all components were investigated to assess the spinal load-sharing distribution.

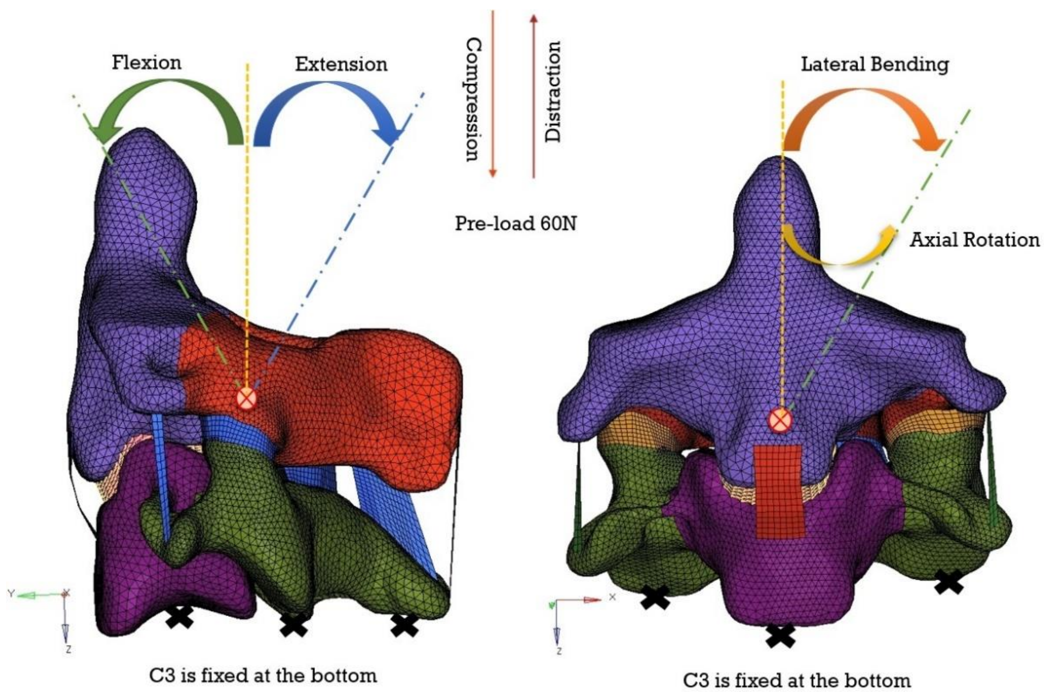

Figure 2: Loading setup for different loading scenarios.

- Boundary conditions:

The sagittal plane, transverse plane, and the coronal plane were defined by the axes “Y” and “Z”, axes “Y” and “X”, and axes “X” and “Z” respectively.

The movement of superior vertebra was allowed in sagittal plane only during flexion-extension rotations, in coronal plane during lateral bending conditions and in transverse plane during axial rotations. The inferior vertebra was fully constrained at the bottom for all cases.

C2-C3 segment model was compared against a variety number of in vitro studies of the human cervical spine segment in accordance to include the response of ligaments and facet joints. These studies were picked for validation purpose based on the type of experiment, the usefulness of the experimental data for validation, the historical use of the experimental data, and the general agreement of the experimental data with other studies in the literature. For each simulation case, the rotation was applied to the centroid of the superior vertebra in the relative plane based on the type of loading and the reaction load was calculated. As loading response was not distinctively different to the placement of center of rotation location for a unit segment in the superior-inferior side, so the loading has been applied on the centroid of C2 vertebra which is consistent with the loading methods adapted in [38]. Most of the experimental studies were load controlled [39] [40] [41], so controlled load was applied in the comparison analyses in accordance with the experimental studies.

- Results

Table-2, lists the progression of failure against the range of motion.

Rotation of the cervical segment at high velocity combined with axial loading conditions produced high peaks of stresses in the ligaments, disc and bony structures. At different degree of rotation, von Mises stress and plastic strain exceeded the yield and ultimate values, respectively, in C2 vertebra for almost all loading cases except the flexion-distraction scenario.

- Cortical and Cancellous Bones

The fracture was initiated near the left side of the vertebral endplate zone in C2 for flexion-compression case (Fig.3). For extension-compression case the fracture initiated in the right side facet region of C2 but it propagated in facets region and endplate region. For C2 vertebra, the fracture in the C2 cancellous bone was initiated around the facets region. For extension-compression case in both C2 and C3 vertebrae the fracture was mainly taken place in facet region. This pattern also found in extension- distraction and axial rotation- distraction cases. But for lateral bending- distraction case fracture propagated in the pedicle region of C2. More details about the locations and instants of ligaments failure and bone fracture are provided in Table 3.

- Intervertebral disc

The nucleus experienced more stresses (2.18 MPa in extension-distraction, 1.65 MPa in extension-compression) than the annulus (1.71 MPa in flexion-distraction 1.57 MPa in flexion-compression) at the same amount of rotation (4.12 degree) in case of flexion and extension (Fig.4). Also the pattern remains similar for axial rotation but for lateral bending with distraction, annulus carried more loading (2.39 MPa) than the nucleus (0.79 MPa).

- Articular Facets

The applied loading did not produce similar contact pressure in left and right facets. For flexion compression and/distraction, extension-compression and lateral bending cases left facet has higher stresses than the right one. In extension- distraction and axial rotation cases right facet takes the higher loading (Fig.5). Fracture of the left facet bone has produced an abrupt change in the contact pressure (Fig.5)

- Ligaments

In flexion all ligaments were recruited except ALL while only ALL and CL ligaments were recruited under extension (Fig.6a). The greatest values were obtained for the CL ligaments (Fig.6a). All the ligaments were recruited under lateral bending and axial rotation. Here, CL reported the maximum stress (Fig.6b).

- Spinal load-sharing

For all the modes of loading conditions of the cervical spine unit, the normalized strain energy curve for the collagen fibres has been plotted against degree of rotation for the flexion and extension cases (Fig. 7).

For all the modes of loading conditions of the cervical spine unit, the strain energy curve has been plotted against the degree of rotation for the flexion, extension, lateral bending and axial rotation cases (Fig. 8). From the curves, the load carrying or sharing capacity of different components can be easily noticeable.
Under flexion with distraction, strain energy of ligaments represented 75% of the total strain energy compared to the disc (26.25%). An alternation in load sharing between cancellous bone and disc occurred around 2 degree of rotation (Fig.8a). Under extension with distraction, strain energy of ligaments represented 57.18% of the total strain energy compared to the disc (32.24%) (Fig.8b). Also an alternation in load sharing between cancellous bone and disc occurred around 1.6 degree of rotation (Fig.8a). While a significant drop is demonstrated for cortical, cancellous, and endplate after around 0.25 degree for both cases. There is almost no strain energy in the articular facets for both cases (Fig.8a).

Under flexion with compression, cancellous bone carried a significant portion (70 %) of the total strain energy compared to the ligaments (51.25%), disc (34%), cancellous bone (40%) and cortical bone (86%) (Fig. 8a). An alternation in load sharing among cancellous bone, ligaments and disc occurred around 1.11 and 1.47 degree of rotation (Fig.8a). Under extension with compression, strain energy of ligaments represented a significant portion (66.85%) of the total strain energy compared to the disc (20.76%), cancellous bone (51%) and cortical bone (35%) (Fig.8b). Also an alternation in load sharing between cancellous bone, ligaments and disc occurred around 0.6 and 1.67 degree of rotation (Fig.8b). While a significant drop is demonstrated around 0.25 degree for extension and 0.10 deg. for flexion. There is almost no strain energy in the articular facets for both cases (Fig.8b).

Under lateral bending with distraction, strain energy of ligaments represented 72.2% of the total strain energy compared to the cortical bone (17.25%), disc (5.7%), cancellous bone (8%) and cortical bone (17%). There is a significant drop is demonstrated for cancellous, and endplate after around 0.25 deg. (Fig.8c).

Under axial rotation with distraction, strain energy of ligaments represented 76.5% of the total strain energy compared to the cortical bone (17.15%) and cancellous bone (8.72%). There is a significant drop is demonstrated for cortical, cancellous, and endplate after around 0.25 deg. (Fig.8c). Disc contributes very less to the strain energy in this case (Fig.8c).

A list has been prepared in table 4, which gives a detail of the components that have been fractured during different injury loading conditions.

Table 2: Progression of failure in different loading scenarios:

Loading Scenario	*Rotation of C2 where the failure initiates (Degree)*	*Component that fails*	*Loading Scenario*	*Rotation of C2 where the failure initiates (Degree)*	*Component that fails*
Distraction + Flexion	0.52	CL	Compression + Flexion	0.20	Vertebral Endplate of C2
	2.67	Vertebral Endplate C2		0.68	Cancellous C2
	4.48	Annulus		3.75	Annulus
	5.18	Nucleus		4.32	Nucleus
Distraction + Extension	3.79	CL	Compression + Extension	0.84	Vertebral Endplate C2
	4.40	IL		1.43	Cancellous C3
	5.16	Cancellous C2		1.47	Cancellous C2
	5.32	Vertebral Endplate C2		1.48	CL
	6.04	Cancellous C3		5.12	LF
	6.48	Facet C2		5.96	ISL
	7.04	LF		7.76	Facet C2
	7.08	ISL			
Distraction + Lateral Bending	0.52	CL	Distraction + Axial Rotation	0.80	Cancellous C3
	1.08	Cancellous C3		0.84	Cancellous C2
	2.0	Cancellous C2		0.88	CL
	2.47	Vertebral Endplate C2		1.95	Vertebral Endplate C2
	3.15	Facet C3		5.20	Facet C3
	3.19	LF		6.40	Facet C2
	3.43	Facet C2		7.36	Annulus
	3.87	Vertebral Endplate C3			
	3.91	IL			

Flexion-Compression

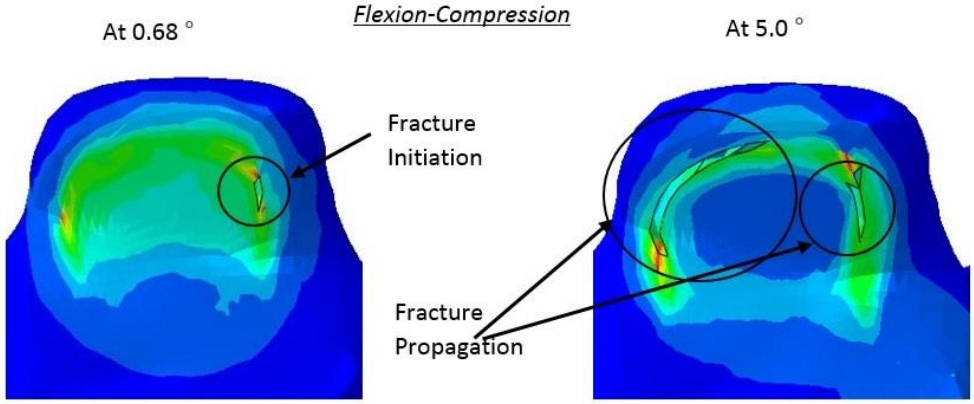

Bottom view of C2 cancellous bone anterior portion

Extension-Compression

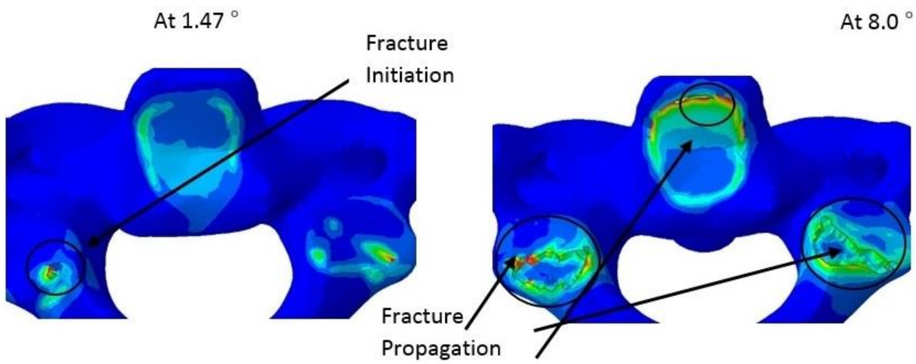

Bottom view of C2 cancellous bone

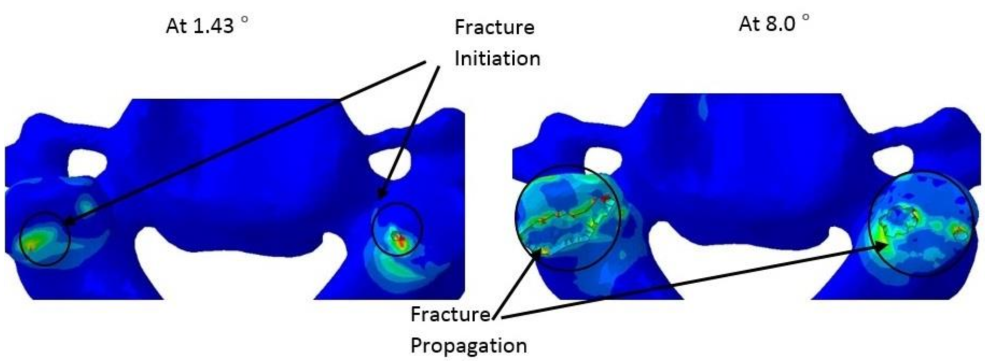

Top view of C3 cancellous bone

Extension-Tension

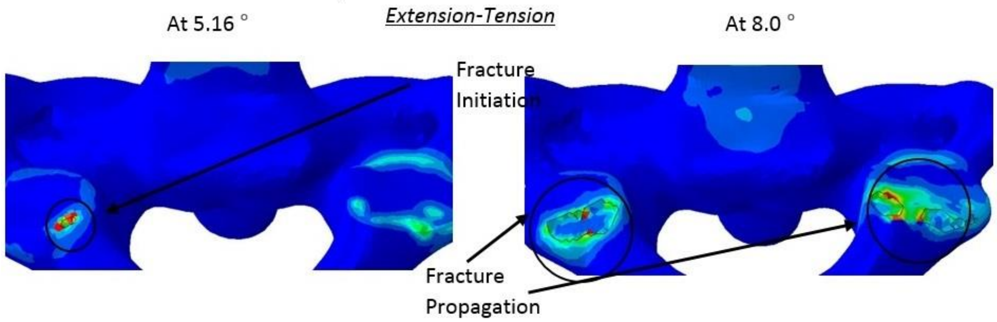

Bottom view of C2 cancellous bone

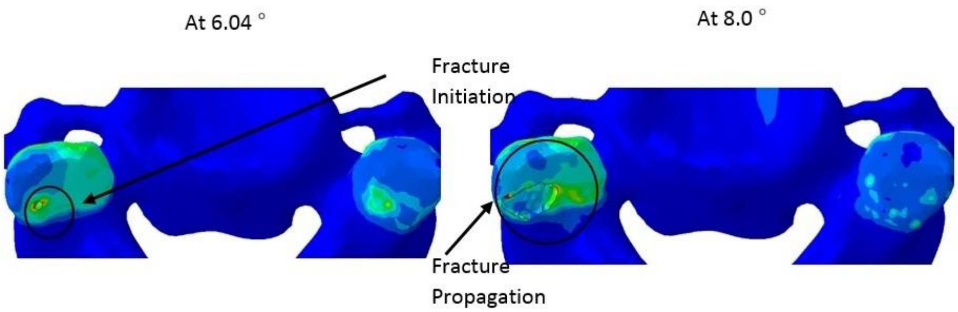

Top view of C3 cancellous bone

Lateral Bending-Tension

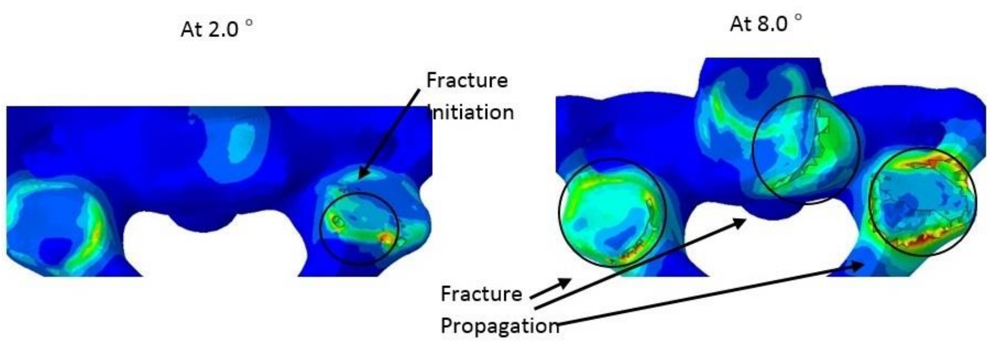

Bottom view of C2 cancellous bone

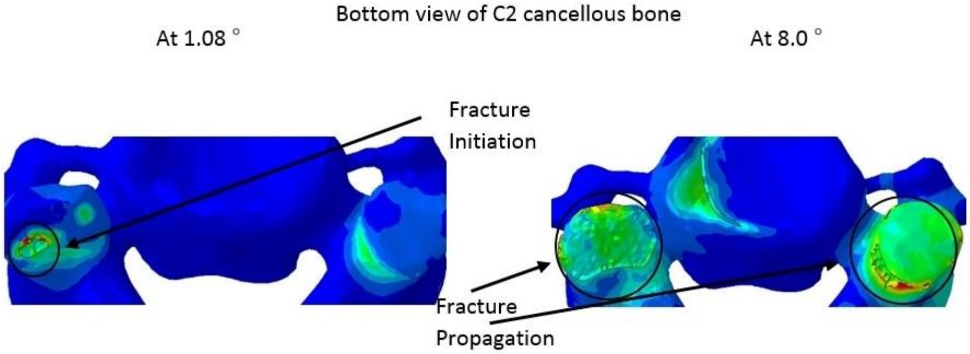

Top view of C3 cancellous bone

At 0.84 ° At 7.58 °

Axial Rotation-Tension

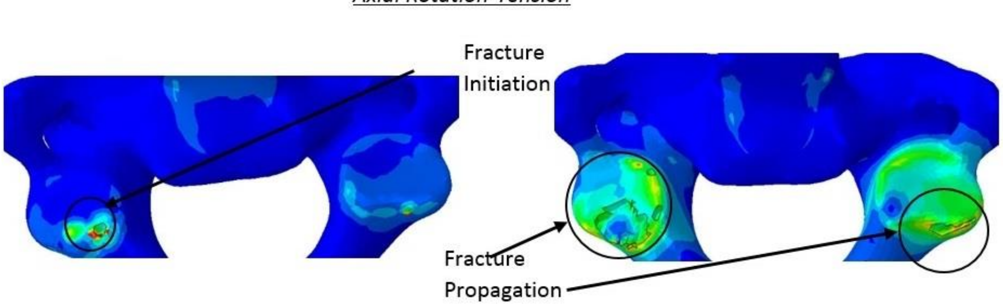

Bottom view of C2 cancellous bone

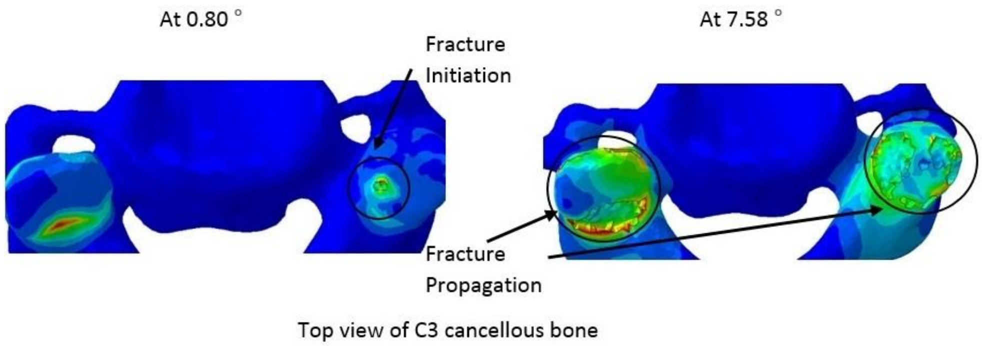

Figure 3: Initiation and propagation of fracture in the C2 and C3 vertebrae under different loading scenarios

Flexion and Extension

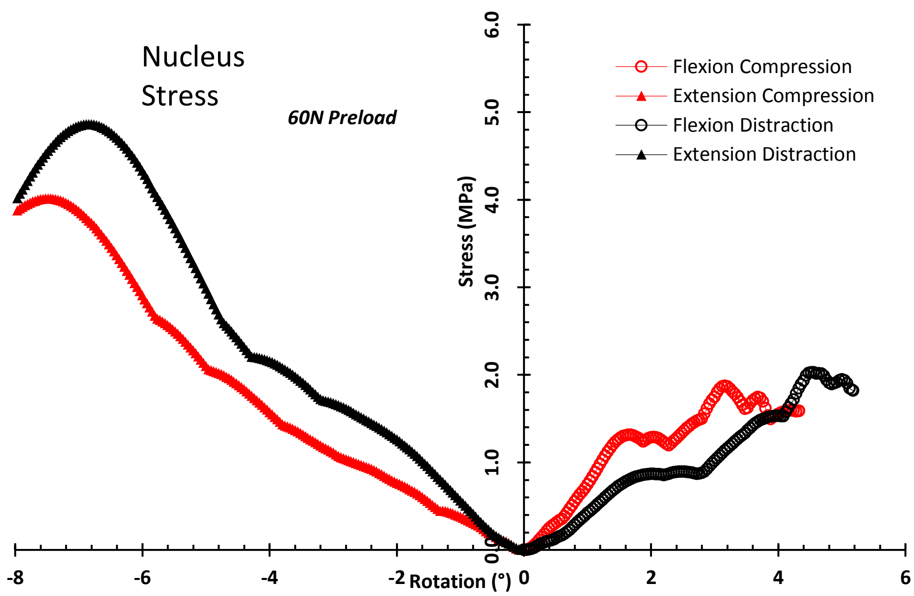

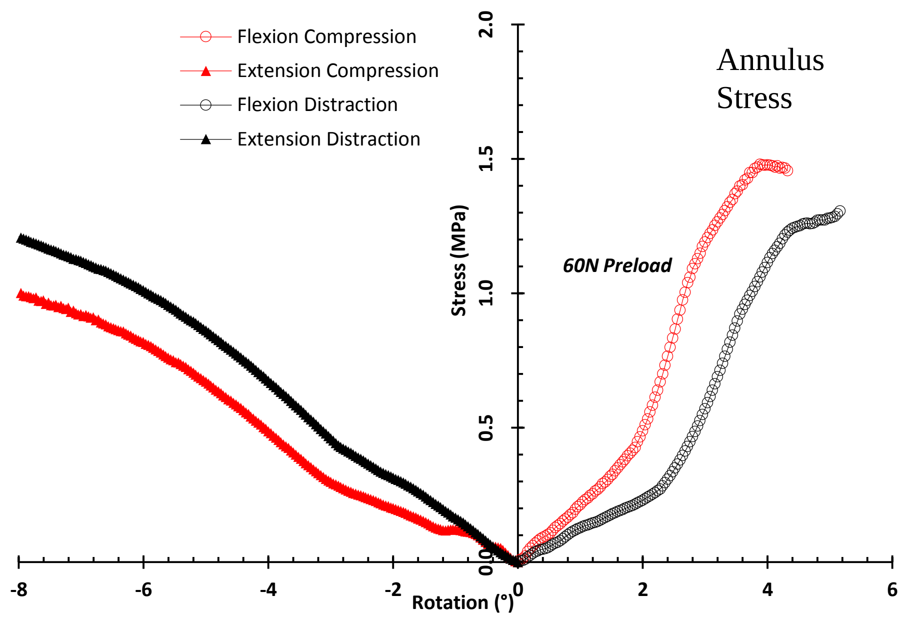

Axial rotation and Lateral bending

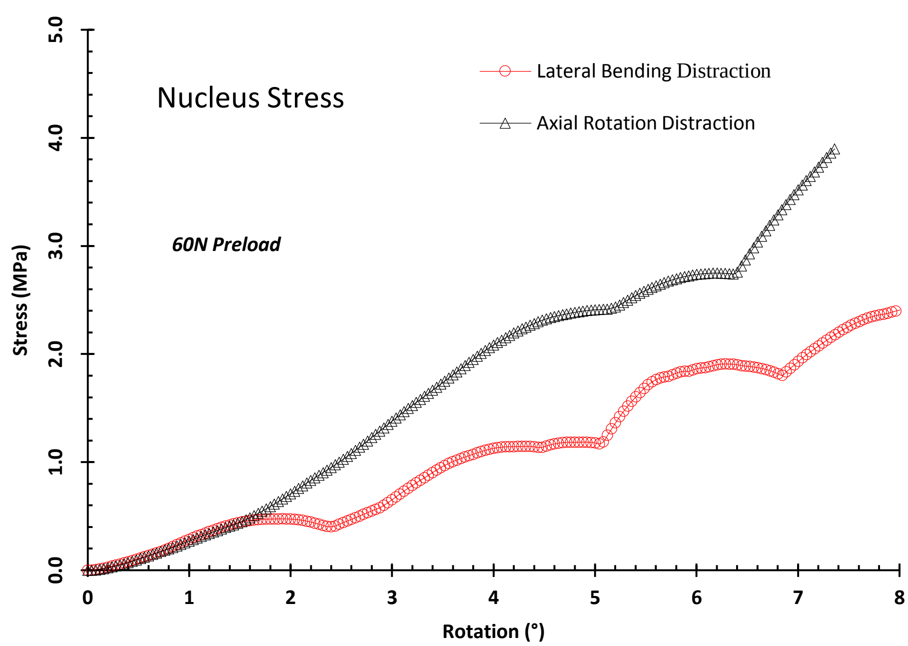

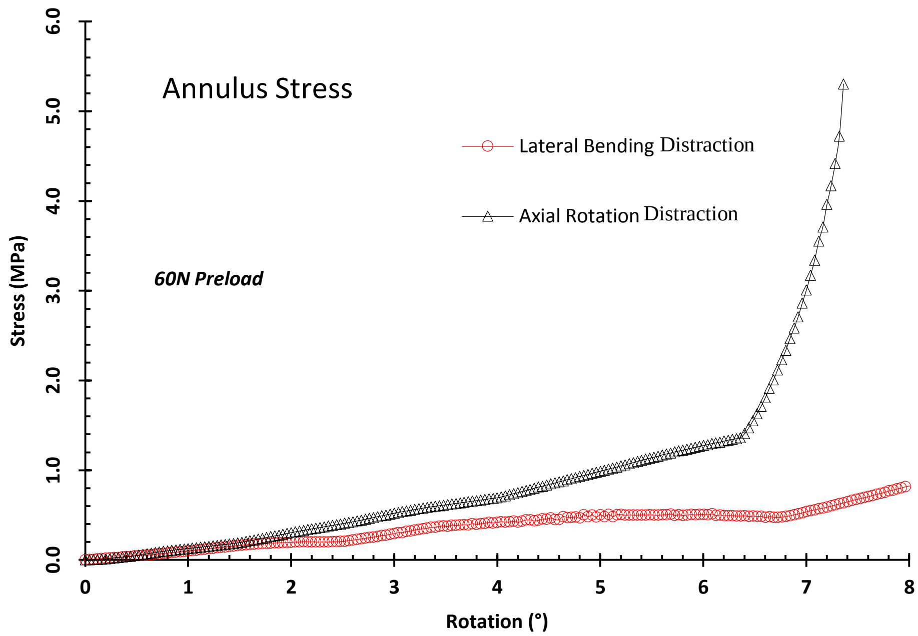

Figure 4: Nucleus and Annulus stress plotted against range of rotation for flexion, extension, lateral bending and axial rotation in combined loading scenarios.

<u>Flexion and Extension</u>

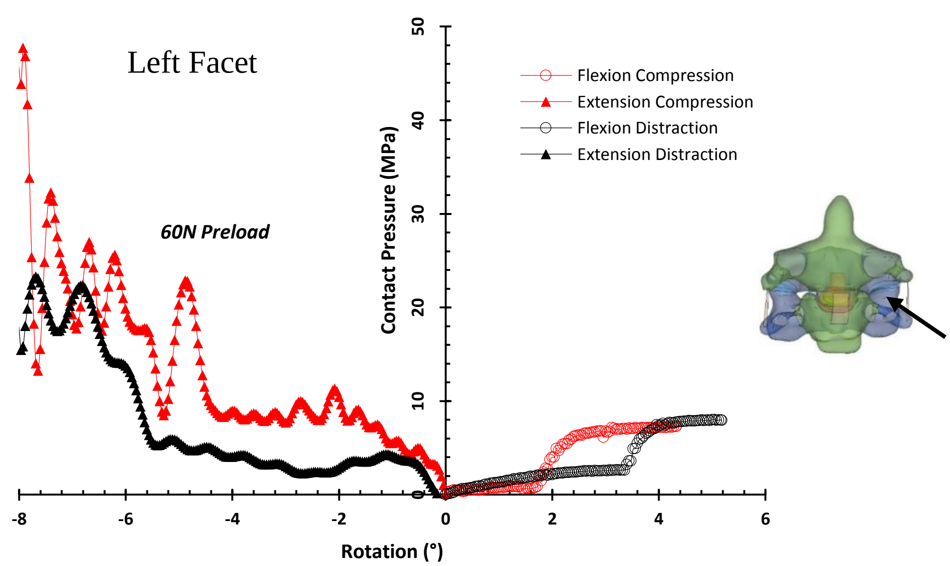

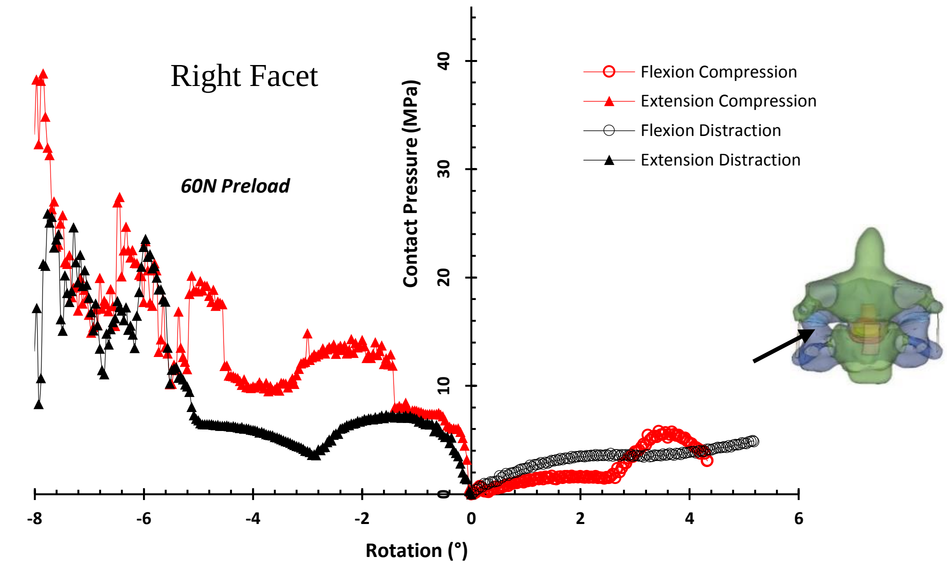

(a)

<u>Lateral bending and Axial rotation</u>

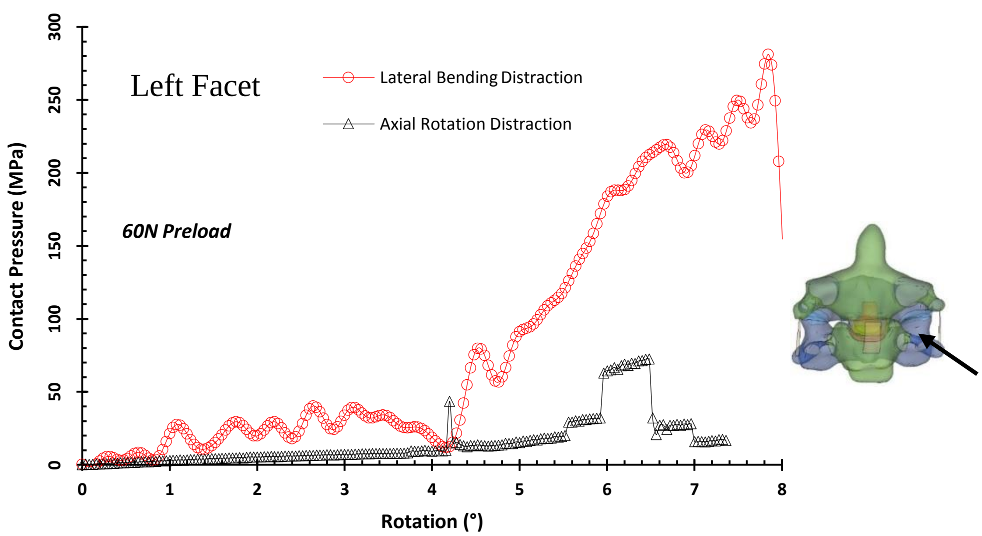

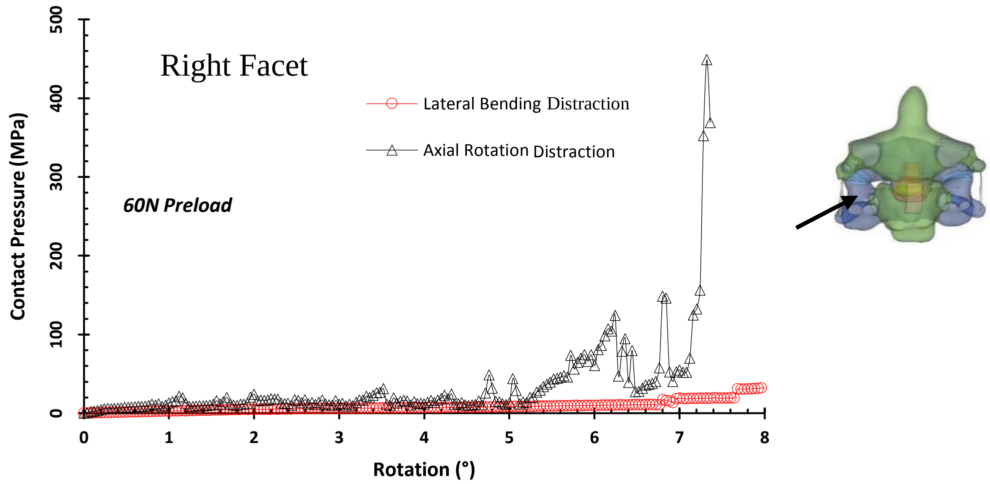

(b)

Figure 5: Contact pressure in facet joint for (5-a) flexion/extension combined with compression/distraction; (5-b) lateral bending/axial rotation combined with distraction

Flexion and Extension

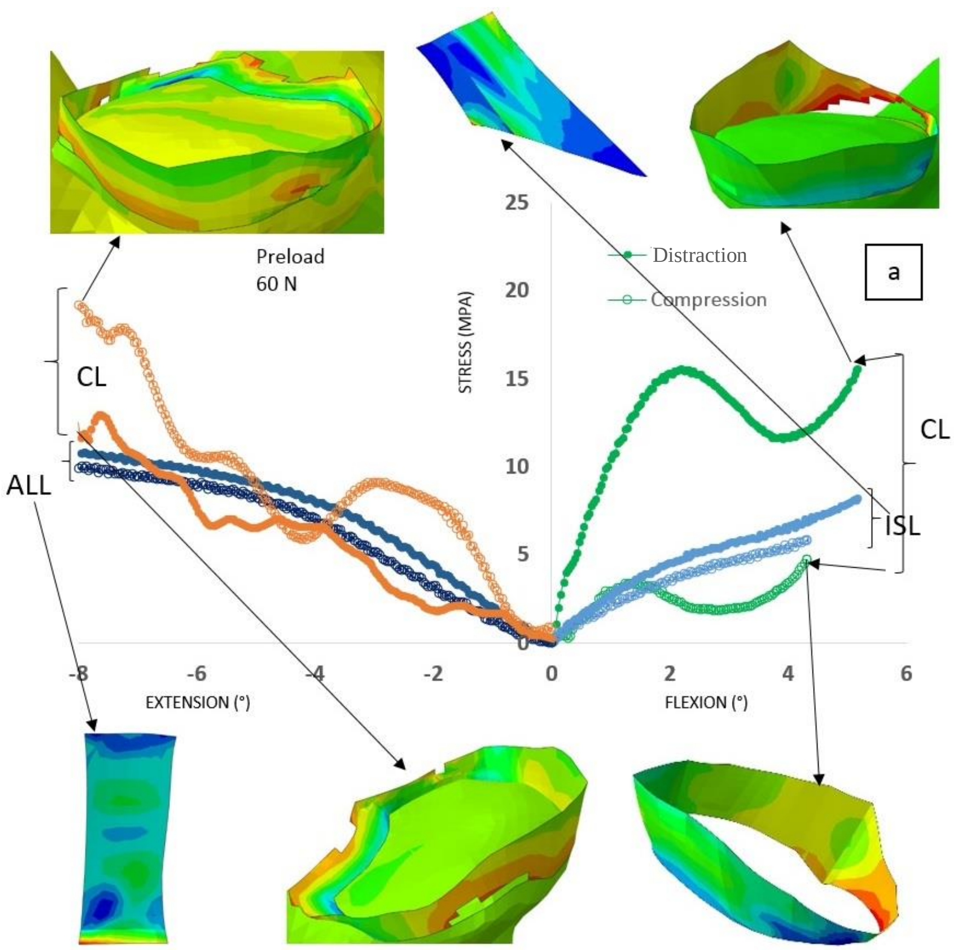

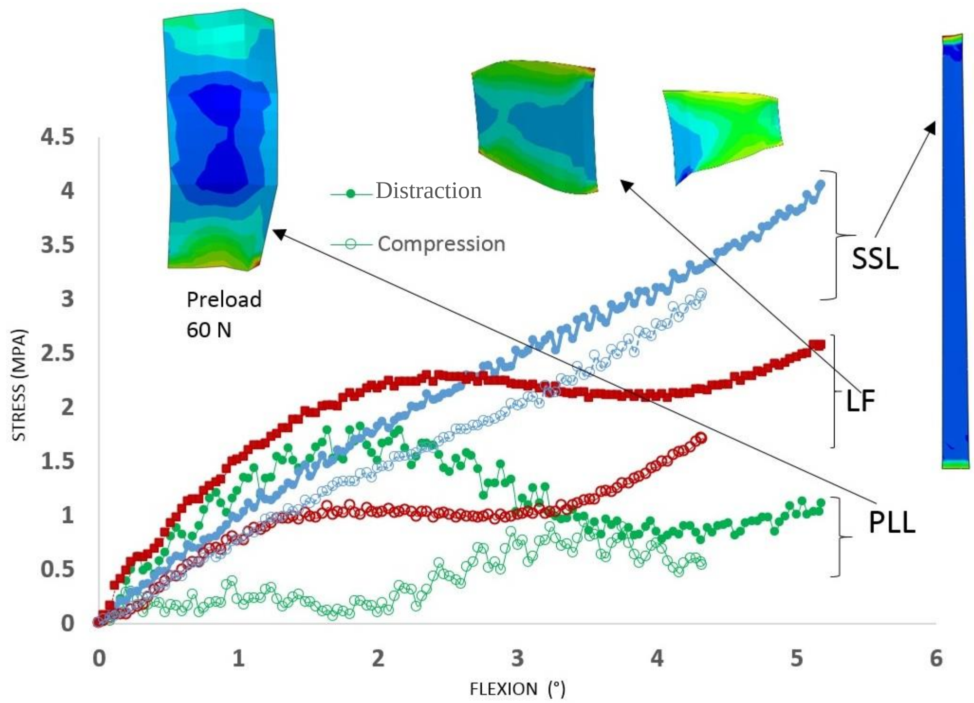

Lateral Bending and Axial Rotation

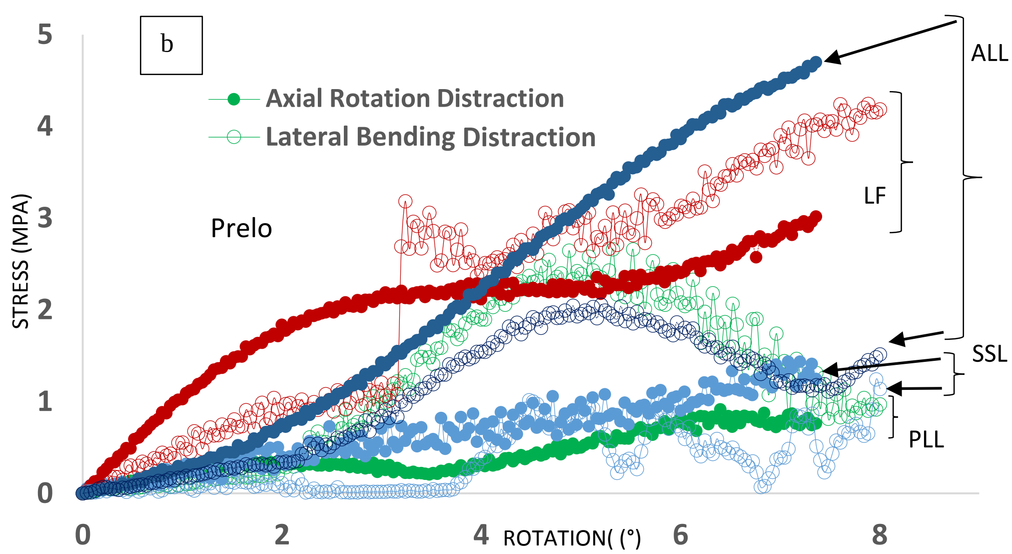

Table 3: Contour plot of ligaments for lateral bending and axial rotation

	Axial Rotation with Distraction	Lateral Bending with Distraction		Axial Rotation with Distraction	Lateral Bending with Distraction
ALL	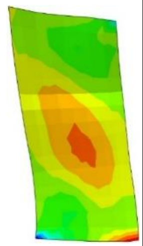	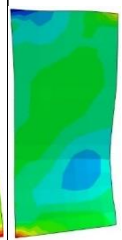	LF	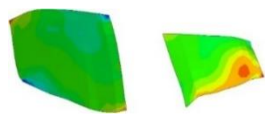	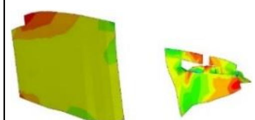
PLL	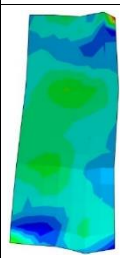		SSL	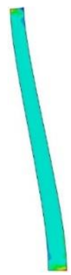	

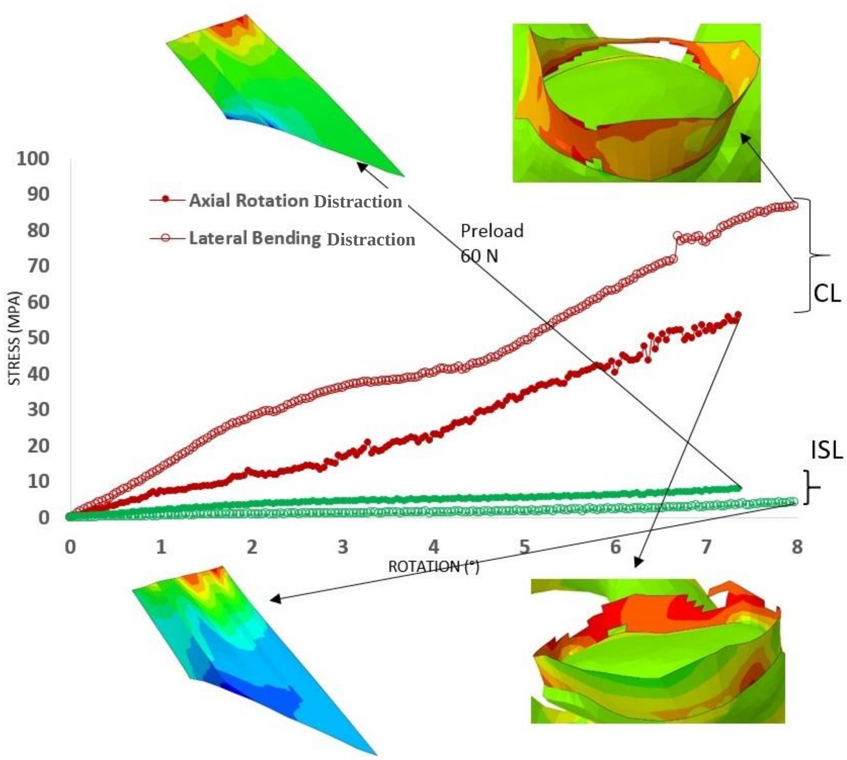

Figure 6: Ligament stresses evaluated in their fiber directions under (6-a) flexion (right) and extension (left) at different loading condition (6-b) Lateral bending and axial rotation with combined distraction cases.

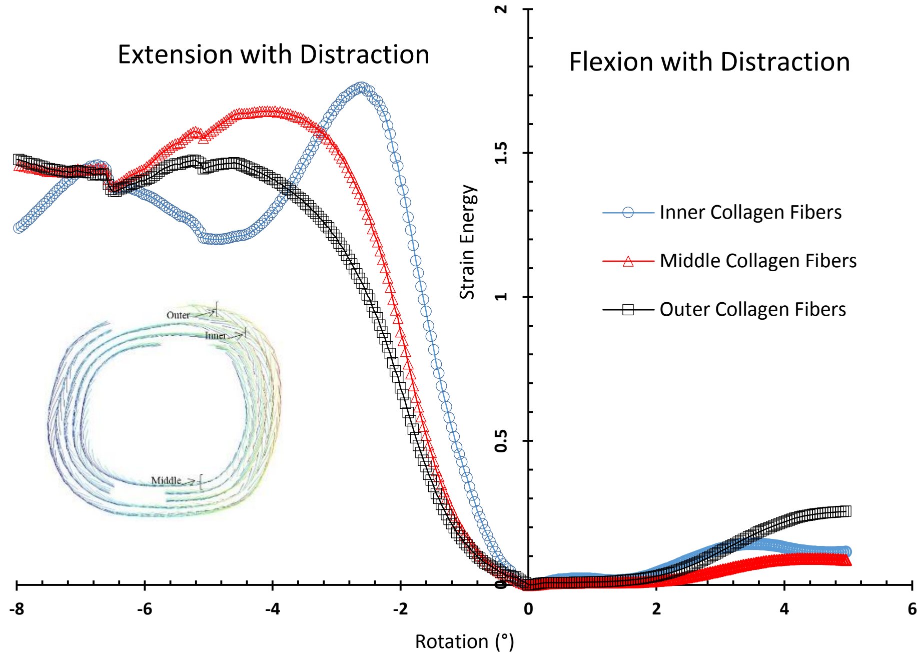
Extension with Distraction
Flexion with Distraction
Strain Energy
Rotation (°)
Inner Collagen Fibers
Middle Collagen Fibers
Outer Collagen Fibers
Outer
Inner
Middle
2
1.5
1
0.5
0
-8
-6
-4
-2
0
2
4
6

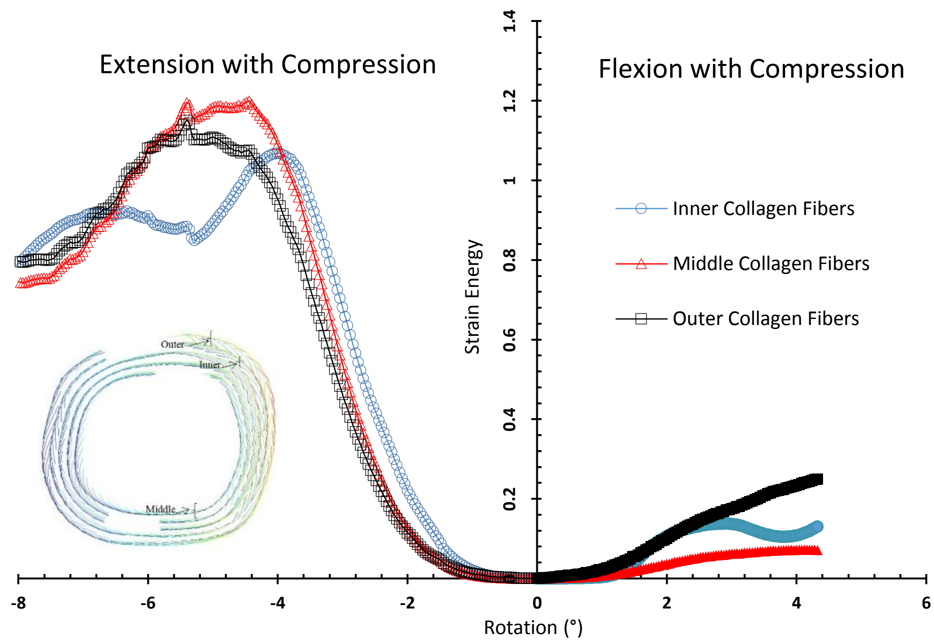
Extension with Compression
Flexion with Compression
Strain Energy
Rotation (°)
Inner Collagen Fibers
Middle Collagen Fibers
Outer Collagen Fibers
Outer
Inner
Middle
1.4
1.2
1
0.8
0.6
0.4
0.2
-8
-6
-4
-2
0
2
4
6

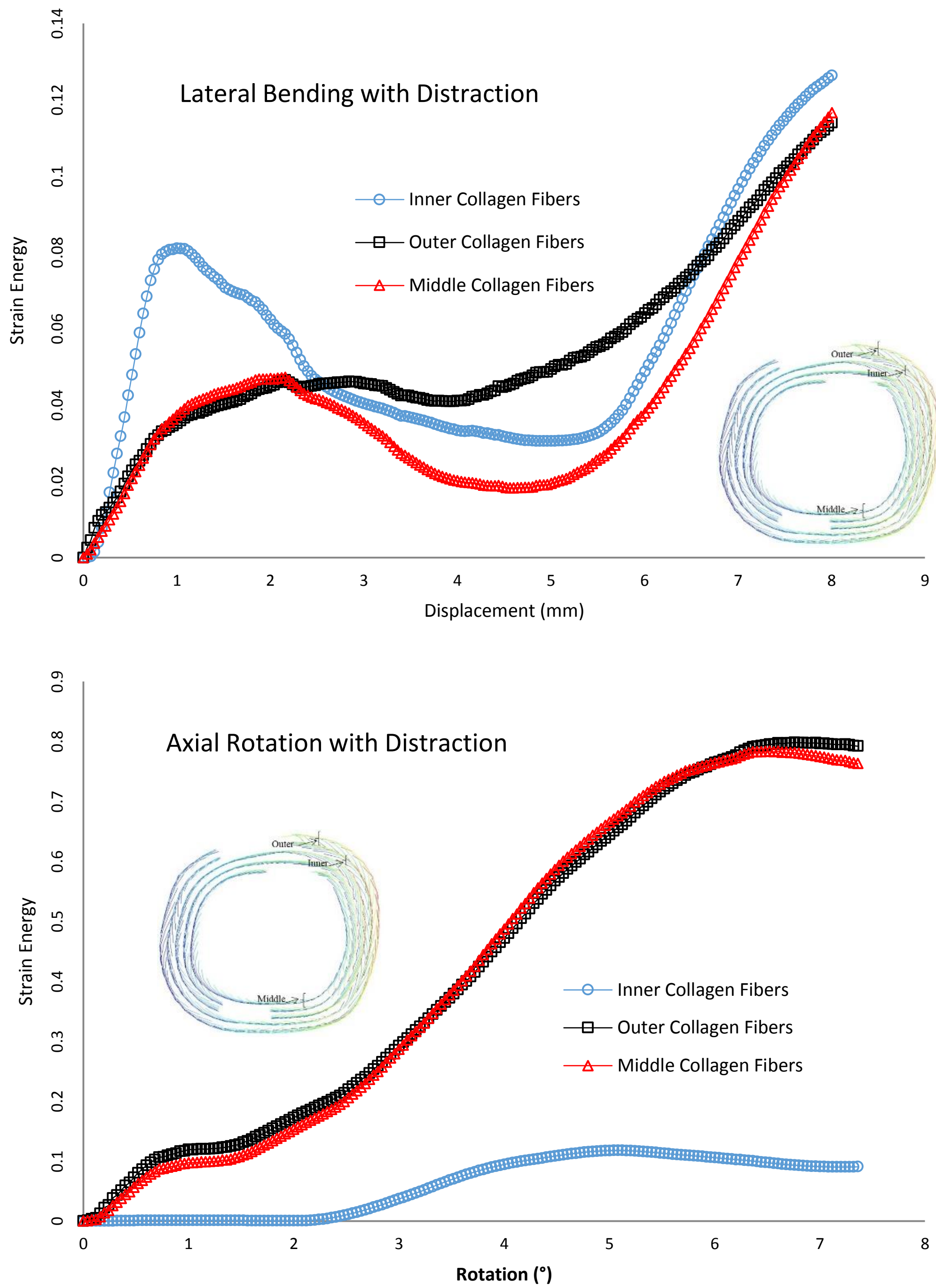

Figure 7: Strain Energy curve for the collagen fibers for all modes of loading

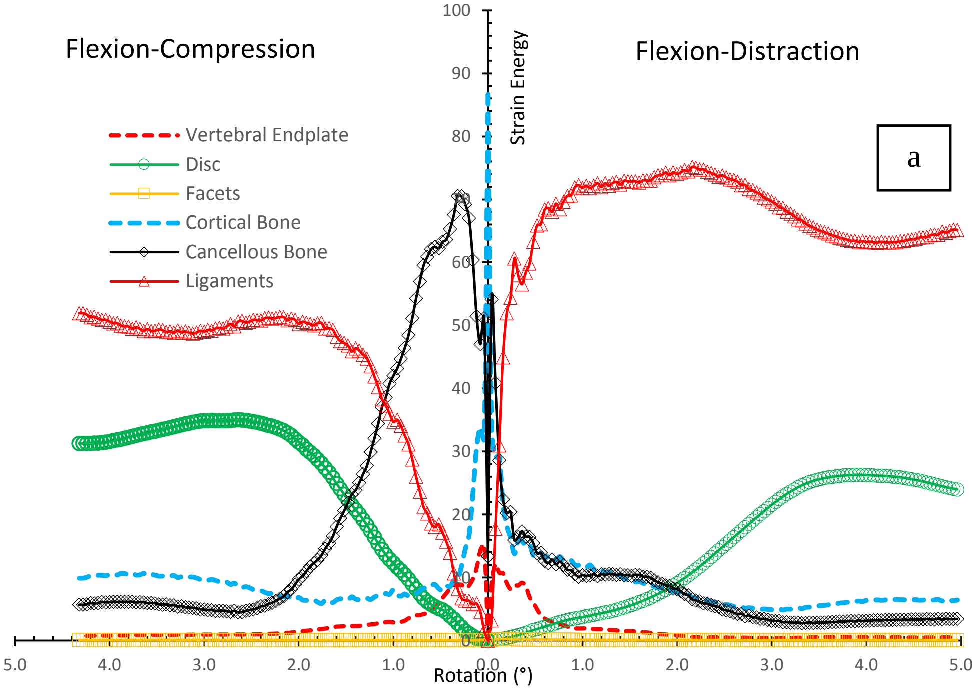

Flexion-Compression
Flexion-Distraction
a
Strain Energy
Vertebral Endplate
Disc
Facets
Cortical Bone
Cancellous Bone
Ligaments
100
90
80
60
50
40
30
20
10
0
5.0
4.0
3.0
2.0
1.0
0.0
0.0
1.0
2.0
3.0
4.0
5.0
Rotation (°)

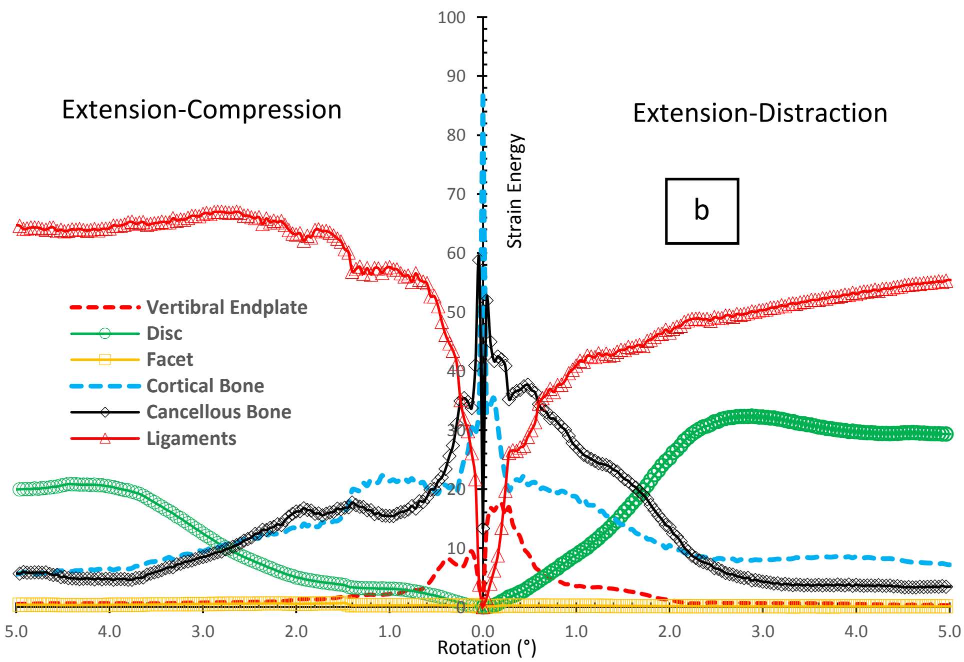

Extension-Compression
Extension-Distraction
b
Strain Energy
Vertibral Endplate
Disc
Facet
Cortical Bone
Cancellous Bone
Ligaments
100
90
80
70
60
50
40
30
20
10
0
5.0
4.0
3.0
2.0
1.0
0.0
1.0
2.0
3.0
4.0
5.0
Rotation (°)

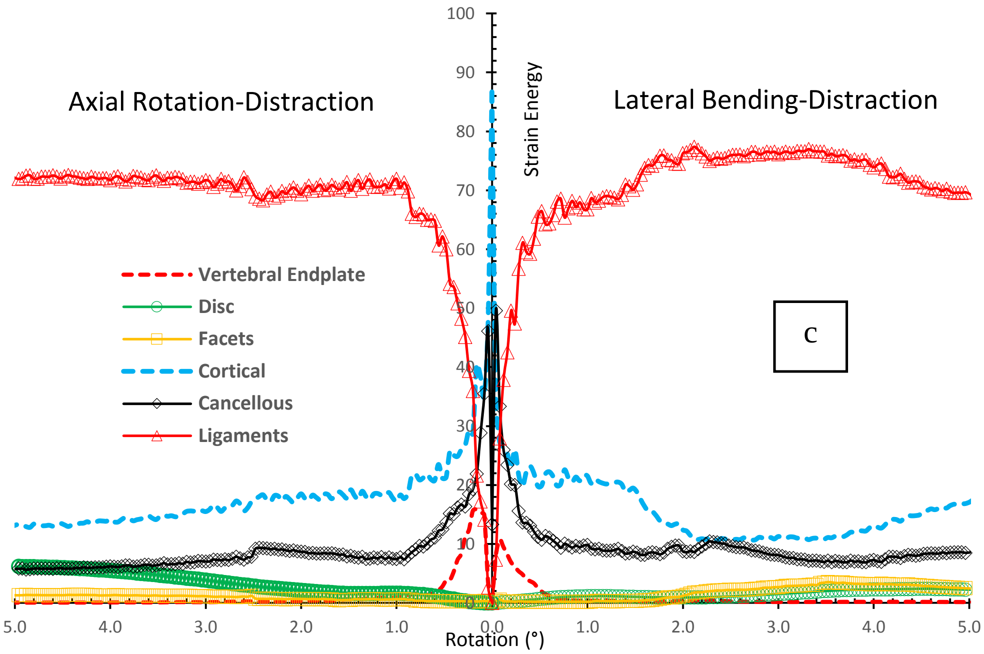

Figure 8: Strain Energy curve for all modes of loading.

Table 4: List of components that failed during different types of loading scenarios:

Components		*Loading Scenarios*					
		Distraction + Flexion	Compression+ Flexion	Distraction + Extension	Compression + Extension	Distraction +Lateral Bending	Distraction +Axial Rotation
		Whether it fails (✓) or not					
Ligaments	ALL						
	PLL						
	CL	✓		✓	✓	✓	✓
	IL			✓		✓	
	ISL			✓	✓		
	LF			✓	✓	✓	
	SSL						
Cancellous Bone	C2		✓	✓	✓	✓	✓
	C3			✓	✓	✓	✓
Cortical Bone	C2						
	C3						
Vertebral Endplate	C2	✓	✓	✓	✓	✓	✓
	C3					✓	
Facets	C2			✓	✓	✓	✓
	C3					✓	✓
Disc(Nucleus)		✓	✓	✓	✓	✓	
Disc(Annulus)							

Discussions

In the current study, a three-dimensional complete ligamentous C2-C3 spine segment has been used to assess the spinal injuries. This numerical model distinguishes itself from other published models [30], [9], [5] by implementing a bio-realistic geometry, a refined mesh, and strain-dependent material constitutive laws that can simulate bone fracture and ligament tear. A detailed/realistic investigation of failure initiation and propagation over the bone is being possible with this model, which was previously limited on defining the failure risk regions based on high-stress concentrations in other literatures [29]; [42]; [43]. Similar compressive and tensile mechanical properties were assigned to cancellous bone except of the yield strain, which is significantly higher in compression [34]. Microstructure and anisotropy of cancellous bone were not included along with the bone fragments at the fracture site. And the fracture initiation depends on the ultimate plastic strain value and location. Implementation of a user pseudo-elasto-plastic material law based on energy formulation which includes unsymmetrical behavior, damage and failure [44] could be used in the future studies. Although the bone fracture and ligament failure are based on element deletion process, the refined mesh used in both components improves the failure propagation path prediction. There is a lack of in vitro data regarding the biomechanical behavior of the spine under combined dynamic loading conditions up to failure. Validation of the ultimate stress and strain values [45] regarding the bone fracture were done in accordance with the experimental procedure [46] and dynamic load test has been conducted with velocities of 3.2 m/s and 5.7 m/s. Drop in the reaction force computed at C3 (since a displacement controlled test) which represents drop in the model resistance demonstrated the failure in the model. The failure force and fracture mechanism shows good agreement with the experimental result [46]. The nucleus was being modelled as a fluid like structure. The annulus was simulated with hyper-elastic material [22]. For flexion combined with both distraction and compression the response load is carried by the annulus resulting in anterior disc compression, bulge and with the simultaneous contribution from the posterior ligaments resulting in tensile stress and strain in the posterior-inferior part of the vertebral bodies. As the disc compressed and the stress in the annulus gets higher than the extension case, after certain degree of rotation the elements get distorted. Similar element distortion condition was noticed during the axial rotation cases where stress in the annulus also gets piled up and the distortion initiates. For the flexion case, the maximum stress in the nucleus occurred in distraction case (1.82 MPa) which is higher than the peak value of the disc 1.18 MPa [47]. This indicates that there was a disc rupture happened during the flexion-distraction analysis. For the extension case, the maximum stress occurred during the distraction case which (4.06 MPa) also exceeded the peak value of the disc pressure in extension [47]. Lateral bending with distraction case resulted the maximum value in nucleus (2.40 MPa) which also exceeded the peak value [47] indicating a disc rupture during the analsysis. The rupture in facets was not initiated in the flexion complex loading. But for extension complex loading facets of C2 got fractured with higher degree of rotation because articular facets carry more load under extension [45] [26]. Which also is in agreement with the curve (Fig.5) where it can be easily noticeable that the stress in the facets shows fluctuations in the curve which has been resulted from the element deletion from the facets. For axial rotation and lateral bending cases, both C2 and C3 facets get fractured which is obvious from the similar pattern of the curve (Fig.5).

In all of the complex loading conditions vertebral endplate of C2 gets ruptured. And the rupture initiates at an early stage of the loading scenario for most of the cases. As a result the stress value in the endplate is seen to reach a high value immediately after the loading starts which can be visualized in strain energy curves (Fig.8) and as it exceeds the ultimate failure stress criterion, the elements get deleted to simulate the fracture mechanism. In flexion cases the fracture starts in the anterior side where as for the extension case it starts in the posterior side. And in lateral bending and axial rotation cases the fractures initiates from a side of the endplate. From the collagen fibers strain energy curves (Fig.7), it can be seen that the trend of the load carrying pattern of the collagen fibres agree with the load carrying pattern of disc. In most of the cases as the stress limit reaches the failure criteria, the CL ligament gets ruptured under this ultimate stress value. A high stress value confirms this failure mechanism (Fig.6a and Fig.6b). The ligaments are modeled to take tensile loading. Another noticeable finding from this investigation is, under all form of tensile combined loading, the ligaments get failed before fracturing any bony elements. This is also another indication that under tensile loading the soft tissue acts first whereas under compressive loading the bony structures function earlier in the analysis which can also be visualized from the flexion-compression case (Fig.8b) where cancellous bone carried a significant portion (70 %) of the total strain energy compared to the ligaments (51.25%). The stress values and distribution in different ligaments are based on their stiffness and orientation [48]. Stress in the ligaments are found mainly concentrated in the attachment regions of ligaments to the bone in most of the cases except for LF and ALL in axial rotation distraction case, where the stress has been found in the mid region of the ligaments (Fig.6-b). Such results could not be found without real 2d geometry of ligaments. For all the modes of loading conditions, strain energy of the components of the cervical unit has been analyzed (Fig.8). For all modes of loading considered, the ligaments were the primary load-bearing structure in the segment. Ligaments carried most of the load at the higher levels of loading. The facet served as the second most load carrier in the segment in flexion and extension cases, at the later stage of the analysis the disc alters it’s position with the facet and it maintained the same trend afterwards. The cortical and cancellous bone were the second most load bearer among other components in lateral bending and axial rotation cases. These results provide insight into cervical spine behavior as the distribution of load within the cervical spine has not yet been measured experimentally. In [10], reported similar conclusions with a C5–C6 FE model that included compressive preload; however, they did not report the load in the ligaments during flexion. In general, the segment model described in this study provides good prediction of response over a wide range of loads and different modes of loading. Importantly, the segment was modeled at the tissue level, with a more detailed disc model than any previously reported in the literature. It should be noted that this model was developed for dynamic loading at injurious levels.

The objective of this study was to predict the tissue level failure under the complex combined loading conditions. The predicted failure locations were in agreement with the reported cervical spine injuries for different modes of loading [19]. A biofidelic model of the cervical spine segment C2-C3 has been used in this study to assess virtually the bone and ligament injuries in complex combined loading scenarios. This model takes into account the rate-dependency and failure behavior of spinal components. But the model is a ligamentous one and hence it did not simulate the active and passive muscular responses which might alter the cervical spine kinematics and loadsharing amongst components. Also, the fluid flow between the disc and the bone is not simulated in this model, which could be achieved by using poroelastic material laws. The simplification of no fluid flow was appropriate here since the study was focused on the immediate mechanical response of the cervical spine to dynamic loadings, as opposed to long-term gravitational loads, which may induce a visco-poroelastic response over a timeframe of minutes or hours [45] [27]. Since these data are not very easily pliable via in vitro studies, the investigation presented in this study represents a first but notable step towards the development of a FEA of models of spine segments under complex combined loading conditions experienced in trauma situations. The comparison between the biomechanical behavior of the cervical spine segment under flexion and extension complex injury cases demonstrates the versatility of our FEM to virtually assess spinal injuries under various complex combined loading scenarios. Also as the model is capable of showing the load-sharing mechanism amongst the different spinal components in response to the different loading cases, the onset of spinal injuries for a given loading direction was also been able to be predicted by the model. Under in vivo conditions, these complex combined loads are usually implemented. But the spinal segment faces those loading with help of muscular, intra-abdominal pressure, inertia and external loads. In the current model, simplifications are made with regard to these individual parameters. This has been mentioned here to emphasize about the fact that the cervical injuries that are modelled with this segment based on the element deletion process which can accurately predicts the initiation site of an injury (bone fracture or ligament rupture), should not be judged as its final state, as observed by clinicians after trauma.

Conclusions

Some of the significant findings of this study include element distortion of disc under flexion-compression loading, C2 vertebral endplate getting ruptured almost in every case, reaching failure stress limit for IL and CL ligaments. Also the study reported facets rupture and cancellous bone fracture in case of extension, axial rotation and lateral bending scenarios. The study also reveals that the ligaments acted as the primary load-bearing structure in the segment in most of the loading scenarios except the flexion-compression case where the cancellous bone carried a major portion (70%) of the total loading. From the injury assessment results it is obvious that the lateral bending-distraction case can be considered as the most critical loading scenario among the other applied ones as a major number of components fail under that loading condition. Future work will address more complex types of loading such as combined rotations and translations that could potentially lead to more severe injuries resulting from early contact between bone components and to an amplified strain level on ligaments. Also the mechanism adapted in this model will be implemented to model the entire cervical spine in future.

Acknowledgements

This study was supported by Department of National Defense, Directorate of Technical Airworthiness and Engineering Support (DTAES 6) and Surgeon General’s Health Research Program (SGHRP). Also some of the valuable data about the processing of the model has been received from the Royal Military College of Canada. Natural Sciences and Engineering Research Council of Canada (NSERC) (engage) grants supported partially this study as well.

References

[1] N. P. F. H. M. J. J. M. D. W. S. L. S. N. H. S. A. Yoganandan, "Epidemiology and Injury Biomechanics of Motor Vehicle Related Trauma to the Human Spine.," 1989.

[2] G. V. T. V. S. J. Clausen JD, "Uncinate processes and Luschkas joints influence the biomechanics of the cervical spine: quantification using a finite element model of the C5-C6 segment," *J. Orthopaedic Research,* vol. 15, no. 3, pp. 342-347, 1997.

[3] N. L. F. a. S. W. Maurel, "A three-dimensional parameterized finite element model of the lower cervical spine. Study of the influence of the posterior articular facets," *Journal of Biomechanics,* vol. 30, pp. 921-931, 1997.

[4] K. S. V. L. P. F. Yoganandan N, "Finite element model of the human lower cervical spine: parametric analysis of the C4-C6 unit," *Jo. Biomechanical Engineering,* vol. 119, no. 1, pp. 87-92, 1997.

[5] H. Ng, "Nonlinear finite-element analysis of the lower cervical spine (C4–C6) under axial loading," *Journal of Spinal Disorders* , vol. 14(3), p. 201–210., 2001.

[6] N. H. Teo EC, "Evaluation of the role of ligaments, facets and disc nucleus in lower cervical spine compression and sagittal moments using finite element method," *Med. Eng. & Physics,* vol. 23, pp. 155-164, 2001.

[7] A. D. B. D. H. R. L. D. D. R. Wilcox R, "An invetsigation of the burst fracture mechanism using a combined experimental and finite element approach," Calgary, 2002.

[8] S. Kumaresan, "Finite element modeling of cervical laminectomy with graded facetectomy.," *Journal of Spinal Disorders* , Vols. 10(1),, p. 40–46., 1997.

[9] S. Kumaresan, "Finite element modeling of the cervical spine:role of intervertebral disc under axial and eccentric loads," *Medical Engineering and Physics* , vol. 21, p. 689–700., 1999.

[10] V. Goel, "Prediction of load sharing among spinal components of a C5–C6 motion segment using the finite element approach," *Spine (6),* vol. 23, p. 684–691, 1998.

[11] Y. N. P. F. Kumaresan S, "Finite element analysis of anterior cervical spine interbody fusion," *Bio-medical mat. and engineering,* vol. 7, pp. 221-230, 1997.

[12] K. S. Y. N. P. F. C. J. Voo LM, "Finite element analysis of cervical facetectomy," *SPINE,* vol. 22, no. 9, pp. 964-969, 1997.

[13] C. B. A. H. A. G. Nataranjan RN, "Anterior cervical fusion - A finite element model study on motion segment stability including the effect of osteoporosis," *SPINE,* vol. 25, no. 8, pp. 955-961, 2000.

[14] K. H. J. C. K. J. S. M. N. R. A. H. A. G. Lim TH, "Effect of Endplate Conditions and Bone Mineral Density on the Compressive Strength of the Graft-Endplate Interface in Anterior Cervical Spine Fusion," *SPINE,* vol. 26, no. 8, pp. 951-956, 2001.

[15] G. V. T. V. C. C. Puttlitz CM, "A Finite Element Investigation of Upper Cervical Instrumentation," *SPINE,* vol. 26, no. 22, pp. 2449-2455, 2001.

[16] M. D. B. D. S. W. Pitzen TR, "Initial stability of cervical spine fixation: predictive value of a finite element model," *J. Neurosurg (Spine 1),* vol. 97, pp. 128-134, 2002.

[17] R. W. N. F. L. C. C. E. F. S. M. Alan T. Dibb, "Tension and Combined Tension-Extension Structural Response and Tolerance Properties of the Human Male Ligamentous Cervical Spine," *Journal of Biomechanical Engineering,* vol. 131, 2009.

[18] B. J. D. J. G. P. B. S. M. G. James H. McElhaney, "Combined Bending and Axial Loading Responses of the Human Cervical Spine".

[19] N. Y. Joseph F. Cusick, "Biomechanics of the cervical spine 4: major injuries," *Clinical Biomechanics,* vol. 17, p. 1–20, 2002.

[20] M. K. Mesfar W., "Effect of the transverse ligament rupture on the biomechanics of the cervical spine under a compressive loading," *Clinical Biomechanics,* 2013.

[21] J. Pooni, "Comparison of the structure of human intervertebral discs in the cervical,thoracic and lumbar regions of the spine.," *Surgical and Radiologic Anatomy,* vol. 8, p. 175–182., 1986..

[22] H. K. A. H. F. S. U. C. L. W. H. Schmidt, "Intradiscal pressure, shear strain, and fiber strain in the intervertebral disc under combined loading," *Spine ,* vol. 32, p. 748–755., 2007.

[23] M. Panzer, *Numerical modelling of the human cervical spine in frontal impact,* Waterloo: University of Waterloo., 2006.

[24] E.-R. M. M. W. a. M. K. Mustafy T., "Investigation of Loading Rate Effects under Impact Conditions on the Ligamentous Cervical Spinal Load-Partitioning Using Finite Element Model of Functional Spinal Unit C2-C3.," *Journal of Biomechanics,* 2013.

[25] K. Yang, "Compressibility measurement of human intervertebral nucleus pulposus," *Journal of Biomechanics ,* vol. 21, p. 865, 1988.

[26] A. A. A. S. S. Shirazi-Adl, "Mechanical response of a lumbar motion segment in axial torque alone and combined with compression," *Spine,* vol. 11, p. 914–927, 1986.

[27] A. C. G. A. E.-R. M. A. P. Wagnac E, "Calibration of hyperelastic material properties of the human lumbar intervertebral disc under fast dynamic compressive loads.," *J Biomech Eng ,* vol. 133, 2011.

[28] A. Inc., *Abaqus Manual 6.12,* 2013.

[29] C. K. Y. L. C. H. Y. J. J. G. V. Lee, "Impact response of the intervertebral disc in a finite-element model," *Spine ,* vol. 25, p. 2431–2439, 2000.

[30] D. Matthew B.Panzer, "C4–C5 segment finite element model development,validation,and load-sharing investigation," *Journal of Biomechanics,* vol. 42, p. 480–490, 2009.

[31] D. Reilly, "The elastic modulus for bone," *Journal of Biomechanics,* vol. 7, p. 271–275., 1974..

[32] P.-J. A. E. W. C. B. C.-E. A. Marwan El-Rich, "Finite element investigation of the loading rate effect on the spinal load-sharing changes under impact conditions," *Journal of Biomechanics ,* vol. 42 , p. 1252–1262, 2009.

[33] D. S. C. Jennifer A. DeWit, "Cervical spine segment finite element model for traumatic injury prediction," *Journal of Mechanical Behaviour of Biomedical Materials,* vol. 10, pp. 138-150, 2012.

[34] D. K. T. Kopperdahl, "Yield strain behavior of trabecular bone," *Journal of Biomechanics ,* vol. 31, p. 601–608, 1998.

[35] R. T. A. C. R. Ochia, "Effect of loading rate on endplate and vertebral body strength in human lumbar vertebrae.," *Journal of Biomechanics,* vol. 36, p. 1875–1881, 2003.

[36] N. Yoganandan, "Finite element applications in cervical spine modeling," *Spine (15),* vol. 21, p. 1824–1834, 1996.

[37] A. e. a. Patwardhan, *J. of Spine* , vol. 25, no. 12, pp. 1548-54, 2000.

[38] M. S. P. V. F. S.-. w. W. Panjabi, "Three-dimensional load–displacement curves due to forces on the cervical spine," *Journal of Orthopaedic Research* , vol. 4, p. 152–161., 1986.

[39] S. A. J. P. F. M. D. R. J. C. J. L. S. Yoganandan N, "Injury Biomechanics of the Human Cervical Column," *Spine (Phila Pa 1976),* vol. 15, no. 10, pp. 1031-9., 1990 Oct.

[40] B. J. W. C. G. B. W. W. W. B. Jaumard NV, "Contact pressure in the facet joint during sagittal bending of the cadaveric cervical spine.," *J Biomech Eng.* , vol. 133, no. 7, 2011.

[41] P. F. S. A. J. R. J. L. S. Yoganandan N, "Strength and kinematic response of dynamic cervical spine injuries.," *Spine (Phila Pa 1976),* vol. 16, no. 10, pp. 511-7., 1991 Oct.

[42] T. K. L. V. T. E. Qiu TX, "Investigation of thoracolumbar T12–L1 burst fracture mechanism using finite element method," *Med Eng Phys,* vol. 28, p. 656–664, 2006.

[43] A. D. H. R. L. D. B. D. D. R. Wilcox RK, "A dynamic investigation of the burst fracture process using a combined experimental and finite element approach," *Eur Spine J* , vol. 13, p. 481–488, 2004.

[44] H. G. Jundt L, "Side-chain truncation of apicularen A by olefin cross-metathesis with ethylene.," *J Nat Prod.* , vol. 70, no. 8, pp. 1377-9. , 2007.

[45] M. A. P. J. W. E. B. C. a. A. C. E. El-Rich, "Finite Element Investigation of the Loading Rate Effect on the Spinal Load- Sharing Changes under Impact Conditions," *J. Biomech.,* , vol. 42, no. 9, p. 1252–1262., 2009.

[46] A. S. J. P. J. R. J. F. a. S. J. Narayan Yoganandan, "Injury Biomechanics of the Human Cervical Column," *Spine,* vol. 15, pp. 1031- 1039.

[47] M. ,. W. H. ,. M. ,. N. H. ,. M. ,. H. U. ,. M. ,. G. I. J. ,. M. P. C. M. ,. M. ,. P. J. T. ,. M. ,. a. B. W. C. ,. M. Ryan M. Kretzer, "Adjacent-Level Range of Motion and Intradiscal Pressure After Posterior Cervical Decompression and Fixation," *SPINE* , vol. 37, no. 13, p. pp E778–E785, 2012.

[48] M. G. V. T. K. Panjabi, "Physiologic strains in the lumbar spinal ligaments. An in vitro biomechanical study.," *Spine* , vol. 7, p. 192–203., 1982.

[49] R. Crowell, "Cervical injuries under flexion and compression loading," *Journal of Spinal Disorders (2),* vol. 6, p. 175–181., 1993.

Chapter 4: Summary and Conclusions

The major novelty and significance of this research is the development of a bio-realistic and anatomically accurate ligamentous C2-C3 finite element model (FEM) which has been capable of predicting injury at the tissue level, showing load sharing mechanisms under different dynamic loading conditions. Another important contribution of this model is that it demonstrated the importance of having 2D ligaments in the model that is mandatory to show the stress concentration at the ligaments and it can demonstrate the progressive failure of ligaments. Until now, there has been no such study at the cervical spine segment level where there has been a successful implementation of the 2D ligaments to investigate the failure propagation mechanism.

One of the objectives was to investigate the loading rate effects on load-sharing at the component level using the complete C2-C3 functional unit of the cervical spine. The finite element modelling results have verified the hypotheses that segment stiffness increases to failure level at higher rates of compression and rotation, indicating the possible influence of the ligament and disc behavior. Ligaments also showed increased stress with the higher rates of loading and load sharing pattern also showed rate dependency, even for vertebral endplates, disc, cancellous bone and ligaments the pattern alters with different loading rates. Hence it can be said that the cervical spine response is indeed rate dependent and load sharing mechanism among different components changes with different rates of loading.

Another objective of the current study is to assess virtually the bone and ligament injuries in complex combined loading scenarios. In order to address this issue a ligamentous segment of the cervical spine has been used to investigate the injury mechanism, load sharing and failure propagation in six different major injury conditions. We have found from the results that for most of the minor injury and in every major injury the vertebral endplate gets fractured which is being confirmed from clinical results. Also, we have found that the articular facets (zygapophyseal joints) responded non-symmetrically as only the right facet failed in majority cases leaving the left facet stressed below the failure limit. Also, we have got an insight about the load sharing at the tissue level, even the model can show the collagen fibers responses in applied injury scenarios.

This numerical model distinguishes itself from other published models by implementing a bio-realistic geometry, a refined mesh, and strain-dependent material constitutive laws that can simulate bone fracture and ligament tear. A detailed/realistic investigation of failure initiation and propagation over the bone is being possible with this model, which can also predict the bone fracture and ligament failure. The comparison between the biomechanical behavior of the cervical spine segment under flexion and extension complex injury cases demonstrates the versatility of our FEM to virtually assess spinal injuries under various complex combined loading scenarios. Also as the model is capable of showing the load-sharing mechanism amongst the different spinal components in response to the different loading cases, the onset of spinal injuries for a given loading direction was also been able to be predicted by the model.

These results provide insight into cervical spine behavior as the distribution of load within the cervical spine has not yet been measured experimentally. Future work will address more complex types of loading such as combined rotations and translations that could potentially lead to more severe injuries resulting from early contact between bone components and to an amplified strain level on ligaments. Also the mechanism adapted in this model will be implemented to model the entire cervical spine in future.